

Cold gas properties of the *Herschel* Reference Survey. I. $^{12}\text{CO}(1-0)$ and H I data \star

A. Boselli¹, L. Cortese^{2,3}, M. Boquien^{1,4}

¹ Aix Marseille Université, CNRS, LAM (Laboratoire d'Astrophysique de Marseille) UMR 7326, 13388, Marseille, France e-mail: Alessandro.Boselli@lam.fr

² Centre for Astrophysics & Supercomputing, Swinburne University of Technology, Mail H30, PO Box 218, Hawthorn, VIC 3122, Australia e-mail: lcortese@swin.edu.au

³ European Southern Observatory, Karl-Schwarzschild Str. 2, 85748 Garching bei Muenchen, Germany

⁴ Institute of Astronomy, University of Cambridge, Madingley Road, Cambridge CB3 0HA, UK e-mail: mboquien@ast.cam.ac.uk

ABSTRACT

We present new $^{12}\text{CO}(1-0)$ observations of 59 late-type galaxies belonging to the *Herschel* Reference Survey (HRS), a complete K-band-selected, volume-limited ($15 \lesssim D \lesssim 25$ Mpc) sample of nearby galaxies spanning a wide range in morphological type and luminosity. We studied different recipes to correct single-beam observations of nearby galaxies of different sizes and inclinations for aperture effects. This was done by comparing single-beam and multiple-beam observations along the major axis, which were corrected for aperture effects using different empirical or analytical prescriptions, to integrated maps of several nearby galaxies, including edge-on systems observed by different surveys. The resulting recipe is an analytical function determined by assuming that late-type galaxies are 3D exponentially declining discs with a characteristic scale length $r_{\text{CO}} = 0.2 r_{24.5}$, where $r_{24.5}$ is the optical, g- (or B-) band isophotal radius at the 24.5 mag arcsec⁻² (25 mag arcsec⁻²), as well as a scale height $z_{\text{CO}} = 1/100 r_{24.5}$. Our new CO data are then combined with those available in the literature to produce the most updated catalogue of CO observations for the HRS, now including 225 out of the 322 galaxies of the complete sample. The 3D exponential disc integration is applied to all the galaxies of the sample to measure their total CO fluxes, which are later transformed into molecular gas masses using a constant and a luminosity-dependent X_{CO} conversion factor. We also collect H I data for 315 HRS galaxies from the literature and present it in a homogenised form.

Key words. Galaxies: ISM; Galaxies: general; Galaxies: spiral; Radio lines: galaxies

1. Introduction

The *Herschel* Reference Survey (HRS) is a complete sample of nearby galaxies defined to study the physical properties of the interstellar medium (ISM) in galaxies of different morphological type and luminosity (Boselli et al. 2010a). Composed of 322 galaxies, it has recently been observed by *Herschel* with the SPIRE (Ciesla et al. 2012) and PACS (Cortese et al. in prep.) instruments. To provide the community with the largest possible set of homogeneous data, our team has undertaken several observational campaigns or collected data from the literature to cover the widest possible range in wavelengths. These data include deep UV imaging with GALEX (Cortese et al. 2012a; Boselli et al. 2011), mid-infrared imaging with IRAC on *Spitzer* and *WISE* (Ciesla et al. in prep.), MIPS *Spitzer* photometry (Bendo et al. 2012), H α imaging (Boselli et al. in prep.), and medium-resolution integrated optical spectroscopy (Boselli et al. 2013a).

This paper presents new CO observations of 59 HRS galaxies obtained at the Kitt Peak 12m radiotelescope. These new CO data, combined with those available for both the other HRS objects and for other nearby galaxies recently mapped in the $^{12}\text{CO}(1-0)$ line with various instruments, are used to compare different prescriptions to correct for aperture-effects single-beam

observations. The new CO data, combined with those already available in the literature for the rest of the sample, are homogenised to produce a complete catalogue of CO fluxes and realistic uncertainties for all the observed HRS. We also collected H I data from the literature and homogenised it for nearly the whole sample. These CO and H I data are crucial for any detailed study of the physical properties of the ISM.

The cold gas is the dominant phase of the ISM in late-type galaxies. It exceeds in mass the dust component by \sim a factor of 100-200 (Sodroski et al. 1994). This cold gas component can be observed easily in local galaxies. The atomic hydrogen (H I) can be observed directly through the emission of the spin inversion line at 21 cm (1420 Mhz). Because of its symmetric structure, the molecular hydrogen (H_2) has no permanent electric dipole moment. Dipole rotational transitions are thus strongly forbidden, making it very hard to directly observe the cold phase of this molecule, which in late-type galaxies has generally a temperature of \sim 10 K. For this reason, the molecular hydrogen mass is generally determined through observing of the second most abundant molecule in the cold ISM, carbon monoxide, under the assumption that CO is a good tracer of H_2 (Young & Scoville 1991). Indeed it has been shown that the dynamical mass of the giant molecular clouds is tightly related to the intensity of the CO line. The most commonly used method of determining the molecular hydrogen mass is based on observing of the $^{12}\text{CO}(1-0)$ rotational line at 2.6 mm (115 GHz) and assuming a given conversion factor X_{CO} between the inten-

\star Tables 1, 2, 10, 11, 12 are available in electronic form at the CDS via anonymous ftp to cdsarc.u-strasbg.fr(130.79.128.5) or via <http://cdsweb.u-strasbg.fr/cgi-bin/qcat?J/A+A/>

sity of the CO line and the H $_2$ column density (see Boselli 2011).

In recent years, several works have questioned the existence of a standard conversion factor, but rather indicated that X_{CO} might change with the different physical conditions characterising the properties of the ISM, such as the hardness of the ionising and non-ionising stellar radiation fields, and the metallicity and the density of the gas (Boselli et al. 2002, Bell et al. 2007, Bolatto et al. 2008, Liszt et al. 2010, Leroy et al. 2011, Shetty et al. 2011a,b, Narayanan et al. 2012, Bolatto et al. 2013, Sandstrom et al. 2013). We thus determined molecular gas masses using both a constant or a luminosity-dependent X_{CO} conversion factor. As constant value we used the one determined in the Milky Way using γ -ray absorption data from COBE ($X_{\text{CO}} = 2.3 \cdot 10^{20} \text{ cm}^{-2}/(\text{K km s}^{-1})$), or else, if expressed as $\alpha_{\text{CO}} = 3.6 M_{\odot}/(\text{K km s}^{-1} \text{ pc}^{-2})$, Strong et al. 1988), which is generally assumed to be representative of environments similar to those encountered in the solar neighbourhood in terms of metallicity and radiation field. As variable conversion factor, we adopt the calibration proposed by Boselli et al. (2002) based on the H-band luminosity, $\log X_{\text{CO}} [\text{cm}^{-2}/(\text{K km s}^{-1})] = -0.38 \times \log L_{\text{H}} [L_{\text{H}\odot}] + 24.23$. We chose this calibration because it can be determined easily for all HRS galaxies, for which an H-band magnitude is available from 2MASS. Furthermore, this calibration is a mean calibration compared to those proposed in the literature (Bolatto et al. 2013).

The paper is structured as follows. Section 2 describes the HRS sample, while Sects. 3 and 4 present the new CO observations. In Sect. 5 we discuss and apply different aperture correction techniques to the whole set of CO data available in the literature for the entire HRS sample, and we thus derive total CO fluxes and molecular gas masses. Section 6 gives homogenised H α data for the whole sample. A brief conclusion is given in Sect. 7. Despite the presence of several complete samples of nearby galaxies with CO data (Sage 1993; FCRAO survey, Young et al. 1995; Boselli et al. 1997; Sauty et al. 2003; Lisenfeld et al. 2011, Saintonge et al. 2011), the HRS is the only one with the complete set of far-infrared and sub-millimetric *Herschel* data necessary for a detailed study of the properties of the ISM of normal galaxies. At the same time, it is a statistically significant, complete sample of nearby galaxies spanning a wide range in morphological type and stellar mass, making it ideally suited to study the cold gas properties of normal galaxies. It can be used, for instance, to extend to lower stellar masses (by a factor of ~ 10) the reference work of Saintonge et al. (2011) on the COLD GASS sample, which only includes massive galaxies. We thus devote three other specific works to the analysis of the gas properties of the HRS using this unique set of data. One, already published, analyses the effects of the environment on the H α scaling relations of the sample (Cortese et al. 2011). A second one is focussed on determining the mean total and molecular gas scaling relations of the HRS (Boselli et al. 2013b), while the last one treats the effects of the environment on the molecular gas content of cluster objects (Boselli et al. 2013c). The interested reader can find the results of other works based on the combined analysis of the *Herschel* and the other multifrequency data in Cortese et al. (2012b; dust scaling relations along the Hubble sequence), Smith et al. (2012; dust properties of early-type galaxies), Boselli et al. (2012; far infrared colours), Boquien et al. (2012, 2013; dust attenuation properties in resolved galaxies) or in the publication of several papers during the science demonstration phase of the instrument (Boselli et al. 2010b; Cortese

et al. 2010; Eales et al. 2010; Gomez et al. 2010; Pohlen et al. 2010; Sauvage et al. 2010).

2. The sample

The *Herschel* Reference Survey (HRS) is an *Herschel*/SPIRE guaranteed time key project aimed at observing a complete, K-band-selected ($K \leq 8.7$ mag for early-types, $K \leq 12$ for type \geq Sa), volume-limited ($15 \lesssim D \lesssim 25$ Mpc) sample of nearby galaxies. The HRS survey, as well as the selected sample, are extensively presented in Boselli et al. (2010a). Briefly, the sample is composed of 322 galaxies out of which 260 are late-type systems¹. Galaxies were selected in the K-band taken as a proxy for galaxy stellar mass (Gavazzi et al. 1996). The sample includes objects in environments of different densities, from the core of the Virgo cluster to loose groups and fairly isolated systems. As defined, the present sample is ideal for any statistical study of the mean galaxy population of the nearby universe.

The galaxies observed in this work are late-type systems of K-band magnitude brighter than $K < 10$, expressly selected to complete the sample down to this K-band magnitude limit (142/151 of the late-types). Including our new observations, 225 out of the 322 HRS galaxies (143 detections), 168/260 for late-type (134 detected), and 57/62 for early-type systems (9 detected) have $^{12}\text{CO}(1-0)$ data.

We also compile and homogenise 21 cm H α data from the literature for all galaxies in the HRS. H α data are available for 315 out of the 322 galaxies of the sample. The whole HRS sample with its main characteristics is given in Table 1, arranged as follows:

- Column 1: *Herschel* Reference Sample (HRS) name, from Boselli et al. (2010a).
- Column 2: Zwicky name, from the Catalogue of Galaxies and of Cluster of Galaxies (CGCG; Zwicky et al. 1961-1968).
- Column 3: Virgo Cluster Catalogue (VCC) name, from Binggeli et al. (1985).
- Column 4: Uppsala General Catalog (UGC) name (Nilson 1973).
- Column 5: New General Catalogue (NGC) name (Dreyer 1888).
- Column 6: Index Catalogue (IC) name (Dreyer 1908).
- Columns 7 and 8: J2000 right ascension and declinations, from NED.
- Column 9: Morphological type, from NED, or from our own classification if not available.
- Column 10: Distance, in Mpc. Distances have been determined from the recessional velocity assuming a Hubble constant $H_0 = 70 \text{ km s}^{-1} \text{ Mpc}^{-1}$ for galaxies outside the Virgo cluster, and assumed to be 23 Mpc for galaxies belonging to the Virgo B cloud, 17 for the other Virgo members (Gavazzi et al. 1999).
- Column 11: Total K-band magnitude ($K_{\text{S tot}}$), from 2MASS (Skrutskie et al. 2006).
- Column 12: g -band optical isophotal diameter (24.5 mag arcsec $^{-2}$), from Cortese et al. (2012a). For the HRS galaxies without SDSS images, the g -band isophotal diameter was determined from the relation $r_{24.5(g)} = 0.871(\pm 0.017)r_{25(B)} +$

¹ With respect to the original sample given in Boselli et al. (2010a), we removed the galaxy HRS 228 whose new redshift indicates it as a background object. We also revised the morphological type for 6 galaxies: NGC 5701, now classified as Sa; NGC 4438 and NGC 4457, now Sb; NGC 4179, now S0; VCC 1549, now dE; and NGC 4691 now Sa.

6.041(± 2.101) (Spearman correlation coefficient $\rho = 0.92$), where $r_{25}(B)$ is the radius given in NED. This relation was determined using the HRS galaxies with both sets of data.

- Column 13: inclination of the galaxy, determined using the prescription based on the morphological type described in Haynes & Giovanelli (1984) and the i -band ellipticity given in Cortese et al. (2012a).
- Column 14: Heliocentric radial velocity (in km s^{-1}), from H α data when available, otherwise from NED.
- Column 15: Cluster or cloud membership, from Gavazzi et al. (1999) for Virgo and Tully (1988) or Nolthenius (1993) whenever available, or from our own estimate otherwise.
- Column 16: Code to indicate whether H α data are available (1) or not (0).
- Column 17: Code to indicate whether CO data are available (1) or not (0).

3. Observations

CO observations were carried out during four remote-observing runs from the Laboratoire d'Astrophysique de Marseille in spring 2008 and 2009 using the NRAO Kitt Peak 12 m telescope². One hundred forty-one hours were allocated to this project, out of which ~ 20 hours lost for bad weather conditions or technical problems. At 115 GHz [$^{12}\text{CO}(1-0)$], the telescope's half-power beam width (HPBW) is $55''$, which corresponds to 5.3 kpc at the average distance of 20 Mpc of the HRS galaxies. Weather conditions were fairly good, with typical zenith opacities of 0.15-0.25. The pointing accuracy was checked every night by broad band continuum observations of nearby planets or the radiogalaxy 3C273, with an average error of $5''$ rms. We used a dual-polarisation SIS mixer, with a receiver temperature for each polarisation of about $T_{\text{sys}}=300-400$ K (in T_R^* scale) at the elevation of the sources. We used a dual beam-switching procedure, with two symmetric reference positions offset by $4'$ in azimuth. The backend was a 256 channel filter bank spectrometer with channel width of 2 MHz. Each six-minute scan began by a chopper wheel calibration on a load at ambient temperature, with an OFF-ON-ON-OFF set of pointings for each scan. Galaxies were observed at their nominal coordinates listed in Table 1. Fifteen objects with an optical diameter exceeding three arcminutes were also mapped along the major axis, with two one-beam off positions. The face-on galaxy HRS 42 (NGC 3596) was observed along a cross with one beam offset. The total integration time was on average 120 minutes ON+OFF (i.e. 60 minutes on the source), yielding rms noise levels of about 3 mK (in the T_R^* scale) after velocity smoothing to 15.7 km s^{-1} . The baselines were flat owing to the use of beam-switching, thereby requiring only linear baselines to be subtracted. The antenna temperature T_R^* was corrected for telescope and atmospheric losses. In the following analysis we use the T_R^* scale. This scale can be transformed into the main-beam brightness temperature scale, T_{mb} , with $T_{\text{mb}}=T_R^*/0.84$ (where the main beam efficiency is $\eta_{\text{mb}}=0.54$ and the forward scattering and spillover efficiency $\eta_{\text{fss}}=0.68$). The T_R^* scale can be converted into flux using 39 Jy/K .

4. Results

4.1. Results of our observations

The $^{12}\text{CO}(1-0)$ spectra of all the observed galaxies, reduced with the CLASS package (Forveille et al. 1990), are shown in Fig. 1.

² The Kitt Peak 12-m telescope was operated by the Arizona Radio Observatory

The observational results are listed in Table 2. Of the 59 observed galaxies, 13 were not detected. Table 2 is arranged as follows:

- Column 1: HRS name.
- Columns 2 and 3: R.A. and Dec. pointing offset, in arcsec.
- Column 4: detection flag, 1 for detected, 0 for undetected sources.
- Column 5: observing run: 1,2 and 3 are for the three 2008 runs, 4 for the 2009 run.
- Column 6: rms noise, in mK, on the T_R^* scale, measured after the spectra are smoothed to a velocity resolution $\delta V_{\text{CO}}=15.7 \text{ km s}^{-1}$.
- Column 7: number of scans (ON+OFF). Each scan is six minutes long.
- Column 8: Intensity of the $I(\text{CO})$ line ($I(\text{CO})=\int T_R^* dv$) in K km s^{-1} (area definition, which corresponds to the area under the profile of the line measured in between the upper and lower limits in velocity within which the line is detected. Galaxies are considered as detected whenever the signal-to-noise, defined as $S/N = \frac{I(\text{CO})}{\Delta I(\text{CO})}$ is greater than 2, where $\Delta I(\text{CO})$ is defined in eq. (2). For undetected galaxies, the reported value is an upper limit determined as follows:

$$I(\text{CO}) = 5\sigma(W_{\text{HI}}\delta V_{\text{CO}})^{1/2} \text{K km s}^{-1} \quad (1)$$

where σ is the rms noise of the spectrum, W_{HI} the H α line width, and δV_{CO} the spectral resolution (here taken at $\delta V_{\text{CO}}=15.7 \text{ km s}^{-1}$). For galaxies with W_{HI} unavailable, the H α width has been determined assuming a standard $W_{\text{HI}} = 300 \sin(i) \text{ km s}^{-1}$, where i is the galaxy inclination, with a minimum value of $W_{\text{HI}} = 50 \text{ km s}^{-1}$ for almost edge-on systems.

- Column 9: Error on the intensity of the CO line, $\Delta I(\text{CO})$, computed as

$$\Delta I(\text{CO}) = 2\sigma(W_{\text{CO}}\delta V_{\text{CO}})^{1/2} \text{K km s}^{-1} \quad (2)$$

where σ is the rms noise of the spectrum, W_{CO} the CO linewidth (given in Col. 11), and δV_{CO} the spectral resolution.

- Column 10: Heliocentric velocity determined from the CO line (Gaussian fit), in km s^{-1} (optical definition $v=c z=\Delta\lambda/\lambda_0$). The estimated error is comparable to the resolution, thus $\sim 15 \text{ km s}^{-1}$.
- Column 11: Full width at zero level of the CO line, in km s^{-1} , with an estimated error of $\sim 20 \text{ km s}^{-1}$. For galaxies with a suffix a the width of the CO line is the full width half maximum (FWHM) determined from a Gaussian fit. The width of the CO line generally corresponds to the width of the H α line, indicated by the red horizontal line in Fig. 1.
- Column 12: Peak temperature, in T_R^* scale (K).

4.2. Uncertainty on the $I(\text{CO})$ data

IN column 9 $\Delta I(\text{CO})$ gives the error on the intensity of the CO line as determined from the typical rms of the observed galaxies. A different estimate of this uncertainty can be determined by comparing independent measurements of the same galaxy. All galaxies observed in this work are new CO observations and thus do not have any similar data in the literature. The only exception is HRS 48 (NGC 3631), observed at the beginning of each run for checking the tuning of the instrument on a CO-bright source and for testing the repeatability of the observations.

We thus have three different CO observations of the same galaxy that can be compared. The same galaxy also has two other independent single-beam observations, one from the FCRAO survey (Young et al. 1995) and a second one from the CO survey of nearby galaxies done with the Onsala radio telescope by Elfhag et al. (1996). Table 3 gives the different $I(\text{CO})$ values obtained within our observing runs and in the literature. Given that the data obtained by the FCRAO (Young et al. 1995) and the Onsala surveys have been obtained in different beams and on different temperature scales, we also compare the total extrapolated CO fluxes obtained as described in the following sections. Table 3 shows that by using exactly the same telescope configuration we have differences from one to another observing run in the CO flux estimate of HRS 48 as large as $\approx 30\%$. The comparison with other data available in the literature, here done on the extrapolated CO fluxes of HRS 48 to remove any first-order dependence on the aperture correction and telescope temperature scale, gives differences with the mean value obtained in this work of the order of $\approx 8-13\%$. These differences are significantly smaller than those observed within our own independent data for the bright HRS 48. We recall, however, that for this particular object, our three independent observations were done with a significantly smaller number of scans (~ 6 scans each) than our typical observations of the other HRS galaxies (~ 20 scans). Given that the uncertainty on the CO intensity $I(\text{CO})$ depends on the rms of the spectrum (see eq. 2), we thus expect that for HRS 48, the quite large dispersion in our data is partly due to the low integration time. Table 3 shows, however, that the difference between our own observations of HRS 48 are larger than the expected uncertainties. Given the peaked distribution of the emitting molecular gas in galaxies, it is conceivable that small pointing offsets can be the origin of this discrepancy. In other words, the relation given in the previous section to estimate the uncertainty on single-beam observations slightly underestimates $\Delta I(\text{CO})$. The error on the CO central beam observations done in this work should thus be of the order of 30%.

5. CO data from the literature

5.1. Unit transformation

The $^{12}\text{CO}(1-0)$ data available in the literature come from a wide variety of references and for this reason are often given on different scales, as summarised in Table 4. Data coming from the FCRAO telescope are generally presented on the T_A^* scale (observed source antenna temperature corrected for atmospheric attenuation, radiative loss, and rearward scattering and spillover), those from the 12 m Kitt Peak telescope on the T_R^* scale (observed source antenna temperature corrected for atmospheric attenuation, radiative loss, and rearward and forward scattering and spillover), while those from the IRAM 30, the SEST, and the Onsala telescopes on the T_{mb} scale (source brightness temperature as measured by the main diffraction beam of the telescope). The different temperature scales can be transformed into a common scale following the prescription of Kutner & Ulich (1981). The T_R^* temperature can be transformed into the antenna temperature as

$$T_R^* = T_A^*/\eta_{fss}, \quad (3)$$

where η_{fss} is the forward spillover and scattering efficiency, while the main beam temperature can be obtained as

$$T_{mb} = T_A^*/\eta_{mb}, \quad (4)$$

where η_{mb} is the main beam efficiency. For the definition of a complete and consistent set of data for the HRS galaxies it is thus necessary that all these observations are homogenised on a common scale. We thus decided to provide, for all galaxies, $^{12}\text{CO}(1-0)$ fluxes in units of Jy km s^{-1} . For a source with a Gaussian profile observed with a Gaussian beam of similar size, the constant necessary to transform main beam temperatures (in K) into fluxes (in Jy) is given by the relation (Wilson et al. 2009) :

$$S(\text{Jy})/T_{mb}(\text{K}) = 8.18 \times 10^{-7} \left(\frac{\theta}{\text{arcsec}} \right)^2 \left(\frac{\nu}{\text{GHz}} \right)^2, \quad (5)$$

where θ is the FWHM of the beam and ν is the frequency. For sources extended with respect to the beam, as is the case for all HRS galaxies, the transformation of main beam temperatures into Jy is much more complex and requires the antenna pattern and the distribution of the emitting source (Wilson et al. 2009). Since a priori the CO distribution of the emitting galaxies within the antenna pattern is unknown, astronomers generally transform antenna temperatures into CO fluxes using a constant whose typical value for each telescope, determined with eq. 5, is listed in Table 4. For consistency with previous works, however, we adopt the same constants as used in the literature and as given in the original references where the CO data have been published. We prefer to use the values published in the original references just to make it easy any direct comparison with the already published data. These conversion constants might differ ($\approx 15\%$) slightly from those given in Table 4, which are mean values determined for galaxies at redshift $z=0$.

5.2. Integrated data of mapped galaxies

5.2.1. Total CO fluxes

Some of the 225 HRS galaxies with CO data have been completely mapped either with a multibeam detector or in interferometric mode and have thus high-quality integrated CO fluxes. Of these, 18 objects have been observed by Kuno et al. (2007) with the 25 beams BEARS array mounted on the 45 m Nobeyama Radio Observatory telescope, 19 objects by Chung et al. (2009a) with the 16 beams SEQUOIA array on the 13.7m FCRAO radio telescope, and 2 other galaxies with the IRAM 30 m radio telescope by our team (see below). Ten galaxies have also been observed during the BIMA SONG survey of nearby galaxies with the Owens Valley Radio Observatory in interferometric mode by Helfer et al. (2003). To these, we can add 71 galaxies observed along the major axis during the FCRAO CO survey of nearby galaxies by Young et al. (1995). Another object, NGC 4565, has also been partly mapped with the IRAM 30 m (Neininger et al. 1996) and with the 45 m Nobeyama (Sofue & Nakai 1994) radiotelescopes. Because of the complete coverage of the stellar disc, in particular for the single-dish observations done at the Nobeyama, IRAM, and FCRAO radio telescopes, we consider that all these data are of much higher quality than other single-beam observations that require aperture corrections. We thus decided to use mapped observations whenever possible instead of single beam data.

A few of these objects have integrated data taken by more than one survey. We compared the different sets of data to isolate those that we consider of higher quality. To do that, we cross-matched the different surveys, including galaxies outside the HRS sample (22 extra objects) to increase the statistics, and compared the different sets of data in Fig. 1. All data were first

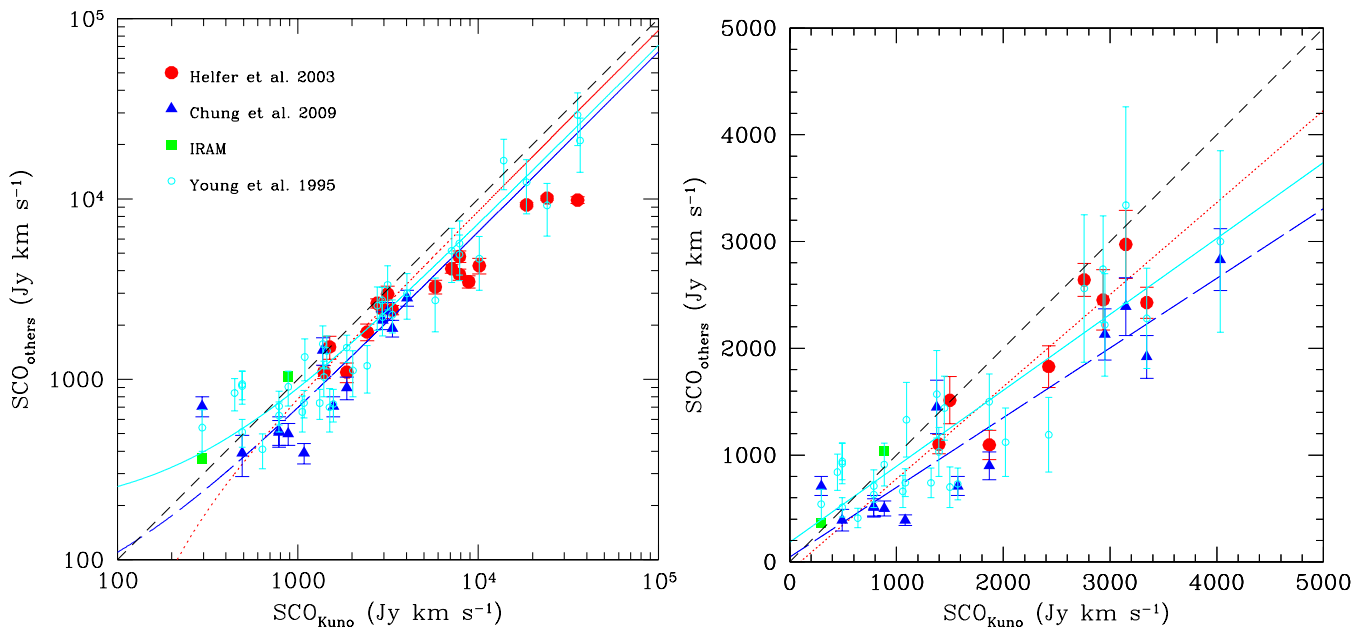


Fig. 1. Comparison between the integrated SCO fluxes determined by Kuno et al. (2007) and those determined by Helfer et al. (2003; red filled dots), Chung et al. (2009a; blue filled triangles), our own observations of the two galaxies NGC 4548 and NGC 4579 with the IRAM radiotelescope (green filled squares) and the extrapolated fluxes of the FCRAO survey (Young et al. 1995; cyan empty circles) on logarithmic scale for all galaxies in common (left) and on linear scale for those objects with SCO in the range 100-5000 Jy km s^{-1} sampled by the HRS (right). The linear best fit to the data, determined assuming the Kuno et al. (2007) data as independent variable in the range 100-5000 Jy km s^{-1} , are shown by the red dotted line (Helfer et al. 2003), the blue long dashed line (Chung et al. 2009a) and the cyan solid line (Young et al. 1995). The short dashed black line shows the 1:1 relationships.

transformed into CO fluxes (in Jy km s^{-1}) using the prescriptions indicated in the original papers for a correct comparison. For the FCRAO data of Young et al. (1995) we used the extrapolated SCO fluxes provided in this reference in the comparison. Figure 1 shows that the multibeam observations of Kuno et al. (2007) and those obtained by our team using the IRAM radio telescope agree within 20% ($SCO_{Kuno}/SCO_{IRAM}=0.83\pm 0.03$), while a certain scatter is present when the data of Kuno et al. (2007) are compared with those obtained by the other teams. All the other datasets give SCO fluxes that are generally smaller than those of Kuno et al. (2007). The difference between the Kuno et al. (2007) and those obtained by the other surveys does not seem to depend on the total flux of the emitting sources, with the exception of the BIMA SONG data of Helfer et al. (2003). Here there is a clear deviation from the one-to-one relation at high SCO fluxes, that could be easily ascribed to a non complete coverage of the stellar disc in the more extended sources combined with a slightly lower sensitivity to the diffuse emission of interferometric observations with respect to the multibeam observations done by Kuno et al. (2007). The difference with Chung et al. (2009a) might also come from a higher sensitivity of the Nobeyama radio telescope with respect to the FCRAO. The difference with the SCO fluxes of Young et al. (1995) probably comes from the rough extrapolation technique applied to the major axis CO data. The difference between these two sets of data is, however, remarkably small, indicating that overall the total SCO flux of spiral galaxies can be fairly well deduced using a very simple observing technique combined with an appropriate aperture correction.

This observational evidence suggests that the set of data of Kuno and collaborators be considered as reference, and the others be corrected using best fitting relations to minimise the scatter in the comparison with Kuno et al. (2007). To avoid any systematic

effect in the correction due to size, we fit the Helfer et al. (2003) and Young et al. (1995) vs. Kuno et al. (2007) CO flux relations using only CO data in the range $100 < SCO < 5000 \text{ Jy km s}^{-1}$, which is the range in the CO flux covered by the HRS galaxies. No restriction in the Chung et al. (2009a) data is required given that the fluxes of all their galaxies are within this range. The best linear fits to the data, shown in Fig. 1, are given in Table 5.

For the Young et al. (1995) data, however, the proposed correction does not significantly decrease the mean ratio and the scatter in the $SCO_{Kuno}/SCO_{Young}(\text{corrected})$ ratio. Indeed, the mean ratio SCO_{Kuno}/SCO_{Young} determined using the full set of original data published by Young et al. (1995) for all galaxies in common between these two surveys is $SCO_{Kuno}/SCO_{Young} = 1.10 \pm 0.44$, while the one determined using the corrected data is $SCO_{Kuno}/SCO_{Young}(\text{corrected}) = 0.90 \pm 0.34$. The majority of the HRS galaxies mapped by Young et al. (1995) without any other higher quality data from Kuno et al. (2007), Helfer et al. (2003), or Chung et al. (2009a), however, have only three detected beams along the major axis, and their total CO flux is $SCO_{Kuno} < 5000 \text{ Jy km s}^{-1}$. If we restrict the comparison of the Young et al. (1995) and Kuno et al. (2007) data to the subsample of HRS galaxies in common, the ratio determined with the originally published data, $SCO_{Kuno}/SCO_{Young} = 1.29 \pm 0.51$, can be compared to that determined using the corrected data, $SCO_{Kuno}/SCO_{Young}(\text{corrected}) = 1.33 \pm 0.55$. The proposed correction does not introduce any significant improvement in the data. We thus decided not to apply any correction to the FCRAO Young et al. (1995) data of the HRS galaxies.

Figure 2 shows the relationship between the different integrated CO fluxes corrected using the prescriptions given in Table 5 and those of Kuno et al. (2007) for the HRS galaxies with $100 < SCO < 5000 \text{ Jy km s}^{-1}$. Given the dispersion in the corrected

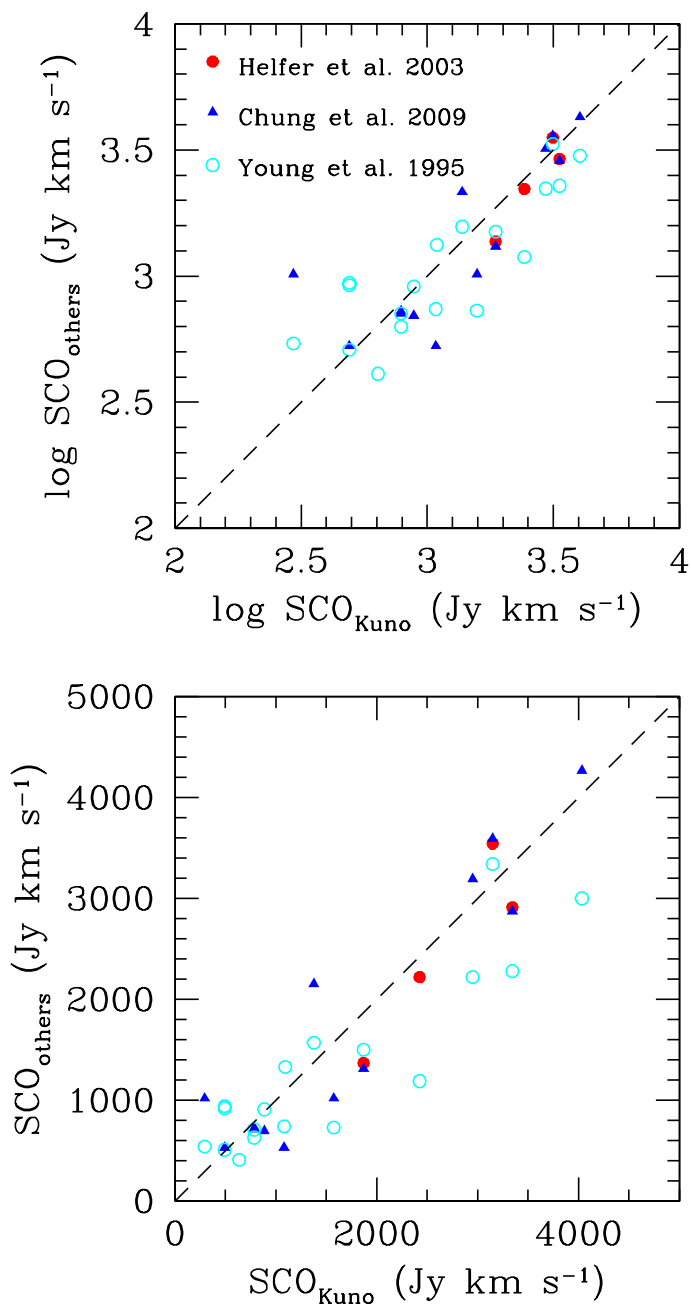


Fig. 2. Comparison between the integrated SCO flux determined by Kuno et al. (2007) and those determined by Helfer et al. (2003; red filled dots), Chung et al. (2009a; blue filled triangles), corrected as described in the text, and the extrapolated fluxes of the FCRAO survey (Young et al. 1995; cyan empty circles), for all HRS galaxies in common, on logarithmic (upper panel) and on linear scales (lower panel). The short dashed black line shows the 1:1 relationships.

relations seen in Fig. 2 and in Table 5, we decided to take the Kuno et al. (2007), Helfer et al. (2003), Chung et al. (2009a), and Young et al. (1995) data in order of priority (whenever multiple datasets are available)³. The quality of the FCRAO data of Young et al. (1995), however, strongly depends on the number

³ The only exception is the galaxy HRS 91, NGC 4192, for which we adopt the flux given in Young et al. (1995) since much closer to three independent estimates from single beam observations. The flux of Kuno et al. (2007) is indeed underestimated by a factor of ~ 2 , as indicated by

of detected beams along the major axis. When only three beam observations are available, the comparison with the Kuno et al. (2007) data indicates that the dispersion in the relation is higher than that we obtained using only the central beam, and we extrapolated it using our own prescriptions (see below). We thus decided to use the extrapolated CO fluxes of Young et al. (1995) only when more than three detections along the major axis are available; otherwise, we consider the galaxies as observed only in the central beam and measure their total emission using our own prescriptions.

We thus end up with 37 HRS galaxies with integrated data, 17 from Kuno et al. (2007), 0 from Helfer et al. (2003)⁴, 6 from Chung et al. (2009a), and 13 from Young et al. (1995). To these we can add a galaxy, NGC 4565 (HRS 213), partly mapped by Neiningner et al. (1996) with the IRAM radiotelescope and by Sofue & Nakai (1994) with the Nobeyama radiotelescope. By correcting their own independent sets of data to extend the measure of the CO flux to the whole galaxy, they end up with a total flux of $SCO = 1672.2 \text{ Jy km s}^{-1}$ and $SCO = 1643 \text{ Jy km s}^{-1}$, respectively. There is also an earlier estimate of the CO flux of this galaxy by Richmond & Knapp (1986) from observations taken with the Bell Laboratories radiotelescope, which gives $SCO = 4487 \text{ Jy km s}^{-1}$. Our own estimate based on the extrapolation of the central single beam as described in sect. 5.3, gives $SCO_{3D} = 1550 \text{ Jy km s}^{-1}$, a value much closer to the estimates of Neiningner et al. (1996) and Sofue & Nakai (1994). We thus decided to take for this object $SCO = 1672.2 \text{ Jy km s}^{-1}$.

5.2.2. Uncertainties on integrated data

Table 5 and Fig. 2 can also be used to estimate the typical uncertainty on the integrated data. The comparison between Kuno et al. (2007) with our own observations of two HRS galaxies done with the IRAM radio telescope indicates that $SCO_{Kuno}/SCO_{IRAM} = 0.83 \pm 0.03$. Despite the lack of statistics, this comparison indicates that the two sets of data are consistent within $\sim 17\%$. This uncertainty should be shared between the two different sets of data. The uncertainty on the Kuno et al. (2007) CO fluxes is thus assumed to be of the order of 12%. The uncertainty in the Helfer et al. (2003) data is also comparable. The one in the Chung et al. (2009a) data is $\sim 40\%$, while in the Young et al. (1995) extrapolated data slightly larger ($\sim 45\%$). It is hard to estimate the uncertainty on the CO flux of NGC 4565 given that the three independent measurements come from the extrapolation of observations of a fraction of this edge-on galaxy. Two independent measurements are consistent within 2%, and the third one is different by a factor of ~ 3 . We thus arbitrarily assume for this source an uncertainty of $\sim 30\%$.

5.3. Single-beam observations of the centres of galaxies

5.3.1. Extrapolation of the central beam

The majority of the 225 HRS galaxies with CO data have only one single-beam observation in their central position. For these objects the beam of the telescope does not necessarily cover the whole surface of the stellar disc. These CO data must thus be corrected for aperture effects to derive total CO fluxes of the observed galaxies. The extrapolation of the central beam obser-

the position that this galaxy would take in the $M(H_2)$ vs. M_{star} scaling relation given in Paper III.

⁴ All HRS galaxies in the BIMA SONG survey have been observed by Kuno et al. (2007).

vation can be done using either empirical relations calibrated on nearby mapped galaxies or analytic functions known to reproduce the radial distribution of the CO emission well. The first method has been proposed by Saintonge et al. (2011), who simulated the observation of the galaxies mapped by Kuno et al. (2007) with Gaussian beams of different sizes. Using this technique, the total CO flux $SCO_{Saintonge}(tot)$ of a galaxy with a central beam flux $SCO(CB)$ is given by the relation

$$SCO_{Saintonge}(tot) = \frac{SCO(CB)}{1.094 - 0.176 * N.Beam + 0.00968 * N.Beam^2}, \quad (6)$$

where $N.Beam$ is the size of the galaxy in number of beams:

$$N.beam = \frac{D_{25}(B)}{\theta}, \quad (7)$$

with $D_{25}(B)$ the 25 mag arcsec $^{-2}$ isophotal B -band diameter⁵, and θ the FWHM of the beam of the radiotelescope (see Table 4), both measured in arcseconds.

The second approach has recently been proposed by Lisenfeld et al. (2011). Considering that the CO emission of nearby mapped galaxies is represented well by an exponential disc of scale length r_{CO} :

$$SCO(r) = SCO(0)e^{-r/r_{CO}}, \quad (8)$$

where $SCO(0)$ is the CO emission in the centre of the galaxy. The total CO flux of an exponential disc is given by the relation:

$$\begin{aligned} SCO_{2D}(tot) &= \int_0^{2\pi} \int_0^{\infty} rSCO(r)drd\theta, \\ &= \int_0^{\infty} 2\pi rSCO(0)e^{-r/r_{CO}}dr, \\ &= 2\pi r_{CO}^2 SCO(0). \end{aligned} \quad (9)$$

As discussed in Lisenfeld et al. (2011), the scale length of the CO emitting disc, r_{CO} , is correlated well with the optical scale length of the stellar disc and with r_{25} , the optical 25 mag arcsec $^{-2}$ isophotal radius⁶. The observations of the THINGS sample of nearby objects done by Leroy et al. (2008) indicates that, on average, $r_{CO}/r_{25} = 0.2$. Lisenfeld et al. (2011) derive a consistent value using different sets of data, from the BIMA SONG survey of Regan et al. (2001), to the sample of Nishiyama & Nakai (2001) observed with the Nobeyama radiotelescope, to the FCRAO galaxies mapped by Young et al. (1995) along the major axis. The CO emission of the observed galaxies within the central beam can be determined by convolving the CO intensity profile with a Gaussian beam:

$$SCO_{2D}(CB) = 4SCO(0) \int_0^{\infty} \int_0^{\infty} \exp\left(-\ln(2) \left[\left(\frac{2x}{\theta}\right)^2 + \left(\frac{2y \cos(i)}{\theta}\right)^2 \right] - \frac{\sqrt{x^2 + y^2}}{r_{CO}}\right) dx dy,$$

⁵ For the sample of galaxies with integrated values in the literature used for comparing the different aperture corrections, D_{25} is the B-band isophotal diameter given in NED.

⁶ For the sample of galaxies with integrated values in the literature used for comparing the different aperture corrections, r_{25} is the isophotal radius derived from the optical diameter given in NED, which generally corresponds to the B-band isophotal diameter at 25 mag arcsec $^{-2}$. For the HRS galaxies we use the g -band isophotal radius $r_{24.5}(g)$ given in Table 1.

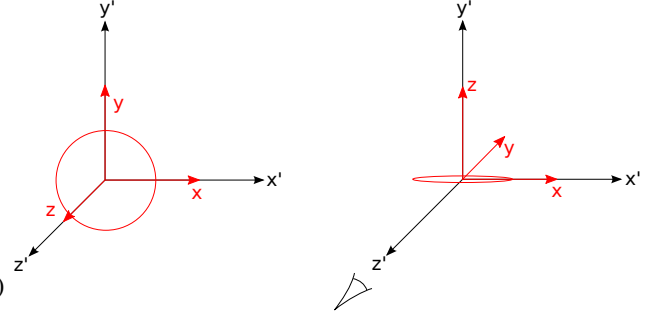


Fig. 3. Definition of the referential of the galaxy (black) and that of the observer (red) in the case of a face-on (left) and an edge-on (right) galaxy. The referential of the observer corresponds to the referential of the galaxy rotated by angle i around the x axis.

where i is the inclination of the disc. The integral given in eq. (10) can be solved numerically, and $SCO(0)$ can be determined by comparing eq. (10) with the CO flux observed in the central beam. With eq. (9), it can be used to derive the total $SCO_{2D}(tot)$ of the observed galaxies.

Our sample includes a large number of edge-on galaxies such as NGC 4565. For these objects the integral given in eq. (10) does not consider that the molecular gas disc also has a given thickness in the z direction orthogonal to the plane of the disc. We thus modify the prescription of Lisenfeld et al. (2011) to take into account that the molecular gas disc has a 3D-distribution. Consistently with what is generally assumed for the dust distribution in edge-on galaxies (Xilouris et al. 1999; De Looze et al. 2012), we assume an exponential distribution even in the z direction:

$$SCO(r, z) = SCO(0)e^{-r/r_{CO}}e^{-|z|/z_{CO}}, \quad (11)$$

where z_{CO} is the scale height of the disc. The total CO flux is then

$$\begin{aligned} SCO_{3D}(tot) &= \int_{-\infty}^{\infty} \int_0^{\infty} \int_0^{2\pi} rSCO(r, z)d\theta dr dz, \\ &= \int_{-\infty}^{\infty} \int_0^{\infty} 2\pi rSCO(0)e^{-r/r_{CO}}e^{-|z|/z_{CO}}dr dz, \\ &= 4\pi r_{CO}^2 z_{CO} SCO(0). \end{aligned} \quad (12)$$

To compute the total CO flux of the galaxy, we first compute the flux detected in the central beam. We do so in the referential of the observer defined by the orthogonal axes x' , y' , and z' , where the last is the coordinate along the line of sight (Fig. 3). The referential of the observer corresponds to the referential of the galaxy rotated by angle i . We obtain the following equation in cartesian coordinates:

$$(10) \quad SCO_{3D}(CB) = 4SCO(0) \int_{-\infty}^{\infty} \int_0^{\infty} \int_0^{\infty} \exp\left[-4\ln(2) \frac{x'^2 + y'^2}{\theta^2} - \frac{\sqrt{x'^2 + (y' \cos(i) - z' \sin(i))^2}}{r_{CO}} - \frac{|y' \sin(i) + z' \cos(i)|}{z_{CO}}\right] dx' dy' dz' \quad (13)$$

Mapped CO observations of edge-on galaxies are needed to estimate the typical scale height of the CO disc in spirals. NGC 891 is the only edge-on galaxy fully mapped in the $^{12}\text{CO}(1-0)$

line (Scoville et al. 1993; Yim et al. 2011). The most recent BIMA-SONG observations of this object have revealed that the scale height of the CO disc is $z_{\text{CO}} \approx 0.185$ kpc (Yim et al. 2011⁷) or, equivalently, $z_{\text{CO}}/r_{25} \sim 1/101$. Previous observations of the same galaxy have given a z -scale ranging from 0.160 kpc in the nucleus to $z_{\text{CO}} = 0.276$ kpc at the edge (Scoville et al. 1993). To check whether these values of z_{CO} are representative of normal, spiral galaxies, we compared them to the typical scale height of the dust component of other edge-on galaxies. Indeed, given the tight correlation between dust and molecular gas, we can reasonably assume that the thickness of the dusty disc is comparable to that of the molecular gas. The scale height of the dust disc can be measured using either far-infrared (dust in emission) or optical (dust in absorption) images. From the analysis of the *Herschel*/SPIRE images of the same galaxy, Bianchi & Xilouris (2011) have determined that $z_{\text{dust}} = 0.200$ kpc, consistently with $z_{\text{CO}} \approx 0.185$ kpc determined by Yim et al. (2011). Using energy transfer models adapted to reproduce the far-infrared emission observed by *Herschel* of the edge-on galaxy NGC 4565, De Looze et al. (2012) derive $z_{\text{dust}} = 2.5$ arcsec, corresponding to $z_{\text{dust}}/r_{25} \sim 1/194$. The analysis of the optical images of seven nearby edge-on galaxies done by Xilouris et al. (1997, 1999) gives values of z_{dust}/r_{25} ranging from 1/50 to 1/184, as summarised in Table 6. The mean value determined from all these data is $z_{\text{dust}}/r_{25} \approx 1/99$, consistent with $z_{\text{CO}}/r_{25} \sim 1/101$ determined by Yim et al. (2011) in NGC 891. A similar value ($z_{\text{dust}}/r_{25} = 1/108$) has been also obtained from the direct analysis of seven edge-on galaxies observed by *Herschel* (Verstappen et al. 2013). Since $r_{24.5}(\text{g}) \approx r_{25}(\text{B})$, we assume $z_{\text{CO}}/r_{25}(\text{B}) = z_{\text{CO}}/r_{24.5}(\text{g}) = 1/100$.

To understand which among these three different recipes is considered the most likely to estimate the total CO emission of galaxies, we applied them to all the objects observed by Kuno et al. (2007) for which single-beam observations are available and compared the extrapolated fluxes to those measured using the CO maps.

Figure 4 shows the relationship between the CO fluxes extrapolated from central-beam observations as described in this text and the total CO fluxes given in Kuno et al. (2007) for those galaxies with single-beam observations available in the literature. The comparison uses the extrapolation prescription proposed by Saintonge et al. (2011) (eq. 6, right panels) and the one proposed in this work based on a 3D-distribution of the molecular gas (eq. 11). The extrapolation recipe proposed by Lisenfeld et al. (2011) gives basically the same results as the one proposed in this work, with the exception of edge-on galaxies where it underestimates the total CO flux by a few percent (see Figure 5).

Figure 4 and Table 7 show that both the 2D- (eq. 8) and the 3D- (eq. 11) analytic prescriptions given above are more appropriate than the empirical relation of Saintonge et al. (2011). Indeed this last recipe systematically underestimates the total CO flux whenever the beam size of the telescope is smaller than one fifth of the optical diameter of the target (empty symbols). We have also tested whether the use of a slightly different exponential disc scale lengths in eqs. (8) and (11) gives better agreement between the CO fluxes extrapolated from the central-beam observations and the integrated values of Kuno et al. (2007). Using a higher $r_{\text{CO}}/r_{24.5}$ ratio than the canonical value of 0.2 indicated by Lisenfeld et al. (2011) leads to ratios $SCO_{3D}/SCO_{Kuno} \approx 1$ in those galaxies with $SCO_{Kuno} < 5000$

⁷ The analytic function adopted in this work to reproduce the z -scale distribution of the molecular gas is Gaussian, not exponential, thus not directly comparable to the one adopted in this work.

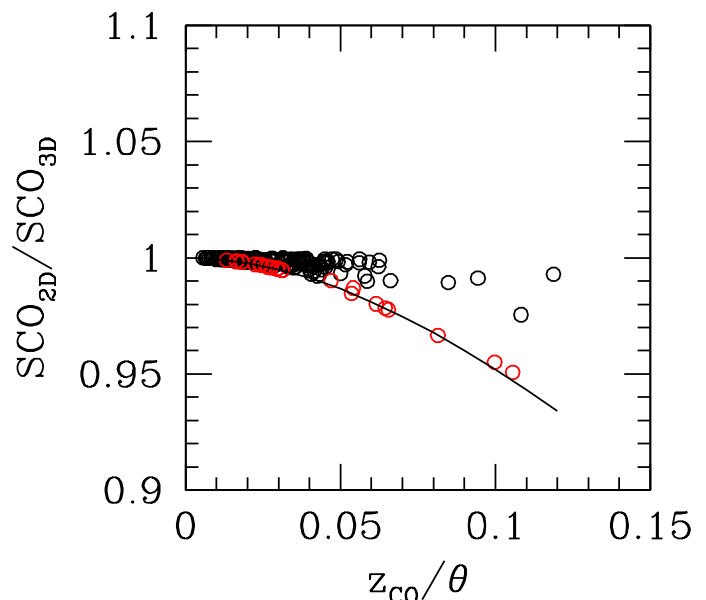


Fig. 5. Relationship between the ratio of the 2D (eq. 9) vs. 3D (eq. 12) aperture corrections SCO_{2D}/SCO_{3D} and the ratio of the molecular gas scale height of the disc to the beam size z_{CO}/θ for the HRS galaxies of the sample. Black open circles are for galaxies with an inclination ≤ 80 deg, red symbols for edge-on systems ($i > 80$ deg). The black solid line gives the relation determined for model edge-on galaxies.

Jy km s^{-1} , but at the same time systematically overestimates $SCO_{3D}(\text{tot})$ in the brightest galaxies. We thus decided to adopt the correction given in eq. (11), keeping $r_{\text{CO}}/r_{24.5} = 0.2$ for all galaxies with only one single-beam observation.

We can also check whether the assumption of a 3D molecular gas disc with $z_{\text{dust}}/r_{24.5} \approx 1/100$ is appropriate for extrapolating single-beam observations of edge-on galaxies. To do that, we extrapolate all single-beam observations of nearby edge-on galaxies with data available in the literature for which accurate estimates of the total CO emission are available from complete or partial CO mapping (see Table 8). Table 8 indicates that, despite the large difference either in the CO fluxes of the central beam observations or in those determined from interferometry, partially mapped or major axis mapped edge-on galaxies, the total CO fluxes determined using the prescriptions given in this work in eq. (8; 2D) or eq. (11; 3D) are close to the broad range of observational data. Equation (8) gives, as expected, slightly lower values (a few per cent) than eq. (11) just because it assumes an infinitely thin disc in the z direction (see Fig. 5). The comparison between aperture-corrected and total CO fluxes given in Table 8 suggests that the 2D extrapolations underestimate the total CO emission more than the 3D one does (but only by a few %). We thus decided to prefer and adopt the 3D recipe given in eq. (11) in this work.

5.3.2. Uncertainties on single beam extrapolated data

By comparing the flux extrapolated from single-beam observations to the integrated value for galaxies in the Kuno et al. (2007) sample, we can quantify the typical uncertainty in the total CO emission due to a combined effect of the uncertainty on the $I(\text{CO})$ measurement and of the aperture correction. Figure 6 shows the relationship between the ratio of the total CO flux as determined from the 3D-extrapolation of the central-beam obser-

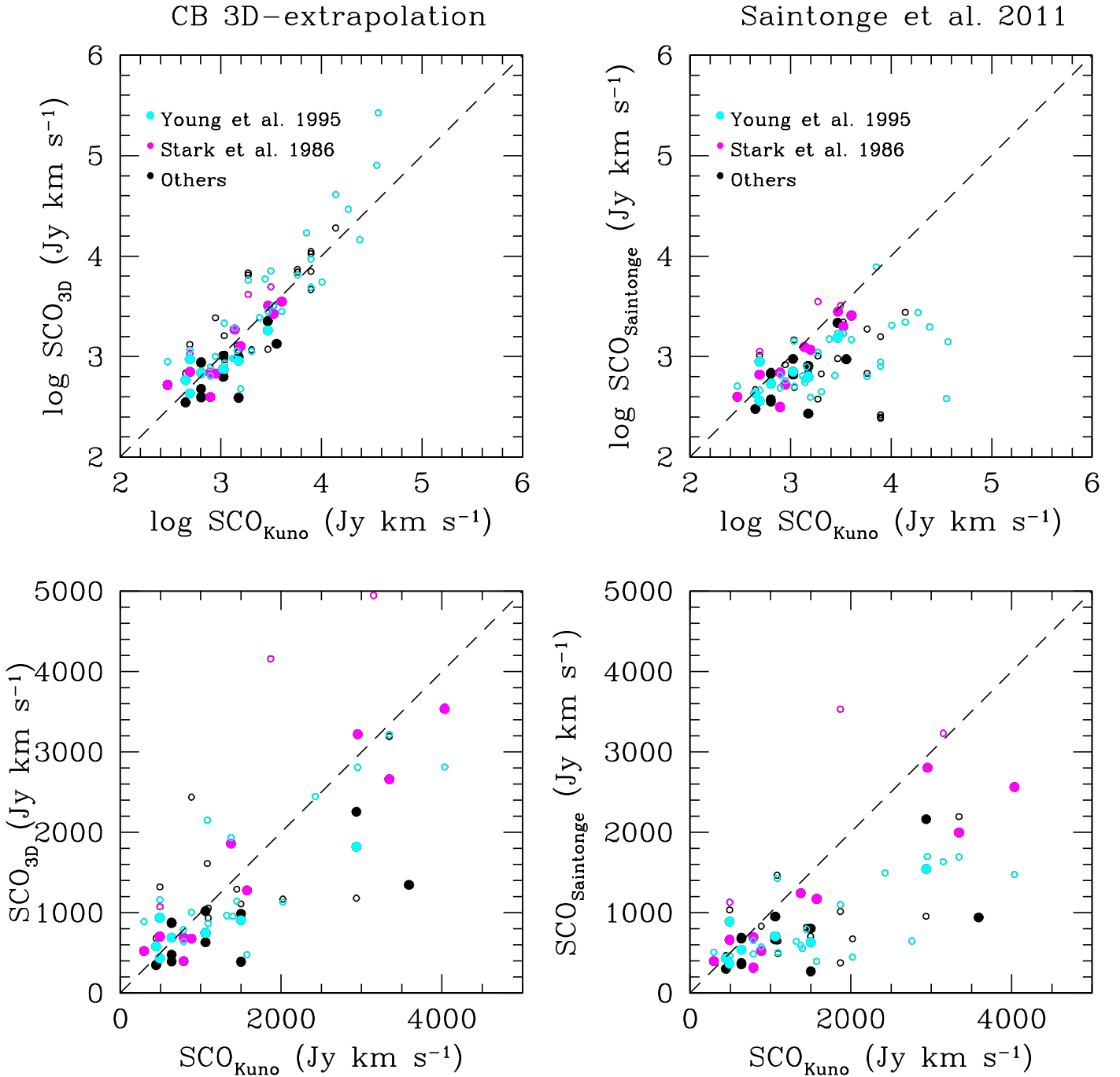


Fig. 4. Comparison of single-beam observations corrected for aperture effects using the prescription based on a 3D-distribution of the molecular gas (eq. 11; left panels) and that of Saintonge et al. (2011) (eq. 6; right panels) on logarithmic (upper panels) and linear (in the range 0-5000 Jy km s $^{-1}$ sampled by the HRS galaxies) scales (lower panels) for galaxies with integrated data from Kuno et al. (2007). Different symbols are used for galaxies observed in the FCRAO survey of Young et al. (1995; cyan), Stark et al. (1986; magenta), and other references (black). Filled dots are for galaxies with $D_{25}(B)/\theta \leq 5$, empty symbols for those objects with $D_{25}(B)/\theta > 5$. The short dashed black line shows the 1:1 relationships.

vation to the total value determined from the maps for galaxies in the Kuno et al. (2007) sample as a function of the surface of the galaxy covered by the telescope beam. Figure 6 shows that whenever the beam covers more than 10 % of the surface of the disc, the mean uncertainty in the total, extrapolated CO flux is of the order of 44 % ($\text{SCO}_{3D}/\text{SCO}_{\text{Kuno}} = 1.01 \pm 0.44$). In the remaining galaxies, where the beam covers less than 10 % of the surface of the galaxy, the mean uncertainty in the total CO

flux estimate is as large as 123 % ($\text{SCO}_{3D}/\text{SCO}_{\text{Kuno}} = 1.46 \pm 1.14$).

5.4. Multiple beam observations

Some HRS galaxies have multiple observations along the major axis. These data can be combined and extrapolated to determine total CO luminosities as done with different techniques found in the literature. Typical examples are the method of Solomon

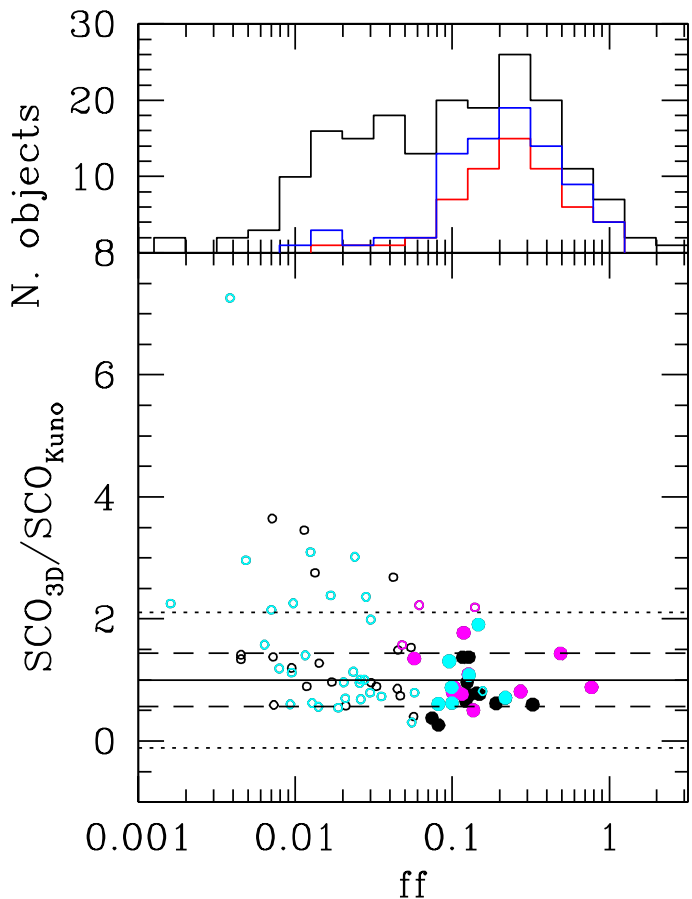


Fig. 6. Relationship between the ratio of the total CO flux as determined from the extrapolation of the central beam observation to the total value determined from the maps for galaxies with integrated data from Kuno et al. (2007) as a function of the filling factor ff , defined as the fraction of the galaxy covered by the central beam (lower panel). Different symbols are used for the galaxies observed in the FCRAO survey of Young et al. (1995; cyan), Stark et al. (1986; magenta) and other references (black). Filled dots are for galaxies with $D_{25}(B)/\theta \leq 5$, empty symbols for those objects with $D_{25}(B)/\theta > 5$. The solid line shows the one ratio, the long dashed lines the typical 1σ uncertainty (44%) for galaxies where the beam size covers more than 10% of the total optical surface of the galaxy, the dotted line 1σ uncertainty (114%) for galaxies where the beam size covers less than or equal to 10% of their surface. The upper panel shows the distribution in the area covered by the central beam for all HRS galaxies with available CO data (black histogram). The blue histogram gives the distribution of all galaxies observed by our team, including previous data (Boselli et al. 1995; 2002, Sauty et al. 2003), while the red one only those observed in this work.

& Sage (1988) or that of the FCRAO team (Young et al. 1995). While the former use different polynomials to combine the emission in the different beams, the latter use the radial variation in the CO emission to deduce a CO profile (exponential, Gaussian, etc.) that is later used to fit and extrapolate the observations. More recently, Saintonge et al. (2011) have proposed a very simple prescription previously determined by simulating the observation through two adjacent beams (one central, the second one beam off-centre) of the Kuno et al. (2007) sample of mapped galaxies. The simulations have been done using beams of different sizes. Multiple beam observations of the HRS galaxies

come mainly from the FCRAO survey of Young et al. (1995), with a few from our own observations. As previously discussed, the FCRAO gives quite accurate extrapolated fluxes for these objects, values that we adopt here. There are, however, a few objects with only two or three detected beams along the major axis, where the extrapolation of the FCRAO is not very accurate. This is probably because, with such a small sampling, it is hard to accurately deduce a radial profile of the CO emission. Eighteen HRS galaxies have two or three detections along the major axis (from the FCRAO survey, 4, and from our own observations presented in this work, 14). It is thus worth understanding whether this radial information can be used to constrain the distribution of the molecular gas along the disc better and thus allow more accurate determination of the total CO emission. To do this we applied an updated version of the technique used by the COLD GASS survey (Saintonge et al. 2011) for galaxies observed in the central position ($SCO(CB)$) and in an adjacent beam ($SCO(adj)$) along the major axis. Following this technique, the total CO flux of the galaxy is given by the relation

$$SCO_{Saintonge_{MB}}(tot) = \frac{SCO(CB)}{1.166 - 3.557 \times f_{OFF} + 3.360 \times f_{OFF}^2}, \quad (14)$$

where f_{OFF} is the ratio of the flux measured in the two beams:

$$f_{OFF} = \frac{SCO(CB)}{SCO(adj)}, \quad (15)$$

where $SCO_{Saintonge_{MB}}(tot)$ stands for the total, extrapolated CO flux determined from multiple beam observations. The variable f_{OFF} gives an empirical estimate of the slope of the radial variation of the CO emission. We then compared the total CO fluxes determined using this relation with the integrated fluxes of Kuno et al. (2007) in Fig. 7. Different and independent sets of data are available from the FCRAO survey of Young et al. (1995), from Stark et al. (1996), from this work, and from several other references in the literature. Table 9 gives for comparison the mean values of the ratio SCO_{3D}/SCO_{Kuno} and $SCO_{Saintonge_{MB}}/SCO_{Kuno}$ for those galaxies in the Kuno et al. (2007) sample with multiple beam observations along the major axis. Figure 7 and Table 9 indicate that the CO fluxes extrapolated using eq. (11), hence not taking the CO observations along the major axis into account, are on average more accurate than those extrapolated using the multi-beam prescription of Saintonge et al. (2011). These last, indeed, generally underestimate the total CO emission of the observed galaxies, while the 3D extrapolation is quite accurate if the size of the galaxy does not exceed about five times the FWHM of the telescope beam. Most of the galaxies of the HRS, and in particular those observed in this work, match this condition. We thus adopted a 3D-extrapolation correction also for these objects with two- or three-beam observations along the major axis.

5.5. The homogenised CO data catalogue

Single-beam observations of HRS galaxies are available from different references in the literature or from our own observations, including those presented in this work. Several objects have multiple, independent observations. Overall there are 344 independent pointings on 225 HRS galaxies. We have collected all these data and listed them in Table 10, arranged as follows

- Column 1: HRS name.
- Column 2: Telescope coded as in Table 4.

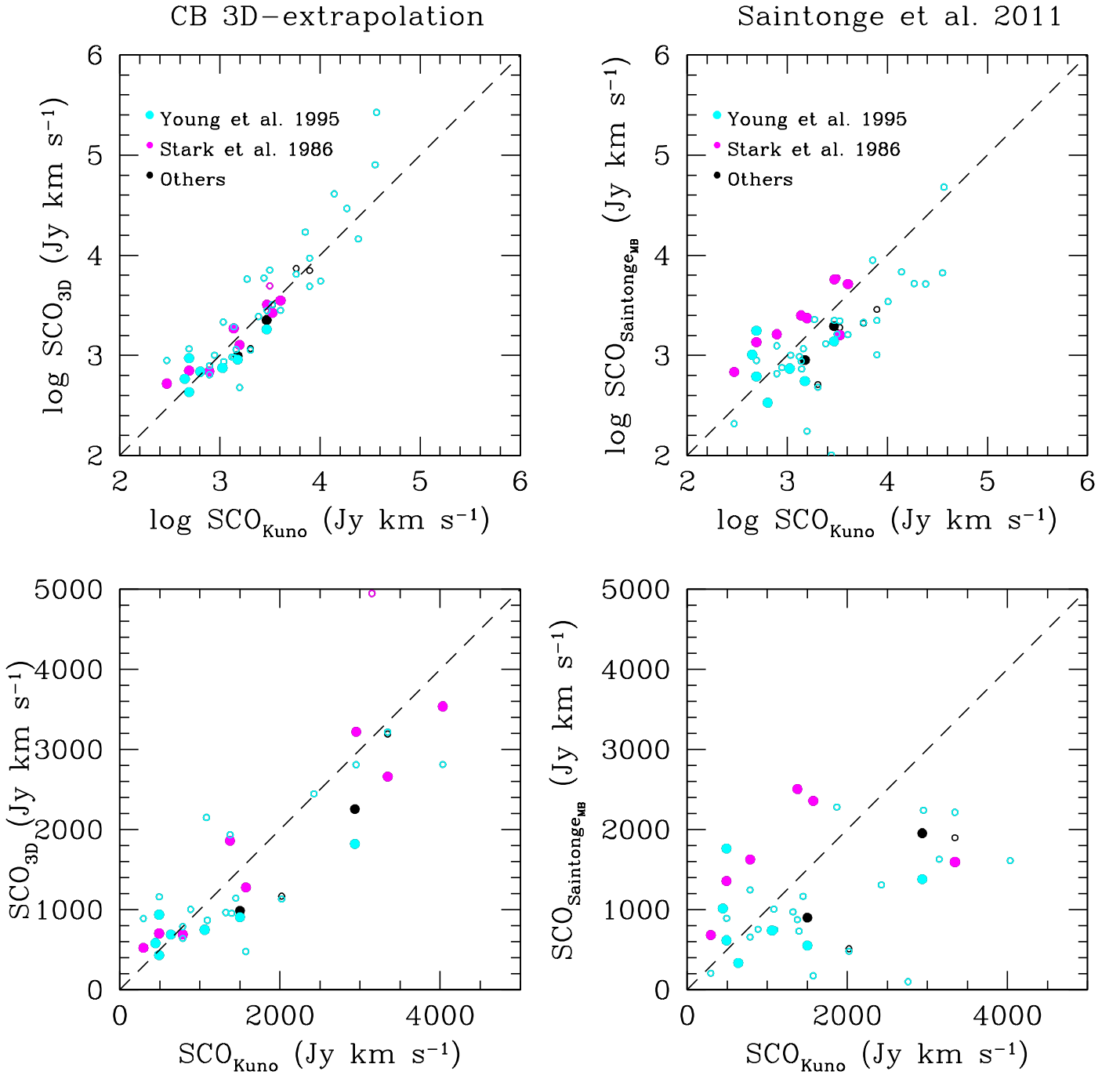


Fig. 7. Comparison of multiple beam observations along the major axis corrected for aperture effects using the prescription based on a 3D-distribution of the molecular gas and assuming only the central beam (eq. 11; left panels) and that of Saintonge et al. (2011) (eq. 13; right panels) on logarithmic (upper panels) and linear (in the range 100-5000 Jy km s^{-1} sampled by the HRS galaxies) scales (lower panels) for galaxies with integrated data from Kuno et al. (2007). Different symbols are used for galaxies observed in the FCRAO survey of Young et al. (1995; cyan), Stark et al. (1986; magenta) and other references (black). Filled dots are for galaxies with $D_{25}/\theta \leq 5$, empty symbols for those objects with $D_{25}/\theta > 5$. The short dashed black line shows the 1:1 relationships.

- Column 3: Number of independent beams for this reference.
- Column 4: Beam size θ , in arcseconds.
- Column 5: Sign for the observation: 1 for detected sources, 0 for undetected objects.
- Column 6: Intensity of the CO line in the central beam, in K km s^{-1} , on the temperature scale (listed in column 9) as indicated in the original paper where the data are presented. No intensities are given for undetected galaxies.
- Column 7: rms the observations, in mK, expressed on the temperature scale as indicated in the original paper where the data are presented (column 9).
- Column 8: Velocity resolution of the smoothed CO spectra, in km s^{-1} .
- Column 9: Temperature scale.
- Column 10: Reference to the data.
- Column 11: Jy/K calibration constant used to transform temperature brightnesses into CO fluxes. These might differ

from those reported in Table 4 if the CO intensities are expressed on other scales than those generally used for the telescope, or if the authors expressly indicate different calibration factors in their original papers.

- Column 12: Extrapolated CO flux SCO_{3D} , or upper limit, in Jy km s^{-1} . CO intensities measured in the central beam, and upper limits are extrapolated to total values using eq. (11). Upper limits in the central beam are determined as described in sect. (3; eq. 1).
- Column 13: Filling factor of the central beam, defined as the ratio of the surface covered by the beam of the telescope to the optical area of the galaxy.
- Column 14: A flag indicates those data used for measuring the total CO emission of HRS galaxies (flag=1) or those not used (flag=0).
- Column 15: Notes to single-beam observations. 1: assumed in T_R^* . 2: transformed from the original table to this scale. 3: partly mapped galaxy, with an equivalent beamsize assumed to be $\theta = 36$ arcsec.

This new set of extrapolated data are then cross-matched with those with available complete mapping (see sect. 5.2) to select the best available data. Total CO emission from mapped galaxies are taken in the order described in sect. 5.2. If no integrated CO data are available, the total SCO emission is taken from extrapolated single-beam observations. When, for the same galaxy, different sets of data are available, we give the mean value determined by combining detections. If detections and undetections are available for the same object, we check that the detections are consistent with the upper limits, and give the detection as final result.

Multiple central-beam observations are useful for inferring a realistic uncertainty on the extrapolated CO emission of the HRS galaxies. For those objects with multiple observations, we quantify the uncertainty by measuring the standard deviation from the mean value determined using only detections. When the uncertainty drops to values lower than 20 %, we assume a conservative error of 20 %. For galaxies with available integrated CO maps from the literature, we assume the standard uncertainties determined as described in sect. 5.2 for the different references. For those with only one central beam detection available, we assume a mean uncertainty determined as described in sect. 5.3 according to the correction factor, namely 44 % if the surface of the beam covers more than 10% of the total surface of the galaxy, 114 % if the sampled area is smaller. Figure 8 shows the ratio of the central beam to the extrapolated CO fluxes, which corresponds to the aperture correction, as a function of the surface of the galaxy covered by the telescope beam (filling factor ff in Table). Figure 8 shows that most of the galaxies observed in this work or by our team in previous observing runs (Boselli et al. 1995; 2002) have been covered by the beam of the telescope by more than 10 % of their surface, thus have relatively low errors in the extrapolated CO flux.

The final results are given in Table 11, arranged as follows:

- Column 1: HRS name.
- Column 2: Sign for the observation: 1 for detected sources, 0 for undetected objects.
- Column 3: SCO flux, in Jy km s^{-1} .
- Column 4: Error on the SCO flux, in Jy km s^{-1} .
- Column 5: Signal-to-noise S/N , defined as the ratio of the total CO flux to the uncertainty in the CO line, this last de-

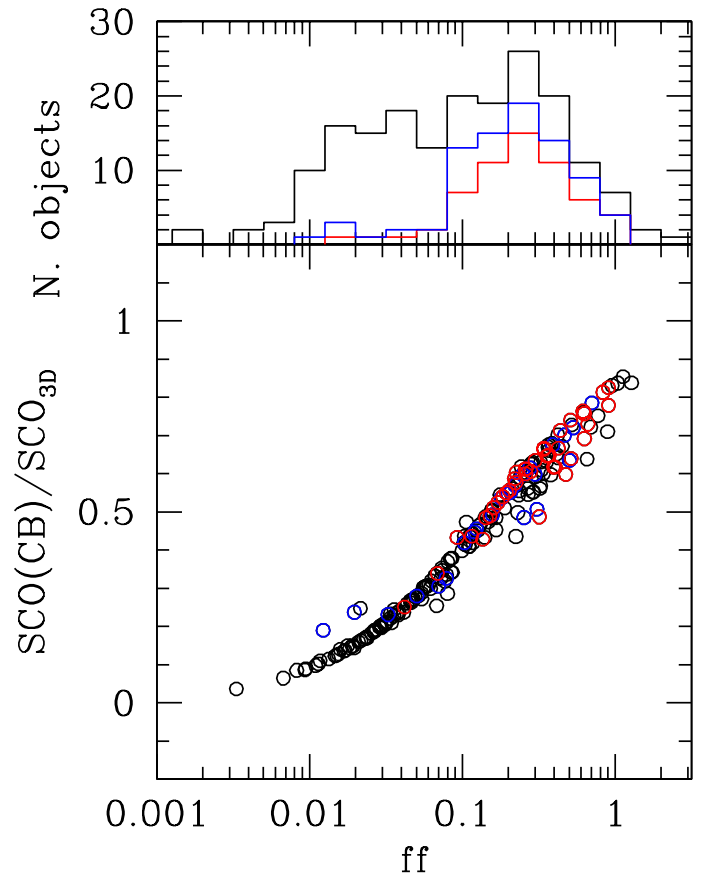


Fig. 8. Relationship between the ratio of the central beam to total extrapolated CO flux ratio (aperture correction) as a function of the filling factor ff , defined as the fraction of the galaxy covered by the central beam for all the HRS galaxies with available single-beam observations (lower panel). Red symbols are for those galaxies observed in this work, blue symbols for other objects observed by our team in previous surveys, while the remaining black circles those with data available in the literature. The upper panel shows the distribution in the filling factor for all the HRS galaxies observed in CO. The blue histogram gives the distribution of all galaxies observed by our team, including previous data (Boselli et al. 1995; 2002, Sauty et al. 2003), while the red one only those observed in this work.

finned as in Column 9 of Table 2. The S/N is given only for galaxies with single-beam observations.

- Column 6: Filling factor ff , defined as the ratio of the surface covered by the beam of the telescope to the optical area of the galaxy. $ff = Int$ indicates galaxies with CO integrated maps, $ff = MA$, those objects mapped along the major axis with more than three detected beams (from the FCRAO survey).
- Column 7: Logarithm of the molecular hydrogen mass, $M(H_2)_c$, determined assuming the standard Galactic conversion factor $X_{CO} = 2.3 \cdot 10^{20} \text{ cm}^{-2}/(\text{K km s}^{-1})$ (Strong et al. 1988). The molecular hydrogen mass of galaxies (in solar units) is determined from the relation:

$$M(H_2) = 3.9 \times 10^{-17} \times X_{CO} \times SCO \times D^2, \quad (16)$$

where D is the distance (in Mpc) given in Table 1.

- Column 8: Logarithm of the molecular hydrogen mass, $M(H_2)_v$, determined by assuming the H-band luminosity dependent conversion factor $\log X_{CO} = -0.38 \times \log L_H + 24.23$,

where X_{CO} is in $\text{cm}^{-2}/(\text{K km s}^{-1})$ and L_{H} in solar units (Boselli et al. 2002).

- Column 8: References to the CO data.

6. H α data

The H α integrated data are available for 315 out of the 322 HRS galaxies. We collected them from a wide variety of references in the literature. Among these, we have favored those coming from the H α survey ALFALFA (Giovanelli et al. 2005) and recently published in Haynes et al. (2011). An important fraction of the HRS galaxies is not observable from Arecibo. For these galaxies, we preferred the homogenised data of Springob et al. (2005), then those available in the literature by choosing those with the highest S/N , lower rms, or with available spectra in the published papers. The H α data for the HRS are given in Table 12, arranged as follows

- Column 1: HRS name.
- Column 2: Sign for the observation: 1 for detected sources, 0 for undetected objects.
- Column 3: rms, in mJy. Not all references in the literature give this entity, thus the rms is available only for a (large) portion of the HRS galaxies.
- Column 4: H α flux SHI , in Jy km s^{-1} . For undetected galaxies, the SHI is an upper limit to the H α flux, defined as

$$SHI = 5 \times rms \times WHI_{exp}, \quad (17)$$

where $WHI_{exp} = 300 \text{ km s}^{-1}$ is the expected H α line width of the observed galaxy.

- Column 5: Logarithm of the H α mass, in M_{\odot} , determined from the relation:

$$M(HI) = 2.356 \times 10^5 \times D^2 \times SHI, \quad (18)$$

where the distance D , expressed in Mpc, is taken from Table 1. The typical uncertainty on the H α mass is $\approx 15\%$.

- Column 6: H α line width WHI measured at 50 % of the peak flux, in km s^{-1} , corrected for instrumental broadening and cosmological redshift as in Catinella et al. (2012). Observed WHI_o are corrected following the relation:

$$WHI = \frac{WHI_o - \Delta s}{1 + z}, \quad (19)$$

where the broadening correction Δs is given by

$$\Delta s = 2 \times \delta V_{HI} \times 0.25, \quad (20)$$

where δV_{HI} is the velocity resolution. The ALFALFA data have been corrected using a different prescription. To have homogenised data, we removed the ALFALFA correction and applied consistently the correction given in eq. 18-19. For some galaxies, the data presented in the original papers cannot be homogeneously corrected using this prescription (line width measured not at 50 % of the intensity peak, lack of any information on the velocity resolution in the data). For these galaxies, we report the value given in the literature, but not corrected for broadening and cosmological redshift. These galaxies can be recognised by the flag given in column 8.

- Column 7: H α -deficiency parameter ($HI - def$), defined as the difference in logarithmic scale between the expected and the observed H α mass of a galaxy of given angular size and morphological type (Haynes & Giovanelli 1984). The H α -deficiency for all the HRS galaxies is determined using the recent calibration of Boselli & Gavazzi (2009).

- Column 8: Flag for the WHI line width measurement: "1" corrected for broadening and cosmological redshift; "2" uncorrected values.

- Column 9: Reference to the H α data.

7. Conclusion

We have presented new $^{12}\text{CO}(1-0)$ observations of 59 late-type galaxies of the *Herschel* Reference Survey done with the 12-metre Kitt Peak radiotelescope. By comparing the total CO emission of fully mapped nearby galaxies, including edge-on systems, to CO fluxes corrected for aperture effects using different prescriptions developed in this work or proposed in the literature, we identified the most accurate recipe for extrapolating central single-beam observations of extended galaxies. The central-beam observation was corrected for the Gaussian shape of the beam and extrapolated assuming a 3D exponential distribution of the molecular gas. The typical scale length of the CO emitting disc is $r_{\text{CO}} = 0.2 r_{24.5}$, where $r_{24.5}$ is the optical, g - (or B -band) isophotal radius at the 24.5 mag arcsec $^{-2}$ (25 mag arcsec $^{-2}$), while its scale height is $z_{\text{CO}} = 1/100 r_{24.5}$. This scale height was calibrated on well known nearby edge-on systems and is comparable to the typical scale height of the dusty disc observed either in absorption using optical images or in emission using far-infrared data.

We applied this new recipe to our new CO data and to all the CO data available in the literature to build the most complete set of molecular gas data for the HRS, which is now available for 225 out of the 322 objects composing the sample. We also collected and homogenised H α data from the literature for 315 HRS galaxies. Both H α and CO data are used to estimate the total H α and H $_2$ molecular gas content of the targets. All these data are available on an HRS-dedicated web page on the HeDaM database: <http://hedam.lam.fr/>. These data are used to study the molecular and total gas scaling relations of the HRS galaxies (Paper II) and the effects of the environment on the molecular gas phase by comparing the molecular gas content of isolated and Virgo cluster galaxies of the sample (Paper III).

Acknowledgements. We are extremely grateful to L. Ziurys for the generous time allocation at the 12-metre Kitt Peak radiotelescope, and to the telescope operators for their assistance during the observations. We want to thank M. Fossati for helping us to write some procedures used to reduce the CO data. This research has made use of data from the HRS project. HRS is a Herschel Key Programme utilising guaranteed time from the SPIRE instrument team, ESAC scientists and a mission scientist. The HRS data was accessed through the Herschel Database in Marseille (HeDaM - <http://hedam.lam.fr/>) operated by CeSAM and hosted by the Laboratoire d'Astrophysique de Marseille. We are grateful to the referee, U. Lisenfeld, for the accurate and detailed reviewing and for the constructive comments that significantly helped increase the quality of the manuscript. A.B. thanks the ESO visiting programme committee for inviting him at the Garching headquarters for a two-month stay.

References

- Albrecht M., Krugel E., Chini R., 2007, *A&A*, 462, 575
- Bell, T., Viti, S., Williams, D., 2007, *MNRAS*, 378, 983
- Bicay, M., Giovanelli, R., 1986, *AJ*, 91, 732
- Bicay, M., Giovanelli, R., 1987, *AJ*, 93, 1326
- Böker T., Lisenfeld U., Schinnerer E., 2003, *A&A*, 406, 87
- Bolatto, A., Leroy, A., Rosolowsky, E., Walter, F., Blitz, L., 2008, *ApJ*, 686, 948
- Bolatto, A., Wolfire, M., Leroy, A., 2013, *ARA&A*, in press
- Boquien, M., Buat, V., Boselli, A., et al., 2012, *A&A*, 539, 145
- Boquien, M., Boselli, A., Buat, V., et al., 2013, *A&A*, in press
- Boselli, A., 2011, in "A Panchromatic View of Galaxies", Wiley-VCH, Berlin (ISBN-10: 3-527-40991-2)
- Boselli, A., Gavazzi, G., 2006, *PASP*, 118, 517
- Boselli, A., Gavazzi, G., 2009, *A&A*, 508, 201

- Boselli, A., Casoli, F., Lequeux, J., 1995, *A&AS*, 110, 521
- Boselli, A., Gavazzi, G., Lequeux, J., Buat, V., Casoli, F., Dickey, J., Donas, J., 1995, *A&A*, 300, L13
- Boselli, A., Gavazzi, G., Lequeux, J., Buat, V., Casoli, F., Dickey, J., Donas, J., 1997, *A&A*, 327, 522
- Boselli, A., Gavazzi, G., Donas, J., Scodreggio, M., 2001, *AJ*, 121, 753
- Boselli, A., Lequeux, J., Gavazzi, G., 2002, *A&A*, 384, 33
- Boselli, A., Boissier, S., Cortese, L., et al., 2006, *ApJ*, 651, 811
- Boselli, A., Boissier, S., Cortese, L., Gavazzi, G., 2008a, *ApJ*, 674, 742
- Boselli, A., Boissier, S., Cortese, L., Gavazzi, G., 2008b, *A&A*, 489, 1015
- Boselli, A., Boissier, S., Cortese, L., Buat, V., Hughes, T., Gavazzi, G., 2009, *ApJ*, 706, 1527
- Boselli, A., Eales, S., Cortese, L., Bendo, G., Chanial, P., Buat, V., Davies, J., Auld, R., et al., 2010a, *PASP*, 122, 261
- Boselli, A., Ciesla, L., Buat, V., et al., 2010b, *A&A*, 518, L61
- Boselli, A., Boissier, S., Heinis, S., et al., 2011, *A&A*, 528, 107
- Boselli, A., Ciesla, L., Cortese, L., et al., 2012, *A&A*, 540, 54
- Boselli, A., Cortese, L., Boquien, M., Boissier, S., Catinella, B., Lagos, C., Saintonge, A., 2013a, submitted to *A&A* (paper I)
- Boselli, A., Cortese, L., Boquien, M., Boissier, S., Catinella, B., Lagos, C., Saintonge, A., 2013b, submitted to *A&A* (paper II)
- Boselli, A., Hughes, T., Cortese, L., Gavazzi, G., Buat, V., 2013b, *A&A*, 550, 114
- Bottinelli, L., Gougouenheim, L., Paturel, G., 1982, *A&AS*, 47, 171
- Bottinelli, L., Gougouenheim, L., Foque, P., Paturel, G., 1990, *A&AS*, 82, 391
- Braine, J., Combes, F., Casoli, F., et al., 1993, *A&AS*, 97, 887
- Bregman, J., Hogg, D., 1988, *AJ*, 96, 455
- Catinella, B., Kauffmann, G., Schiminovich, D., et al., 2012, *MNRAS*, 420, 1959
- Chamaraux, P., Balkowski, C., Fontanelli, P., 1987, *A&AS*, 69, 263
- Chung, E., Rhee, M., Kim, H., Yun, M., Heyer, M., Young, J., 2009a, *ApJS*, 184, 199
- Chung, A., van Gorkom, J., Kenney, J., Crowl, H., Vollmer, B., 2009b, *AJ*, 138, 1741
- Ciesla, L., Boselli, A., Smith, M., et al., 2012, *A&A*, 543, 161
- Combes, F., Young, L., Bureau, M., 2007, *MNRAS*, 377, 1795
- Cortese, L., Bendo, G., Boselli, A., et al., 2010, *A&A*, 518, L63
- Cortese, L., Catinella, B., Boissier, S., Boselli, A., Heinis, S., 2011, *A&A*, 415, 1797
- Cortese, L., Boissier, S., Boselli, A., et al., 2012a, *A&A*, 544, 101
- Cortese, L., Ciesla, L., Boselli, A., et al., 2012b, *A&A*, 540, 52
- Courtois, H., Tully, B., Fisher, R., et al., 2009, *AJ*, 138, 1938
- Davis, L., Seaquist, E., 1983, *ApJ*, 53, 269
- de Vaucouleurs, G., de Vaucouleurs, A., Corwin, H., Buta, R., Paturel, G., Foque, P., 1991, in "The Third Reference Catalogue of Bright Galaxies", Springer, New York
- Dreyer, J.L.E., 1888, *MmRAS*, 49, 1
- Dreyer, J.L.E., 1908, *MmRAS*, 59, 105
- Dumke, M., Braine, J., Krause, M., Zylka, R., Wielebinski, R., Guélin, M., 1997, *A&A*, 325, 124
- Eales, S., Smith, M., Wilson, C., et al., 2010, *A&A*, 518, L62
- Elfhag T., Booth R., Höglund B., Johansson L., Sandqvist A., 1996, *A&AS*, 115, 439
- Fisher, J., Tully, B., 1981, *ApJS*, 47, 139
- Gavazzi, G., Boselli, A., van Driel, W., O'Neil, K., 2005, *A&A*, 429, 439
- Giovanardi, C., Krumm, N., Salpeter, E., 1983a, *AJ*, 88, 1719
- Giovanardi, C., Helou, G., Salpeter, E., Krumm, N., 1983b, *ApJ*, 267, 35
- Giovanelli, R., Haynes, M., Kent, B., et al., 2005, *AJ*, 130, 2598
- Gomez, H., Baes, M., Cortese, L., et al., 2010, *A&A*, 518, L45
- Gondhalekar P., Johansson L., Brosch N., Glass I., Brinks E., 1998, *A&A*, 335, 152
- Haynes, M., Giovanelli, R., 1984, *AJ*, 89, 758
- Haynes, M., Giovanelli, R., 1986, *ApJ*, 306, 466
- Haynes, M., Giovanelli, R., 1991, *ApJS*, 77, 331
- Haynes, M., Jore, K., Barrett, E., Broelis, A., Murray, B., 2000, *AJ*, 120, 703
- Haynes, M., Giovanelli, R., Martin, A., et al., 2011, *AJ*, 142, 170
- Helfer, T., Thornley, M., Regan, M., et al., 2003, *ApJS*, 145, 259
- Helou, G., Salpeter, E., Giovanardi, C., Krumm, N., 1981, *ApJS*, 46, 267
- Helou, G., Salpeter, E., Terzian, Y., 1982, *AJ*, 87, 1443
- Helou, G., Hoffman, G., Salpeter, E., 1984, *ApJS*, 55, 433
- Hoffman, L., Helou, G., Salpeter, E., Glosson, J., Sandage, A., 1987, *ApJS*, 63, 247
- Hoffman, G., Lewis, B., Helou, G., Salpeter, E., Williams, B., 1989, *ApJS*, 69, 65
- Huchtmeier, W., Seiradakis, J., 1985, *A&A*, 143, 216
- Huchtmeier, W., Richter, O., 1989, in "A General Catalog of H I Observations of Galaxies. The Reference Catalog", ISBN 0-387-96997-7 Springer-Verlag Berlin Heidelberg
- Huchtmeier, W., Krishna, G., Petrosian, A., 2005, *A&A*, 434, 887
- Jackson, J., Snell, R., Ho, P., Barrett, A., 1989, *ApJ*, 337, 680
- Jaffe W., 1987, *A&A*, 171, 378
- Koribalski, B., Staveley-Smith, L., Kilborn, V., et al., 2004, *AJ*, 128, 16
- Krumm, N., Salpeter, E., 1979, *ApJ*, 227, 776
- Kuno, N., Sato, N., Nakanishi, H., et al., 2007, *PASJ*, 59, 117
- Kutner, M., Ulich, B., 1981, *ApJ*, 250, 341
- Lake, G., Schommer, R., 1984, *ApJ*, 280, 107
- Leroy, A., Bolatto, A., Simon, J., Blitz, L., 2005, *ApJ*, 625, 763
- Leroy, A., Bolatto, A., Gordon, K., et al., 2011, *ApJ*, 737, 12
- Lewis, B., 1987, *ApJS*, 63, 515
- Lisenfeld, U., Espada, D., Verdes-Montenegro, L., et al., 2011, *A&A*, 534, 102
- Liszt, H., Pety, J., Lucas, R., 2010, *A&A*, 518, 45
- Lu, N., Hoffman, G., Groff, T., Roos, T., Lamphear, C., 1993, *ApJS*, 88, 383
- Magri, C., 1994, *AJ*, 108, 896
- Narayanan, D., Krumholz, M., Ostriker, E., Hernquist, L., 2012, *MNRAS*, 421, 3127
- Neininger, N., Guélin, M., Garcia-Burillo, S., Zylka, R., Wielebinski, R., 1996, *A&A*, 310, 725
- Noordermeer, E., van der Hulst, J., Sancisi, R., Swaters, R., van Albada, T., 2005, *A&A*, 442, 137
- O'Neil K., 2004, *AJ*, 128, 2080
- Peterson, S., 1979, *ApJS*, 40, 527
- Pohlen, M., Cortese, L., Smith, M., et al., 2010, *A&A*, 518, L72
- Richmond, M., Knapp, G., 1986, *AJ*, 91, 517
- Richter, O., Huchtmeier, W., 1987, *A&AS*, 68, 427
- Sage, L., *A&A*, 1993, 272, 123
- Sage, L., Wrobel, J., 1989, *ApJ*, 344, 204
- Sage, L., Welch, G., Young, L., 2007, *ApJ*, 657, 232
- Sakamoto, S., Handa, T., Sofue, Y., Honma, M., Sorai, K., 1997, *ApJ*, 475, 134
- Saintonge, A., Kauffmann, G., Kramer, C., et al., 2011, *MNRAS*, 415, 32
- Sandstrom, K., Leroy, A., Walter, F., et al., 2013, *ApJ*, in press (astro-ph/1212.1208)
- Sauty S., Casoli F., Boselli A., et al., 2003, *A&A*, 411, 381
- Sauvage, M., Sacchi, N., Bendo, G., et al., 2010, *A&A*, 518, L64
- Schneider, S., Thuan, T., Magnum, J., Miller, J., 1992, *ApJS*, 81, 5
- Scoville, N., Thakkar, D., Carlstrom, J., Sargent, A., 1993, *ApJ*, 404, L59
- Shetty, R., Glover, S., Dullemond, C., Klessen, R., 2011a, *MNRAS*, 412, 1686
- Shetty, R., Glover, S., Dullemond, C., Ostriker, E., Harris, A., Klessen, R., 2011b, *MNRAS*, 415, 3253
- Smith, B., Madden, S., 1997, *AJ*, 114, 138
- Smith, M., Eales, S., Gomez, H., et al., 2012, *ApJ*, 756, 40
- Smoker, J., Davies, R., Axon, D., Hummel, E., 2000, *A&A*, 361, 19
- Sodroski, T., Bennett, C., Boggess, N., et al., 1994, *ApJ*, 428, 638
- Sofue, Y., Nakai, N., 1993, *PASJ*, 45, 139
- Sofue, Y., Nakai, N., 1994, *PASJ*, 46, 147
- Springob, C., Haynes, M., Giovanelli, R., Kent, B., 2005, *ApJS*, 160, 149
- Stark, A., Knapp, G., Bally, J., Wilson, R., Penzias, A., Rowe, H., 1986, *ApJ*, 310, 660
- Staveley-Smith, L., Davies, R., 1988, *MNRAS*, 231, 833
- Strong, A., Bloemen, J., Dame, T., et al., 1988, *ApJ*, 207, 1
- Taylor, R., Davies, J., Auld, R., Minchin, R., 2012, *MNRAS*, 423, 787
- Theureau, G., Bottinelli, L., Coudreau, N., Gougouenheim, L., Hallet, N., Loulergue, M., Paturel, G., Teerikorpi, P., 1998, *A&AS*, 130, 333
- Thronson, H., Tacconi, L., Kenney, J., et al., 1989, *ApJ*, 344, 747
- van Driel, W., Ragaingne, D., Boselli, A., Donas, J., Gavazzi, G., 2000 *A&AS*, 144, 463
- Verstappen, J., Fritz, J., Baes, M., et al., 2013, *A&A*, in press
- Wardle, M., Knapp, G., 1986, *AJ*, 91, 23
- Welch, G., Sage, L., 2003, *ApJ*, 584, 260
- Wilson, T., Rohlf, K., Huttemeister, S., 2009, in "Tools of Radio Astronomy", Springer-Verlag, Berlin (ISBN 978-3-540-85121-9)
- Wong, O., Rayan-Weber, E., Garcia-Appadoo, D., et al., 2006, *MNRAS*, 371, 1855
- Young, J., Scoville, N., 1991, *ARA&A*, 29, 581
- Young, L., Bureau, M., Davies, T., et al., 2011, *MNRAS*, 414, 940
- Young, J., Xie, S., Tacconi, L., et al., 1995, *ApJS*, 98, 219 (FCRAO)

Table 1. Herschel Reference Survey.

HRS	CGCG	VCC	UGC	NGC	IC	RA(2000)	dec	type	D	K _S rot	D _{24,5} (g)	incl	vel	memb	HI	CO
(1)	(2)	(3)	(4)	(5)	(6)	h m s	° ' " . . .	(9)	(10)	(11)	(12)	(13)	(14)	(15)	(16)	(17)
1	123035	-	-	-	-	101759.66	224835.9	Pec	16.79	11.59	0.92	67.09	1175	Leo Cl.	0	0
2	124004	-	5588	-	-	102057.13	252153.4	S?	18.44	11.03	0.73	44.82	1291	Leo Cl.	1	0
3	94026	-	5617	3226	-	102327.01	195354.7	E2:pec;LINER;Sy3	16.70	8.57	3.15	34.97	1169	Leo Cl.	1	1
4	94028	-	5620	3227	-	102330.58	195154.2	SAB(s)pec;Sy1.5	16.40	7.64	4.80	61.37	1148	Leo Cl.	1	1
5	94052	-	-	-	610	102628.37	201341.5	Sc	16.71	9.94	1.96	77.41	1170	Leo Cl.	1	0
6	154016	-	5662	3245A	-	102701.16	283821.9	SB(s)b	18.89	11.83	2.21	90.00	1322	Leo Cl.	1	0
7	154017	-	5663	3245	-	102718.39	283026.6	SA(r)0+?:HII;LINER	18.77	7.86	3.13	55.29	1314	Leo Cl.	1	1
8	154020	-	5685	3254	-	102919.92	292929.2	SA(s)bc;Sy2	19.37	8.80	3.92	70.43	1356	Leo Cl.	1	1
9	154026	-	5731	3277	-	103255.45	283042.2	SA(r)ab;HII	20.21	8.93	2.60	49.22	1415	Leo Cl.	1	1
10	183028	-	5738	-	-	103429.82	351524.4	S?	21.66	11.31	0.92	46.50	1516	Leo Cl.	1	0
11	124038	-	5742	3287	-	103447.31	213854.0	SB(s)d	18.93	9.78	2.40	62.51	1325	Leo Cl.	1	1
12	124041	-	-	-	-	103542.07	260733.7	cl	19.89	11.98	0.74	49.03	1392	Leo Cl.	1	0
13	183030	-	5753	3294	-	103616.25	371928.9	SA(s)c	22.47	8.38	3.59	63.21	1573	Leo Cl.	1	1
14	124045	-	5767	3301	-	103656.04	215255.7	(R')SB(rs)0/a	19.16	8.52	2.80	70.35	1341	Leo Cl.	1	1
15	65087	-	5826	3338	-	104207.54	134449.2	SA(s)c	18.57	8.13	4.82	55.69	1300	Leo Cl.	1	1
16	94116	-	5842	3346	-	104338.91	145218.7	SB(rs)cd	18.00	9.59	2.65	27.27	1260	Leo Cl.	1	1
17	95019	-	5887	3370	-	104704.05	171625.3	SA(s)c	18.30	9.43	2.68	58.49	1281	Leo Cl.	1	1
18	155015	-	5906	3380	-	104812.17	283606.5	(R')SBA?	22.91	9.92	1.51	18.71	1604	Leo Cl.	1	0
19	184016	-	5909	3381	-	104824.82	344241.1	SB pec	23.29	10.32	1.79	21.68	1630	Leo Cl.	1	0
20	184018	-	5931	3395	2613	104950.11	325858.3	SAB(rs)cd pec;	23.10	9.95	2.31	61.85	1617	Leo Cl.	1	1
21	155028	-	5958	-	-	105115.81	275054.9	Sbc	16.89	11.56	1.56	80.13	1182	Leo Cl.	1	0
22	155029	-	5959	3414	-	105116.23	275830.0	S0 pec;LINER	20.20	7.98	3.31	43.72	1414	Leo Cl.	1	1
23	184028	-	5972	3424	-	105146.33	325402.7	SB(s)b?:HII	21.44	9.04	2.91	78.74	1501	Leo Cl.	1	1
24	184029	-	5982	3430	-	105211.41	325701.5	SAB(rs)c	22.64	8.90	3.48	60.53	1585	Leo Cl.	1	1
25	125013	-	5995	3437	-	105235.75	225602.9	SAB(rs)c	18.24	8.88	2.39	68.42	1277	Leo Cl.	1	1
26	184031	-	5990	-	-	105238.34	342859.3	Sab	22.41	11.71	1.26	90.00	1569	Leo Cl.	1	0
27	184034	-	6001	3442	-	105308.11	335437.3	Sa?	24.77	10.90	0.72	29.21	1734	Leo Cl.	1	1
28	155035	-	6023	3451	-	105420.86	271422.9	Sd	19.03	10.23	1.66	60.50	1332	Leo Cl.	1	0
29	95060	-	6026	3454	-	105429.45	172038.3	SB(s)c?	15.73	10.67	2.46	80.08	1101	Leo Cl.	1	0
30	95062	-	6028	3455	-	105431.07	171704.7	(R')SAB(rs)b	15.79	10.39	2.20	61.59	1105	Leo Cl.	1	0
31	267027	-	6024	3448	-	105439.24	541818.8	10	19.63	9.47	2.97	70.30	1374	Ursa Maj. S S	1	1
32	95065	-	6030	3457	-	105448.63	173716.3	S?	16.54	9.64	1.05	18.49	1158	Leo Cl.	1	1
33	95085	-	6077	3485	-	110002.38	145029.7	SB(r)b;	20.46	9.46	2.08	18.49	1432	Leo Cl.	1	1
34	95097	-	6116	3501	-	110247.32	175922.2	Scd	16.14	9.41	3.36	79.98	1130	Leo Cl.	1	1
35	267037	-	6115	3499	-	110311.03	561318.2	10	21.74	10.23	0.83	30.85	1522	Ursa Maj. S S	0	1
36	155049	-	6118	3504	-	110311.21	275821.0	(R)SAB(s)ab;HII	21.94	8.27	2.60	19.92	1536	Leo Cl.	1	1
37	155051	-	6128	3512	-	110402.98	280212.5	SAB(rs)c	19.61	9.65	1.54	28.52	1373	Leo Cl.	1	1
38	38129	-	6167	3526	-	110656.63	071026.1	SAC pec sp	20.27	10.69	2.32	77.41	1419	Leo Cl.	1	1
39	66115	-	6169	-	-	110703.35	120336.2	Sb;	22.24	11.13	1.46	72.78	1557	Leo Cl.	1	0
40	67019	-	6209	3547	-	110955.94	104315.0	Sb;	22.63	10.44	1.62	60.18	1584	Leo Cl.	1	0
41	96011	-	6267	3592	-	111427.25	171536.5	Sc? sp	18.61	10.78	2.06	77.41	1303	Leo Cl.	1	0
42	96013	-	6277	3596	-	111506.21	144713.5	SAB(rs)c	17.04	8.70	2.75	28.52	1193	Leo Cl.	1	1
43	96022	-	6299	3608	-	111658.96	180854.9	E2;LINER;	15.83	8.10	3.21	37.06	1108	Leo Cl.	1	1
44	96026	-	6320	-	-	111817.24	185049.0	S?	16.01	10.99	1.10	18.49	1121	Leo Cl.	1	0
45	291054	-	6330	3619	-	111921.60	574527.8	(R)SA(s)0+;	22.06	8.58	2.79	30.44	1544	Ursa Major Cl.	1	1
46	96029	-	6343	3626	-	112003.80	182124.5	(R)SA(rs)0+	21.34	8.16	2.92	48.89	1494	Leo Cl.	1	1
47	156064	-	6352	3629	-	112031.82	265748.2	SA(s)cd;	21.53	10.50	1.90	39.89	1507	Leo Cl.	1	0
48	268021	-	6360	3631	-	112102.85	531011.0	SA(s)c	16.50	7.99	4.16	25.99	1155	Ursa Major Cl.	1	1
49	39130	-	6368	3640	-	112106.85	031405.4	E3	17.87	7.52	3.96	30.44	1251	Leo Cl.	1	1

Continued on next page...

Table 1. Herschel Reference Survey.

HRS	CGCG	VCC	UGC	NGC	IC	RA(2000) h m s	dec ° ' "	type	D Mpc	K _S rot mag	D _{24,5} (g)	incl deg	vel km s ⁻¹	memb	HI	CO
(1)	(2)	(3)	(4)	(5)	(6)	(7)	(8)	(9)	(10)	(11)	(12)	(13)	(14)	(15)	(16)	(17)
50	96037	-	6396	3655	-	112254.62	163524.5	SA(s)c;:HII	21.43	8.83	1.95	49.05	1500	Leo Cl.	1	1
51	96038	-	6405	3659	-	112345.49	174906.8	SB(s)m;?	18.56	10.28	1.71	53.52	1299	Leo Cl.	1	0
52	268030	-	6406	3657	-	112355.57	52515.5	SAB(rs)c pec	17.20	10.29	1.20	31.98	1204	Ursa Major Cl.	1	0
53	67071	-	6420	3666	-	112426.07	112032.0	SA(rs)c:	15.14	9.23	3.64	73.54	1060	Leo Cl.	1	1
54	96045	-	6445	3681	-	112629.80	165147.5	SAB(r)bc:LINER	17.77	9.79	2.08	18.38	1244	Leo Cl.	1	1
55	96047	-	6453	3684	-	112711.18	170149.0	SA(rs)bc:HII	16.54	9.28	2.69	43.65	1158	Leo Cl.	1	1
56	291072	-	6458	3683	-	112731.85	565237.4	SB(s)c?;HII	24.40	8.67	2.10	60.53	1708	Ursa Major Cl.	1	1
57	96049	-	6460	3686	-	112743.95	171326.8	SB(s)bc	16.51	8.49	3.12	40.12	1156	Leo Cl.	1	1
58	96050	-	6464	3691	-	112809.41	165513.7	SB?	15.24	10.51	1.43	43.09	1067	Leo Cl.	1	0
59	67084	-	6474	3692	-	112824.01	092427.5	Sb;LINER;HII	24.53	9.52	3.11	82.22	1717	Leo Cl.	1	1
60	268051	-	6547	3729	-	113349.34	530731.8	SB(r)a pec	15.14	8.73	2.80	47.21	991	Ursa Major Cl.	1	1
61	292009	-	6575	-	-	113626.47	581129.0	Sed;HII	17.39	11.40	1.73	72.21	1217	Ursa Major Cl.	1	0
62	186012	-	6577	3755	-	113633.37	362437.2	SAB(rs)c pec	22.44	10.60	3.29	70.35	1571	Ursa Major Cl.	1	0
63	268063	-	6579	3756	-	113648.02	541736.8	SAB(rs)bc	18.41	8.78	3.81	61.00	1289	Ursa Maj. S S	1	1
64	292017	-	6629	3795	-	114006.84	583647.2	Sc;HII	17.33	10.64	1.89	72.27	1213	Ursa Major Cl.	1	0
65	292019	-	6640	3794	-	114053.42	561207.3	SAB(s)d	19.76	11.60	2.27	57.07	1383	Ursa Major Cl.	1	0
66	186024	-	6651	3813	-	114118.65	363248.3	SA(rs)b:	20.97	8.86	2.57	65.10	1468	Ursa Maj. S S	1	0
67	268076	-	6706	-	-	114414.83	550205.9	SB(s)m:	20.51	11.28	2.01	50.56	1436	Ursa Major Cl.	1	0
68	186045	-	-	-	-	114625.96	345109.2	S?	20.17	11.44	0.53	18.49	1412	Ursa Maj. S S	1	0
69	268088	-	6787	3898	-	114915.37	560503.7	SA(s)ab;LINE;HII	16.73	7.66	4.12	61.76	1171	Ursa Major Cl.	1	1
70	-	-	-	-	2969	115231.27	-035220.1	SB(r)bc?;HII	23.10	11.15	1.27	50.90	1617	Crater Cl.	1	0
71	292042	-	6860	3945	-	115313.73	604032.0	SB(rs)0+;LINER	17.99	7.53	4.84	56.83	1259	Ursa Major Cl.	0	1
72	-	-	-	3952	2972	115340.63	-035947.5	IBm; sp;HII	22.53	11.01	1.58	59.15	1577	Crater Cl.	1	0
73	269013	-	6870	3953	-	115348.92	521936.4	SB(r)bc;HII/LINER	15.00	7.05	6.19	61.69	1050	Ursa Major Cl.	1	1
74	269019	-	6918	3982	-	115628.10	550730.6	SAB(r)b;HII/LINER	15.83	8.85	1.94	34.51	1108	Ursa Major Cl.	1	1
75	269020	-	6919	-	-	115637.51	553759.5	Sdm:	18.33	11.56	1.33	71.57	1283	Ursa Major Cl.	1	0
76	269022	-	6923	-	-	115649.43	530937.3	Im:	15.27	11.32	1.94	67.09	1069	Ursa Major Cl.	1	0
77	13033	-	6993	4030	-	120023.64	-010600.0	SA(s)bc;HII	20.83	7.33	3.86	40.12	1458	Crater Cl.	1	1
78	98019	-	6995	4032	-	120032.82	200426.0	Im:	18.13	10.45	1.63	33.05	1269	Coma I Cl.	1	1
79	69024	-	7001	4019	755	120110.39	140616.2	SBb? sp	21.54	11.33	1.94	84.36	1508	Virgo Out.	1	0
80	69027	-	7002	4037	-	120123.67	132403.7	SB(rs)b:	17.00	10.11	2.57	28.84	932	Virgo Out.	1	0
81	13046	-	7021	4045	-	120242.26	015836.4	SAB(r)a;HII	17.00	8.75	2.73	52.14	2011	Virgo Out.	1	0
82	98037	-	-	-	-	120335.94	160320.0	Sab	17.00	11.19	0.87	56.01	931	Virgo Out.	1	0
83	41031	-	7035	-	-	120340.14	023828.4	SB(r)a;:HII	17.60	11.82	1.38	75.09	1232	Crater Cl.	1	0
84	69036	-	7048	4067	-	120411.55	105115.8	SA(s)b:	17.00	9.90	1.23	39.46	2424	Virgo Out.	1	1
85	243044	-	7095	4100	-	120608.60	493456.3	(R')SA(rs)bc;HII	15.31	8.03	4.88	72.43	1072	Ursa Major Cl.	1	1
86	41041	-	7111	4116	-	120736.82	024132.0	SB(rs)dm	17.00	10.27	3.40	54.24	1309	Ursa Major Cl.	1	1
87	69058	-	7117	4124	-	120809.64	102243.4	SA(r)0+	17.00	8.49	4.19	72.67	1652	Virgo Out.	1	0
88	41042	-	7116	4123	-	120811.11	025241.8	SB(r)c;Sbrst;HII	17.00	8.79	3.57	47.49	1326	Virgo Out.	1	1
89	69088	66	7215	4178	-	121246.45	105157.5	SB(rs)dm;HII	17.00	9.58	5.02	71.57	3679	Virgo N Cl.	1	1
90	13104	-	7214	4179	-	121252.11	011758.9	S0 edge-on	17.00	7.92	4.11	80.56	1279	Virgo N Cl.	1	1
91	98108	92	7231	4192	-	121348.29	145401.2	SAB(s)ab;HII;Sy	17.00	6.89	9.83	90.00	-135	Virgo N Cl.	1	1
92	69101	131	7255	-	3061	121504.44	140144.3	SBc? sp	17.00	10.64	1.91	77.41	2317	Virgo N Cl.	1	0
93	187029	-	7256	4203	-	121505.06	331150.4	SAB0-;:LINER;Sy3	15.59	7.41	3.47	23.75	1091	Coma I Cl.	1	1
94	69104	145	7260	4206	-	121516.81	130126.3	SA(s)bc:	17.00	9.39	4.45	81.71	702	Virgo N Cl.	1	1
95	69107	152	7268	4207	-	121530.50	093505.6	Scd	17.00	9.44	1.71	55.67	592	Virgo N Cl.	1	1
96	69110	157	7275	4212	-	121539.36	135405.4	SAC;:HII	17.00	8.38	2.99	50.58	-83	Virgo N Cl.	1	1
97	69112	167	7284	4216	-	121554.44	130857.8	SAB(s)b;:HII/LINER	17.00	6.52	8.16	81.28	140	Virgo N Cl.	1	1
98	69119	187	7291	4222	-	121622.52	131825.5	Sc	17.00	10.33	3.03	81.47	226	Virgo N Cl.	1	1
99	69123	213	7305	-	3094	121656.00	133731.0	S;BCD	17.00	11.25	0.76	18.49	-162	Virgo N Cl.	1	0

Continued on next page...

Table 1. Herschel Reference Survey.

HRS	CGCG	VCC	UGC	NGC	IC	RA(2000)	dec	type	D	K _S rot	D _{24,5} (g)	incl	vel	memb	HI	CO
(1)	(2)	(3)	(4)	(5)	(6)	h m s	° ' " "	(9)	(10)	(11)	(12)	(13)	(14)	(15)	(16)	(17)
100	98130	226	7315	4237	-	121711.42	151926.3	SAB(rs)bc;HII	17.00	10.03	2.27	49.35	864	Virgo N Cl.	1	1
101	158060	-	7338	4251	-	121808.31	281031.1	SB0? sp	15.30	7.73	3.45	55.29	1014	Coma I Cl.	1	1
102	98144	307	7345	4254	-	121849.63	142459.4	SA(s)c	17.00	6.93	5.64	39.90	2405	Virgo N Cl.	1	1
103	42015	341	7361	4260	-	121922.24	060555.2	SB(s)a	23.00	8.54	3.51	72.67	1935	Virgo B	1	1
104	99015	-	7366	-	-	121928.66	171349.4	Spiral	17.00	11.99	1.05	55.09	925	Virgo Out.	0	0
105	99014	355	7365	4262	-	121930.58	145239.8	SB(s)0?-?	17.00	8.36	1.82	25.22	1369	Virgo A	1	1
106	42032	393	7385	4276	-	122007.50	074131.2	S(s)c II	23.00	10.69	1.62	28.52	2617	Virgo B	1	0
107	42033	404	7387	-	-	122017.35	041205.1	Sd(f)	17.00	10.74	1.87	79.98	1733	Virgo S Cl.	1	0
108	42037	434	-	4287	-	122048.49	053823.5	Sc(f)	23.00	11.02	1.29	71.63	2155	Virgo B	1	0
109	42038	449	7403	4289	-	122102.25	034319.7	SA(s)cd; sp	17.00	9.89	3.13	83.55	2541	Virgo S Cl.	1	0
110	70024	465	7407	4294	-	122117.79	113040.0	SB(s)cd	17.00	9.70	2.59	60.50	357	Virgo N Cl.	1	1
111	99024	483	7412	4298	-	122132.76	143622.2	SA(rs)c	17.00	8.47	3.62	57.10	1136	Virgo A	1	1
112	42044	492	7413	4300	-	122141.47	052305.4	Sa	23.00	9.53	1.81	61.37	2310	Virgo B	1	1
113	99027	497	7418	4302	-	122142.48	143553.9	Sc; sp	17.00	7.83	7.05	81.47	1150	Virgo A	1	1
114	42045	508	7420	4303	-	122154.90	042825.1	SAB(rs)bc;HII;Sy2	17.00	6.84	5.81	26.12	1568	Virgo S Cl.	1	1
115	42047	517	7422	-	-	122201.30	050600.2	SBab(s)	17.00	10.79	1.11	78.46	1864	Virgo S Cl.	1	0
116	70031	522	7432	4305	-	122203.60	124427.3	SA(r)a	17.00	9.83	2.08	58.36	1888	Virgo A	1	0
117	70029	524	7431	4307	-	122205.63	090236.8	Sb	23.00	8.72	3.19	74.94	1035	Virgo B	1	1
118	42053	552	7439	-	-	122227.25	043358.7	SAB(s)cd	17.00	11.20	1.73	45.87	1296	Virgo S Cl.	1	0
119	99029	559	7442	4312	-	122231.36	153216.5	SA(rs)ab; sp	17.00	8.79	3.98	90.00	153	Virgo A	1	1
120	70034	570	7445	4313	-	122238.55	114803.4	SA(rs)ab; sp	17.00	8.47	4.12	90.00	1443	Virgo A	1	1
121	70035	576	7447	4316	-	122242.24	091956.9	Sbc	23.00	9.25	2.50	76.52	1254	Virgo B	1	1
122	99030	596	7450	4321	-	122254.90	154920.6	SAB(s)bc;LINER;HII	17.00	6.59	6.74	23.32	1575	Virgo A	1	1
123	42063	613	7451	4324	-	122306.18	051501.5	SA(r)0+	17.00	8.48	2.60	68.83	1670	Virgo S Cl.	1	1
124	70039	630	7456	4330	-	122317.25	112204.7	Scd	17.00	9.51	4.73	83.55	1564	Virgo A	1	1
125	42068	648	7461	4339	-	122334.94	060454.2	E0;Sy2	23.00	8.54	2.38	25.22	1298	Virgo B	1	1
126	99036	654	7467	4340	-	122335.31	164319.9	SB(r)0+	17.00	8.32	2.93	47.21	930	Virgo A	1	1
127	42070	656	7465	4343	-	122338.70	065714.7	SA(rs)b;	23.00	8.97	2.18	58.74	1014	Virgo B	1	1
128	42072	667	7469	-	3259	122348.52	071112.6	SAB(s)dm?	23.00	11.06	1.79	61.85	1420	Virgo B	1	0
129	99038	685	7473	4350	-	122357.81	164136.1	SA0;LINER	17.00	7.82	2.85	55.29	1241	Virgo A	1	1
130	70045	692	7476	4351	-	122401.56	121218.1	SB(rs)ab pec;	17.00	10.24	2.10	54.09	2324	Virgo A	1	1
131	42079	697	7474	-	3267	122405.53	070228.6	SA(s)cd	23.00	10.95	1.26	18.29	1231	Virgo B	1	0
132	42080	699	7477	-	3268	122407.44	063626.9	Sm/Im	23.00	11.49	1.15	21.68	727	Virgo B	1	0
133	158099	-	7483	4359	-	122411.06	313117.8	SB(rs)c? sp	17.90	10.81	2.62	68.42	1253	Coma I Cl.	1	0
134	70048	713	7482	4356	-	122414.53	083208.9	Sc	23.00	9.69	3.07	76.76	1137	Virgo B	1	0
135	42083	731	7488	4365	-	122428.23	071903.1	E3	23.00	6.64	6.71	48.89	1240	Virgo B	1	1
136	42089	758	7492	4370	-	122454.93	072640.4	Sa	23.00	9.31	1.68	48.89	784	Virgo B	1	1
137	70057	759	7493	4371	-	122455.43	114215.4	SB(r)0+	17.00	7.72	4.44	64.35	943	Virgo A	1	1
138	70058	763	7494	4374	-	122503.78	125313.1	Im	17.00	6.22	7.58	18.71	910	Virgo A	1	1
139	42093	785	7497	4378	-	122518.06	054428.3	E1;LIERG;LINER;Sy2	23.00	11.23	1.54	53.52	1136	Virgo B	1	0
140	42092	785	7497	4378	-	122518.06	045530.2	(R)SA(s)ab;Sy2	17.00	8.51	3.33	39.05	2557	Virgo S Cl.	1	1
141	70061	792	7503	4380	-	122522.17	100100.5	SA(rs)bc;?	23.00	8.33	3.58	59.46	971	Virgo B	1	1
142	99044	801	7507	4383	-	122525.50	162812.0	Sa? pec;HII	17.00	9.49	2.17	56.06	1710	Virgo A	1	1
143	42095	827	7513	-	-	122542.63	071300.1	SB(s)cd; sp	23.00	9.79	2.82	77.33	992	Virgo B	1	0
144	70068	836	7520	4388	-	122546.82	123943.5	SA(s)b; sp;Sy2	17.00	8.00	6.10	79.55	2515	Virgo A	1	1
145	70067	849	7519	4390	-	122550.67	102732.6	Sbc(s) II	23.00	10.33	1.76	46.16	1103	Virgo B	1	1
146	42098	851	7518	-	-	122554.12	073317.4	SAB(s)cd; sp	23.00	10.47	2.27	75.40	1195	Virgo B	1	0
147	42099	859	7522	-	3322	122558.30	032547.3	Sd(f)	17.00	10.18	2.58	80.66	1428	Virgo S Cl.	1	0
148	99049	865	7526	4396	-	122558.80	154017.3	SAd; sp	17.00	10.34	3.49	75.40	-124	Virgo A	1	1
149	70071	873	7528	4402	-	122607.56	130646.0	Sb	17.00	8.49	4.12	75.67	234	Virgo A	1	1

Continued on next page...

Table 1. Herschel Reference Survey.

HRS	CGCG	VCC	UGC	NGC	IC	RA(2000)	dec	type	D	K _S rot	D _{24,5} (g)	incl	vel	memb	HI	CO
(1)	(2)	(3)	(4)	(5)	(6)	h m s	° ' " . . .	(9)	(10)	(11)	(12)	(13)	(14)	(15)	(16)	(17)
150	70072	881	7532	4406	-	122611.74	125646.4	S0(3)E3	17.00	6.10	12.37	54.51	-221	Virgo A	1	1
151	70076	912	7538	4413	-	122632.25	123639.5	(R')SB(rs)ab:	17.00	9.80	2.35	55.05	105	Virgo A	1	1
152	42104	921	7536	4412	-	122636.10	035752.7	SB(r)b? pec:LINER	17.00	9.65	1.63	23.46	2289	Virgo S Cl.	1	1
153	42105	938	7541	4416	-	122646.72	075508.4	SB(rs)cd::Sbrst	17.00	10.97	1.67	27.27	1395	Virgo S Cl.	1	1
154	70082	939	7546	-	-	122647.23	085304.6	SAB(s)cd	23.00	10.71	2.50	18.29	1271	Virgo B	1	1
155	70080	944	7542	4417	-	122650.62	093503.0	SB0: s	23.00	8.17	3.31	68.83	832	Virgo B	1	1
156	99054	958	7551	4419	-	122656.43	150250.7	SB(s)a:LINER:HI	17.00	7.74	3.29	74.27	-273	Virgo A	1	1
157	42106	957	7549	4420	-	122658.48	022939.7	SB(r)bc:	17.00	9.66	2.03	61.69	1695	Virgo S Cl.	1	1
158	42107	971	7556	4423	-	122708.97	055248.6	Sdm:	23.00	11.05	2.71	81.35	1120	Virgo B	1	1
159	70090	979	7561	4424	-	122711.59	092514.0	SB(s)a:HI	23.00	9.09	3.66	62.11	438	Virgo B	1	1
160	42111	1002	7566	4430	-	122726.41	061546.0	SB(rs)b:	23.00	9.35	2.44	27.59	1450	Virgo B	1	1
161	70093	1003	7568	4429	-	122726.56	110627.1	SA(r)0+:LINER:HI	17.00	6.78	6.22	65.09	1130	Virgo A	1	1
162	70098	1030	7575	4435	-	122740.49	130444.2	SB(s)0:LINER:HI	17.00	7.30	3.37	45.49	775	Virgo A	1	1
163	70097	1043	7574	4438	-	122745.59	130031.8	Sb(t)ides):LINER	17.00	7.27	8.68	68.57	70	Virgo A	1	1
164	70099	1047	7581	4440	-	122753.57	121735.6	SB(rs)a	17.00	8.91	1.87	26.61	724	Virgo A	1	1
165	42117	1048	7579	-	-	122755.39	054316.4	Sdm:	23.00	11.58	1.33	74.76	2252	Virgo B	1	0
166	70100	1062	7583	4442	-	122803.89	094813.0	SB(s)0	23.00	7.29	4.32	68.83	517	Virgo B	1	1
167	70104	1086	7587	4445	-	122815.94	092610.7	Sab: sp	23.00	9.83	2.51	90.00	328	Virgo B	1	0
168	70108	1091	7590	-	-	122818.77	084346.1	Sbc	23.00	11.77	1.26	61.00	1119	Virgo B	1	0
169	99063	-	7595	-	3391	122827.28	182455.1	Sed:	24.30	10.45	1.58	44.22	1701	Coma I Cl.	1	0
170	99062	1110	7594	4450	-	122829.63	170505.8	SA(s)ab:LINER:Sy3	17.00	7.05	5.59	56.97	1954	Virgo A	1	1
171	70111	1118	7600	4451	-	122840.55	091532.2	Sbc:	23.00	9.99	1.62	49.35	865	Virgo B	1	1
172	99065	1126	7602	-	-	122843.26	145958.2	SAB:	17.00	9.26	2.57	65.79	1687	Virgo A	1	1
173	42124	1145	7609	4457	-	122859.01	033414.2	(R)SB(rs)l:LINER	17.00	7.78	3.38	18.49	884	Virgo S Cl.	1	1
174	70116	1154	7614	4459	-	122900.03	135842.9	SA(r)0+:HI:LINER	17.00	7.15	4.11	41.90	1210	Virgo A	1	1
175	70115	1158	7613	4461	-	122903.01	131101.5	SB(s)0+:	17.00	8.01	3.31	68.83	1919	Virgo A	1	1
176	70121	1190	7622	4469	-	122928.03	084459.7	SB(s)0a? sp	23.00	8.04	4.20	76.78	508	Virgo B	1	0
177	42132	1205	7627	4470	-	122937.78	074927.1	Sa?:HI	17.00	10.12	1.52	50.53	2339	Virgo S Cl.	1	1
178	42134	1226	7629	4472	-	122946.76	080001.7	E2/S0:Sy2:LINER	17.00	5.40	11.29	40.97	868	Virgo S Cl.	1	1
179	70125	1231	7631	4473	-	122948.87	132545.7	E5	17.00	7.16	4.69	54.51	2236	Virgo A	1	1
180	70129	1253	7638	4477	-	123002.17	133811.2	SB(s)0?:Sy2	17.00	7.35	3.56	23.75	1353	Virgo A	1	1
181	70133	1279	7645	4478	-	123017.42	121942.8	E2	17.00	8.36	1.83	33.89	1370	Virgo A	1	1
182	42139	1290	7647	4480	-	123026.78	041447.3	SAB(s)c	17.00	9.75	2.10	59.17	2438	Virgo S Cl.	1	1
183	70139	1316	7654	4486	-	123049.42	122328.0	E+0-1 pec:NLRG:Sy	17.00	5.81	9.42	41.90	1292	Virgo A	1	1
184	70140	1326	7657	4491	-	123057.13	112900.8	SB(s)a:	17.00	9.88	1.95	61.37	497	Virgo A	1	1
185	42141	1330	7656	4492	-	123059.74	080440.6	SA(s)a?	17.00	9.08	2.48	18.71	1777	Virgo S Cl.	1	1
186	129005	-	7662	4494	-	123124.03	254629.9	E1-2:LINER	18.71	7.00	4.59	30.44	1310	Coma I Cl.	1	1
187	42144	1375	7668	4505	-	123139.21	035622.1	SB(rs)m	17.00	9.56	3.36	38.04	1732	Virgo S Cl.	1	1
188	99075	1379	7669	4498	-	123139.57	165110.1	SAB(s)cd	17.00	9.66	2.86	60.50	1505	Virgo A	1	1
189	99077	1393	7676	-	797	123154.76	150726.2	SB(s)c II.5	17.00	10.80	1.71	50.58	2100	Virgo A	1	0
190	99076	1401	7675	4501	-	123159.22	142513.5	SA(rs)b:HI:Sy2	17.00	6.27	6.78	61.59	2284	Virgo A	1	1
191	99078	1410	7677	4502	-	123203.35	164115.8	Sed:	17.00	11.90	1.14	53.52	1629	Virgo A	1	0
192	70152	1419	7682	4506	-	123210.53	132510.6	Sa pec?	17.00	10.26	1.69	41.90	737	Virgo A	1	0
193	70157	1450	7695	-	3476	123241.88	140301.8	IB(s)lm:	17.00	10.91	2.13	49.80	-173	Virgo A	1	1
194	14063	-	7694	4517	-	123245.59	000654.1	SA(s)cd: sp	17.00	7.33	9.92	82.79	1129	Virgo Out.	1	1
195	99087	1479	7703	4516	-	123307.56	143429.8	SB(rs)ab?	17.00	9.99	1.97	72.01	958	Virgo A	1	1
196	70167	1508	7709	4519	-	123330.25	083917.1	SB(rs)cd	17.00	9.56	2.80	46.67	1212	Virgo S Cl.	1	1
197	70168	1516	7711	4522	-	123339.66	091029.5	SB(s)cd: sp	17.00	10.35	3.62	74.76	2330	Virgo S Cl.	1	1
198	159016	-	7714	4525	-	123351.19	301639.1	Sed:	16.77	9.99	2.31	57.77	1174	Coma I Cl.	1	0
199	99090	1532	7716	-	800	123356.66	152117.4	SB(rs)c pec?	17.00	10.58	1.69	45.89	2335	Virgo A	1	0

Continued on next page...

Table 1. Herschel Reference Survey.

HRS	CGCG	VCC	UGC	NGC	IC	RA(2000)	dec	type	D	K _s rot	D _{24,5} (g)	incl	vel	memb	HI	CO
(1)	(2)	(3)	(4)	(5)	(6)	h m s	° ' " . . .	(9)	(10)	(11)	(12)	(13)	(14)	(15)	(16)	(17)
200	42155	1535	7718	4526	-	123403.03	074156.9	SAB(s)0:	17.00	6.47	7.94	75.93	448	Virgo S Cl.	1	1
201	42156	1540	7721	4527	-	123408.50	023913.7	SAB(s)bc;HII;LINER	17.00	6.93	6.23	71.76	1736	Virgo S Cl.	1	1
202	70173	1549	7728	-	3510	123414.79	110417.7	dE3,N	17.00	11.42	0.81	18.71	1357	Virgo A	1	0
203	42158	1554	7726	4532	-	123419.33	062803.7	IBm;HII	17.00	9.48	2.95	66.45	2021	Virgo S Cl.	1	1
204	42159	1555	7727	4535	-	123420.31	081151.9	SAB(s)c;HII	17.00	7.38	6.76	48.27	1962	Virgo S Cl.	1	1
205	14068	1562	7732	4536	-	123427.13	021116.4	SAB(rs)bc;HII;Sbst	17.00	7.52	7.50	69.76	1807	Virgo S Cl.	1	1
206	42162	1575	7736	-	3521	123439.42	070936.0	SBm pec;BCD	17.00	11.01	1.51	44.22	597	Virgo S Cl.	1	1
207	99093	1588	7742	4540	-	123450.87	153305.2	SAB(rs)cd;LINER;Sy1	17.00	9.24	2.31	30.85	1288	Virgo A	1	1
208	99096	1615	7753	4548	-	123526.43	142946.8	SB(rs);LINER;Sy	17.00	7.12	5.44	40.39	484	Virgo A	1	1
209	-	-	-	4546	-	123529.51	-034735.5	SB(s)0:-	15.00	7.39	3.08	67.33	1050	Virgo Out.	1	1
210	70182	1619	7757	4550	-	123530.61	121315.4	SB0: sp;LINER	17.00	8.69	2.45	70.35	381	Virgo A	1	1
211	70184	1632	7760	4552	-	123539.88	123321.7	E;LINER;HII;Sy2	17.00	6.73	5.60	32.77	322	Virgo A	1	1
212	99098	-	7768	4561	-	123608.14	191921.4	SB(rs)dm	20.14	10.63	1.65	38.04	1410	Coma I Cl.	1	1
213	129010	-	7772	4565	-	123620.78	255915.6	SA(s)b? sp;Sy3;Sy1.9	17.61	6.06	11.97	87.55	1233	Coma I Cl.	1	1
214	70186	1664	7773	4564	-	123626.99	112621.5	E6	17.00	7.94	3.23	65.09	1165	Virgo A	1	1
215	70189	1673	7777	4567	-	123632.71	111528.8	SA(rs)bc	17.00	8.30	3.41	44.50	2277	Virgo A	1	1
216	70188	1676	7776	4568	-	123634.26	111420.0	SA(rs)bc	17.00	7.52	4.97	67.76	2255	Virgo A	1	1
217	70192	1690	7786	4569	-	123649.80	130946.3	SAB(rs)ab;LINER;Sy	17.00	6.58	9.23	90.00	-216	Virgo A	1	1
218	42178	1692	7785	4570	-	123653.40	071448.0	S07/E7	17.00	7.69	3.84	77.67	1730	Virgo S Cl.	1	1
219	70195	1720	7793	4578	-	123730.55	093318.4	SA(r)0:	17.00	8.40	2.93	46.35	2284	Virgo E Cl.	1	1
220	70197	1727	7796	4579	-	123743.52	114905.5	SAB(rs)b;LINER;Sy1.9	17.00	6.49	5.91	39.46	1520	Virgo A	1	1
221	42183	1730	7794	4580	-	123748.40	052206.4	SAB(rs)a pec	17.00	8.77	2.33	44.61	1032	Virgo S Cl.	1	1
222	70199	1757	7803	4584	-	123817.89	130635.5	SAB(s)a?	17.00	10.46	1.55	48.89	1783	Virgo A	1	0
223	42186	1758	7802	4586	-	123820.82	075328.7	Sdm	17.00	11.76	1.84	79.98	1788	Virgo A	1	0
224	42187	1760	7804	4586	-	123828.44	041908.8	SA(s)a: sp	17.00	8.47	3.78	76.78	792	Virgo S Cl.	1	1
225	70202	1778	7817	4591	3611	123904.14	132148.7	S?	17.00	11.42	1.47	63.00	2750	Virgo E Cl.	1	0
226	42191	1780	7821	4592	-	123912.44	060044.3	Sb	17.00	10.24	1.57	59.46	2424	Virgo S Cl.	1	0
227	14091	-	7819	4592	-	123918.74	0-3155.2	SA(s)dm:	15.27	10.22	4.25	73.48	1069	Virgo Out.	1	0
228	-	-	-	-	-	123922.26	-053953.3	Pec	17.13	11.95	0.58	37.09	12000	Background	1	0
229	70204	1809	7825	-	3631	123948.02	125826.1	S?	17.00	11.11	1.09	54.34	2839	Virgo E Cl.	1	1
230	99106	1811	7826	4595	-	123951.91	151752.1	SAB(rs)b?	17.00	10.03	1.95	52.84	632	Virgo E Cl.	1	1
231	70206	1813	7828	4596	-	123955.94	101033.9	SB(r)0+;LINER:	17.00	7.46	4.35	39.05	1834	Virgo E Cl.	1	1
232	70213	1859	7839	4606	-	124057.56	115443.6	SB(s)a:	17.00	9.17	3.01	67.33	1645	Virgo E Cl.	1	0
233	70216	1868	7843	4607	-	124112.41	115311.9	SB6? sp	17.00	9.58	3.01	81.28	2255	Virgo E Cl.	1	1
234	70214	1869	7842	4608	-	124113.29	100920.9	SB(r)0	17.00	8.16	3.40	32.77	1864	Virgo E Cl.	1	1
235	42205	1883	7850	4612	-	124132.76	071853.2	(R)SAB0	17.00	8.56	2.70	38.06	1875	Virgo S Cl.	1	1
236	70223	1903	7858	4621	-	124202.32	113848.9	E5	17.00	6.75	5.26	26.61	444	Virgo E Cl.	1	1
237	42208	1923	7871	4630	-	124231.15	035737.3	IB(s)m?	17.00	9.89	1.97	41.66	742	Virgo S Cl.	1	1
238	14109	-	7869	4629	-	124232.67	-012102.4	SAB(s)m pec	15.94	11.84	1.33	38.97	1116	Virgo Out.	1	0
239	99112	1932	7875	4634	-	124240.96	141745.0	SBcd: sp	17.00	9.25	3.59	79.98	1116	Virgo E Cl.	1	1
240	70229	1938	7880	4638	-	124247.43	112632.9	S0-	17.00	8.21	2.36	44.61	1147	Virgo E Cl.	1	1
241	43002	1939	7878	4636	-	124249.87	024116.0	E/S0/1;LINER;Sy3	17.00	6.42	8.71	48.89	1094	Virgo S Cl.	1	0
242	70230	1943	7884	4639	-	124252.37	131526.9	SAB(rs)bc;Sy1.8	17.00	8.81	2.92	54.63	1048	Virgo E Cl.	1	1
243	15008	-	7895	4643	-	124320.14	015842.1	SB(rs)0/a;LINER	17.00	7.41	3.97	34.97	1346	Virgo Out.	1	1
244	71015	1972	7896	4647	-	124332.45	113457.4	SAB(rs)c	17.00	8.05	4.16	44.24	1422	Virgo E Cl.	1	1
245	71016	1978	7898	4649	-	124340.01	113309.4	E2	17.00	5.74	8.33	37.06	1095	Virgo E Cl.	1	1
246	100004	-	7901	4651	-	124342.63	162336.2	SA(rs)c;LINER	17.00	8.03	3.84	49.05	797	Virgo Out.	1	1
247	71019	1987	7902	4654	-	124356.58	130736.0	SAB(rs)cd;HII	17.00	7.74	5.18	54.96	1039	Virgo E Cl.	1	1
248	71023	2000	7914	4660	-	124431.97	111125.9	E5	17.00	8.21	2.19	43.72	1115	Virgo E Cl.	1	1
249	71026	2006	7920	-	3718	124445.99	122105.2	S	17.00	11.91	2.19	72.78	844	Virgo E Cl.	1	0

Continued on next page...

Table 1. Herschel Reference Survey.

HRS	CGCG	VCC	UGC	NGC	IC	RA(2000)	dec	type	D	K_s rot	$D_{24,5}(g)$	incl	vel	memb	HI	CO
(1)	(2)	(3)	(4)	(5)	(6)	h m s	° ' " . . .	(9)	(10)	(11)	(12)	(13)	(14)	(15)	(16)	(17)
250	43018	-	7924	4665	-	124505.96	030320.5	SB(s)0/a	17.00	7.43	3.99	20.52	785	Virgo Out.	1	0
251	15015	-	7926	4666	-	124508.59	-002742.8	SABc::HI;LINER	21.61	7.06	4.93	70.35	1513	Virgo Out.	1	1
252	15016	-	7931	4668	-	124532.14	-003205.0	SB(s);NL;AGN	23.13	10.58	1.57	55.67	1619	Virgo Out.	1	0
253	15019	-	7951	4684	-	124717.52	-024338.6	SB(r)0+;HII	21.29	8.39	2.94	70.35	1490	Virgo Out.	1	1
254	71043	2058	7965	4689	-	124745.56	134546.1	SA(rs)bc	17.00	7.96	4.05	41.02	1620	Virgo E.Cl.	1	1
255	43028	-	7961	4688	-	124746.46	042009.9	SB(s)cd	17.00	11.16	2.31	25.98	984	Virgo Out.	1	1
256	15023	-	7961	4691	-	124813.63	-031957.8	Aa pec;HII	15.99	8.54	3.38	40.02	1119	Virgo Out.	1	1
257	71045	2070	7970	4698	-	124822.92	082914.3	SA(s)ab;Sy2	17.00	7.56	6.03	90.00	1008	Virgo E.Cl.	1	1
258	-	-	-	4697	-	124835.91	-054803.1	Eg;AGN	17.73	6.37	7.93	48.05	1241	Virgo Out.	0	1
259	43034	-	7975	4701	-	124911.56	032319.4	SA(s)cd	17.00	9.77	2.17	38.04	727	Virgo Out.	1	1
260	100011	-	7980	4710	-	124938.96	150955.8	SA(r)0+;? sp;HII	17.00	7.57	4.30	74.27	1129	Virgo Out.	1	1
261	43040	-	7982	-	-	124950.19	025110.4	Sd(f)	16.54	10.17	2.89	79.30	1158	Virgo Out.	1	0
262	43041	-	7985	4713	-	124957.87	051841.1	SAB(rs)cd;LINER	17.00	9.75	2.43	40.78	652	Virgo Out.	1	1
263	129027	-	7989	4725	-	125026.61	253002.7	SAB(r)ab pec;Sy2	17.27	6.17	9.34	51.19	1209	Coma I Cl.	1	1
264	15027	-	7991	-	-	125038.96	012752.3	Sd(f)	18.17	11.61	2.04	79.98	1272	Virgo Out.	1	0
265	-	-	-	4720	-	125042.78	-040921.0	Pec	21.49	10.77	0.77	40.78	1504	Virgo Out.	0	0
266	-	-	-	4731	-	125101.09	-062335.0	SB(s)cd	21.30	9.79	5.96	44.22	1491	Virgo Out.	1	1
267	129028	-	8005	4747	-	125145.96	254638.3	SBcd? pec sp	16.84	10.29	4.12	71.57	1179	Coma I Cl.	1	0
268	71060	-	8007	4746	-	125155.37	120458.9	Sb; sp	17.00	9.50	1.96	69.97	1779	Virgo Out.	1	1
269	71062	2092	8010	4754	-	125217.56	111849.2	SB(r)0+;	17.00	7.41	4.40	61.37	1377	Virgo E.Cl.	1	0
270	15029	-	8009	4753	-	125222.11	-011158.9	10	17.70	6.72	6.92	58.46	1239	Virgo Out.	1	1
271	100015	-	8014	4758	-	125244.04	155055.9	Im;HII	17.00	10.93	3.48	78.64	1240	Virgo Out.	1	0
272	71065	2095	8016	4762	-	125256.05	111350.9	SB(r)0 sp;LINER	17.00	7.30	7.99	85.96	985	Virgo E.Cl.	1	1
273	15031	-	8020	4771	-	125321.27	011609.0	SA d? sp;NL;AGN	17.00	9.01	3.58	76.04	1119	Virgo Out.	1	1
274	15032	-	8021	4772	-	125329.17	021006.0	SA(s)a;LINER;Sy3	17.00	8.36	4.25	61.37	1038	Virgo Out.	1	1
275	-	-	-	4775	-	125345.70	-063719.8	SA(s)d	22.37	9.22	2.06	23.20	1566	Virgo Out.	1	1
276	71068	-	8022	4779	-	125350.86	094235.7	SB(rs)bc;Sbrst	17.00	9.87	1.96	37.30	2832	Virgo Out.	1	1
277	43060	-	-	4791	-	125443.97	080310.7	cl	17.00	11.35	0.71	50.56	2529	Virgo Out.	1	0
278	71071	-	8032	-	-	125444.19	131414.2	S	16.01	10.39	2.46	81.28	1121	Virgo Out.	1	0
279	15037	-	8041	-	-	125512.68	000700.0	SB(s)d	17.00	11.98	3.09	61.18	1321	Virgo Out.	1	0
280	43066	-	8043	4799	-	125515.53	025347.9	S?	17.00	9.89	1.44	63.00	2802	Virgo Out.	1	1
281	43068	-	8045	-	-	125523.62	075434.0	IBm:	17.00	11.82	0.90	18.29	2801	Virgo Out.	1	0
282	43069	-	-	4803	-	125533.67	081425.8	Comp	17.00	10.71	0.89	45.87	2664	Virgo Out.	1	1
283	43071	-	8054	4808	-	125548.94	041814.7	SA(s)cd;HII	17.00	9.04	2.54	65.15	760	Virgo Out.	1	1
284	-	-	-	-	3908	125640.62	-073346.1	SB(s)d?;HII	18.51	9.10	1.79	69.02	1296	Virgo Out.	1	1
285	15049	-	8078	4845	-	125801.19	013433.0	SA(s)ab sp;HII	17.00	7.79	4.65	90.00	1097	Virgo Out.	1	1
286	71092	-	8102	4866	-	125927.14	141015.8	SA(r)0+; sp;LINER	17.00	7.92	4.49	84.22	1986	Virgo Out.	1	1
287	15055	-	8121	4904	-	130058.67	-000138.8	SB(s)cd;Sbrst	17.00	9.50	2.24	45.05	1174	Virgo Out.	1	1
288	-	-	-	4941	-	130413.14	-053305.8	(R)SAB(r)ab;Sy2	15.91	8.22	3.36	81.97	1114	Virgo Out.	1	1
289	-	-	-	4981	-	130848.74	-064639.1	SAB(r)bc;LINER	23.97	8.49	2.60	53.16	1678	Virgo Out.	1	1
290	189037	-	8271	5014	-	131131.16	361654.9	Sa? sp	16.23	10.11	1.52	70.35	1136	Canes Ven. Spur	1	1
291	217031	-	8388	5103	-	132030.08	430502.3	Sab	18.53	9.49	1.56	48.22	1297	Canes Ven. Spur	1	1
292	218010	-	8439	5145	-	132513.92	431602.2	S?;HII;Sbrst	17.50	9.33	1.30	41.31	1225	Canes Ven. Spur	1	1
293	16069	-	8443	5147	-	132619.71	020602.7	SB(s)dm	15.60	9.73	1.97	36.11	1092	Virgo Out.	1	1
294	246017	-	8593	-	902	133601.22	495739.0	Sb	22.97	10.42	2.09	79.55	1608	Canes Ven. Spur	1	0
295	73054	-	8616	5248	-	133732.07	085306.2	(R)SB(rs)bc;Sy2;HII	16.46	7.25	5.50	42.79	1152	Virgo-Libra Cl.	1	1
296	190041	-	8675	5273	-	134208.34	353915.2	SA(s)0;Sy1.9	15.20	8.67	2.43	31.62	1064	Canes Ven. Spur	1	1
297	246023	-	8711	5301	-	134624.61	460626.7	SA(s)bc; sp	21.54	9.11	3.69	76.52	1408	Canes Ven. Spur	1	1
298	218047	-	8725	5303	-	134744.97	381816.4	Pec	20.27	10.23	1.05	49.80	1519	Canes Ven. Spur	1	0
299	45108	-	8727	5300	-	134816.04	035703.1	SAB(r)c	16.73	9.50	3.30	49.82	1171	Virgo-Libra Cl.	1	1

Continued on next page...

Table 1. Herschel Reference Survey.

HRS	CGCG	VCC	UGC	NGC	IC	RA(2000) h m s	dec ° ' ''	type	D Mpc	K _s rot mag	D _{24,5} (g)	incl deg	vel km s ⁻¹	memb	HI	CO
(1)	(2)	(3)	(4)	(5)	(6)	(7)	(8)	(9)	(10)	(11)	(12)	(13)	(14)	(15)	(16)	(17)
300	218058	-	8756	-	-	135035.89	423229.5	Sab	19.34	10.34	1.54	90.00	1354	Canes Ven. Spur	1	0
301	17088	-	8790	5334	4338	135254.46	-010652.7	SB(rs)bc:	19.71	9.94	3.64	45.89	1380	Virgo-Libra Cl.	1	1
302	45137	-	8821	5348	-	135411.27	051338.8	SBbc: sp	20.61	10.87	3.00	82.55	1443	Virgo-Libra Cl.	1	0
303	295024	-	8843	5372	-	135446.01	583959.4	S?	24.53	10.65	0.81	37.55	1717	Canes Ven-Came. Cl.	0	0
304	46001	-	8831	5356	-	135458.46	052001.4	SABbc: sp, HII	19.57	9.64	3.07	75.82	1370	Virgo-Libra Cl.	1	1
305	46003	-	8838	5360	958	135538.75	045906.2	10	16.73	11.15	1.74	66.45	1171	Virgo-Libra Cl.	1	0
306	46007	-	8847	5363	-	135607.21	051517.2	10?	16.23	6.93	5.81	49.03	1136	Virgo-Libra Cl.	1	1
307	46009	-	8853	5364	-	135612.00	050052.1	SA(rs)bc pec; HII	17.74	7.80	6.20	50.13	1242	Virgo-Libra Cl.	1	1
308	46011	-	8857	-	-	135626.61	042348.0	Sb(f)	15.59	11.93	1.02	72.07	1091	Virgo-Libra Cl.	1	0
309	272031	-	9036	5486	-	140724.97	550611.1	SA(s)m:	19.76	11.95	1.63	52.79	1383	Canes Ven-Came. Cl.	1	0
310	47010	-	9172	5560	-	142005.42	035928.4	SB(s)b pec	24.54	9.98	2.51	68.57	1718	Virgo-Libra Cl.	1	1
311	47012	-	9175	5566	-	142019.95	035600.9	SB(r)ab; LINER	21.31	7.39	5.75	90.00	1492	Virgo-Libra Cl.	1	1
312	47020	-	9183	5576	-	142103.68	031615.6	E3	21.17	7.83	3.78	46.35	1482	Virgo-Libra Cl.	1	1
313	47022	-	9187	5577	-	142113.11	032608.8	SA(rs)bc:	21.29	9.75	3.05	75.14	1490	Virgo-Libra Cl.	1	1
314	19012	-	9215	-	-	142327.12	014334.7	SB(s)d	19.84	10.54	2.64	63.18	1389	Virgo-Libra Cl.	1	0
315	220015	-	9242	-	-	142521.02	393222.5	Sc	20.57	11.73	4.07	90.00	1440	Canes Ven. Spur	1	0
316	47063	-	9308	5638	-	142940.39	031400.2	E1	23.94	8.25	2.62	30.44	1845	Virgo-Libra Cl.	1	1
317	47066	-	9311	-	1022	143001.85	034622.3	S?	24.51	11.70	1.22	72.07	1716	Virgo-Libra Cl.	1	0
318	47070	-	9328	5645	-	143039.35	071630.3	SB(s)d	19.57	9.69	2.54	55.67	1370	Virgo-Libra Cl.	1	1
319	75064	-	9353	5669	-	143243.88	095330.5	SAB(rs)cd	19.54	10.35	3.26	42.53	1368	Virgo-Libra Cl.	1	1
320	47090	-	9363	5668	-	143324.34	042701.6	SA(s)d	22.61	11.71	2.85	21.68	1583	Virgo-Libra Cl.	1	1
321	47123	-	9427	5692	-	143818.12	032437.2	S?	22.59	10.54	1.03	48.94	1581	Virgo-Libra Cl.	1	0
322	47127	-	9436	5701	-	143911.06	052148.8	(R')SBa; LINER	21.50	8.14	4.12	18.71	1505	Virgo-Libra Cl.	1	0
323	48004	-	9483	-	1048	144257.88	045324.5	S	23.43	9.55	2.15	72.07	1640	Virgo-Libra Cl.	1	1

Table 2. Results of the CO observations of the HRS galaxies.

HRS	$\Delta(x)$ arcsec	$\Delta(y)$ arcsec	sgn	Run	rms mK	N. scan	$I(\text{CO})$ K km s $^{-1}$	$\Delta I(\text{CO})$ K km s $^{-1}$	Vel km s $^{-1}$	W_{CO} km s $^{-1}$	Peak T K
(1)	(2)	(3)	(4)	(5)	(6)	(7)	(8)	(9)	(10)	(11)	(12)
8	0	0	0	1	3.00	20	1.18	-	-	-	-
9	0	0	1	1	3.00	20	1.79	0.31	1391	167	7.14E-3
11	0	0	0	4	5.00	20	1.16	-	-	-	-
16	0	0	1	1	4.00	30	1.85	0.29	1267	83	1.66E-2
17	0	0	1	2	4.00	20	4.17	0.41	1293	164	1.87E-2
17N	-35	+42	1	2	4.00	20	1.03	0.26	1403	69 ^a	1.10E-2
17S	+35	-42	1	2	3.00	20	0.62	0.16	1166	44 ^a	1.33E-2
31	0	0	0	1	3.00	20	1.17	-	-	-	-
32	0	0	0	4	4.00	20	1.07	-	-	-	-
33	0	0	1	2	4.00	20	1.81	0.27	1440	73	1.82E-2
34	0	0	1	2	3.00	28	1.94	0.27	1107	133	1.00E-2
37	0	0	1	2	3.00	26	2.00	0.29	(1413)	151	9.59E-3
42	0	0	1	2	3.00	8	4.34	0.21	1182	76	4.53E-2
42E	+55	0	1	2	3.00	20	1.69	0.14	1237	33	3.26E-2
42W	-55	0	1	2	3.00	20	1.38	0.19	1150	66	2.65E-2
42N	0	+55	1	1	3.00	20	1.05	0.13	1191	30	1.38E-2
42S	0	-55	1	1	3.00	22	1.41	0.16	1173	48	2.02E-2
48	0	0	1	4	4.00	16	6.22	0.25	1155	62	7.60E-2
53	0	0	1	2	3.00	20	2.64	0.30	1072	160	1.34E-2
53W	-54	+10	1	3	3.00	20	0.56	0.18	1153	58 ^a	9.20E-3
53E	+54	-10	1	3	3.00	20	0.84	0.10	959	18	1.74E-2
54	0	0	1	2	3.00	26	0.81	0.21	1219	79 ^a	7.93E-3
55	0	0	1	1	4.00	16	2.76	0.37	1152	138	1.67E-2
57	0	0	1	2	4.00	20	4.55	0.32	1148	105	3.29E-2
57N	+17	+52	1	2	4.00	12	2.09	0.17	1224	29	4.15E-2
57S	-17	-52	1	2	4.00	12	1.71	0.16	1079	26	4.18E-2
59	0	0	0	4	4.00	22	1.59	-	-	-	-
60	0	0	1	1	3.00	20	4.18	0.29	1059	145	2.23E-2
63	0	0	1	3	3.00	20	2.67	0.24	1268	103	1.63E-2
63N	0	+55	1	3	3.00	14	1.41	0.13	1185	31	2.19E-2
63S	0	-55	1	3	4.00	14	0.79	0.22	1404	47	1.25E-2
66	0	0	1	1	4.00	12	5.97	0.45	1436	200	2.37E-2
69	0	0	0	1	2.00	38	0.85	-	-	-	-
74	0	0	1	1	4.00	12	5.48	0.37	1120	137	3.13E-2
81	0	0	1	2	3.00	14	8.51	0.35	1995	219	3.01E-2
81E	+55	0	1	2	3.00	20	1.44	0.21	1885	80	9.49E-3
81W	-55	0	1	2	3.00	20	0.84	0.15	(2120)	40 ^a	1.44E-2
84	0	0	1	2	3.00	28	1.29	0.39	2416	269 ^a	4.71E-3
85	0	0	1	1	5.00	8	8.29	0.50	1083	160	3.79E-2
85N	-14	+53	1	1	4.00	20	2.28	0.22	1210	50	1.93E-2
85S	+14	-53	1	1	3.00	20	3.30	0.24	941	101	2.72E-2
112	0	0	1	4	3.00	36	0.63	0.16	2374	48 ^a	7.90E-3
117	0	0	1	3	3.00	20	3.27	0.29	1057	148	1.55E-2
117N	+22	+50	1	3	3.00	20	0.43	0.13	1200	31 ^a	0.94E-2
117S	-22	-50	1	3	3.00	20	0.74	0.10	917	18	1.39E-2
120	0	0	1	3	3.00	20	3.41	0.30	1439	160	1.56E-2
120N	-33	+44	1?	3	3.00	20	0.57	0.25	1521	115 ^a	0.47E-2
120S	+33	-44	1?	3	3.00	20	0.60	0.15	1342	42 ^a	0.93E-2
121	0	0	1	1	4.00	20	1.12	0.37	1212	136 ^a	0.89E-2
124	0	0	1	4	4.00	20	1.98	0.36	1550	127	1.25E-2
124E	+48	+25	1	4	4.00	20	0.64	0.20	1661	41 ^a	1.20E-2
124W	-48	-25	1	4	4.00	20	0.90	0.13	1480	18	1.16E-2
136	0	0	0	1	4.00	26	1.37	-	-	-	-
140	0	0	0	1	3.00	16	1.09	-	-	-	-
152	0	0	1	2	4.00	14	1.72	0.21	2297	42	2.16E-2
171	0	0	1	4	4.00	32	1.79	0.30	844	92	9.92E-3
172	0	0	1	2	4.00	16	2.70	0.35	1676	121	1.73E-2
185	0	0	1	2	3.00	20	1.10	0.22	1768	83	1.01E-2
195	0	0	0	4	4.00	20	0.64	-	-	-	-
232	0	0	1	2	3.00	20	1.48	0.22	1637	86	1.27E-2
233	0	0	1	4	4.00	10	4.03	0.36	2262	128	2.48E-2
233N	0	+55	1	4	4.00	26	1.53	0.13	2203	18	9.86E-3
233S	0	-55	1	4	4.00	26	0.71	0.24	2351	55 ^a	1.02E-2
266	0	0	1	4	4.00	32	0.77	0.26	(1464)	68 ^a	8.74E-3
273	0	0	1	3	3.00	20	2.42	0.25	1105	113	1.34E-2
273N	-39	+39	1	3	4.00	20	0.97	0.13	1242	18	1.59E-2
273S	+39	-39	1	3	3.00	20	0.88	0.10	1023	18	1.63E-2
274	0	0	0	1	3.00	36	1.28	-	-	-	-
280	0	0	0	4	5.00	22	1.92	-	-	-	-
284	0	0	1	2	5.00	20	5.07	0.49	1292	153	2.39E-2
287	0	0	1	2	3.00	20	2.24	0.21	1200	80	1.43E-2

Continued on next page...

Table 2 – Continued

HRS	$\Delta(x)$ arcsec	$\Delta(y)$ arcsec	sgn	Run	rms mK	N. scan	$I(\text{CO})$ K km s^{-1}	$\Delta I(\text{CO})$ K km s^{-1}	Vel km s^{-1}	W_{CO} km s^{-1}	Peak T K
(1)	(2)	(3)	(4)	(5)	(6)	(7)	(8)	(9)	(10)	(11)	(12)
288	0	0	1	2	3.00	20	2.05	0.34	1116	206	8.82E-3
289	0	0	1	1	4.00	16	4.01	0.42	1673	177	1.79E-2
291	0	0	0	2	3.00	34	0.59	-	-	-	-
292	0	0	1	2	4.00	10	6.44	0.41	1228	167	3.08E-2
293	0	0	1	2	3.00	24	0.99	0.10	1076	18	9.43E-3
297	0	0	1	3	4.00	16	2.35	0.44	1521	196	1.21E-2
297N	-27	+48	1	3	3.00	16	1.43	0.15	1397	41	1.91E-2
297S	+27	-48	1	3	3.00	20	1.30	0.18	1617	59	1.53E-2
299	0	0	1	2	3.00	20	1.01	0.23	1158	92	6.26E-3
301	0	0	1	4	3.00	40	1.17	0.25	1370	114	7.95E-3
304	0	0	1	2	4.00	24	1.69	0.21	1393	45	1.22E-2
304N	+14	+53	1	3	3.00	20	0.43	0.17	1476	50 ^a	0.84E-2
304S	-14	-53	1	3	3.00	20	0.74	0.10	1257	18	1.47E-2
310	0	0	1	2	3.00	20	2.11	0.23	1696	95	1.23E-2
310E	+54	-10	1	2	4.00	18	0.44	0.16	1830	26 ^a	1.66E-2
310W	-54	+10	1	2	3.00	16	1.67	0.32	1762	183	7.38E-3
311	0	0	1	1	3.00	32	3.64	0.37	1560	236	0.97E-2
313	0	0	1	2	3.00	34	0.77	0.31	1510	168 ^a	(4.24E-3)
318	0	0	0	1	5.00	26	1.33	-	-	-	-
323	0	0	1	1	4.00	32	2.03	0.38	1616	147	0.97E-2

Table 3. Independent observations of HRS 48 (NGC 3631)

Run	Telescope	θ "	Units	$I(\text{CO})$ K km s^{-1}	SCO_{3D} Jy km s^{-1}
2008,1	Kitt Peak	55	T_R^*	6.77 ± 0.30	1003 ± 44
2008,2				7.33 ± 0.24	1086 ± 36
2009				4.90 ± 0.39	726 ± 58
Mean ^a				6.22 ± 0.25	922 ± 37
Elfhag et al. (1998)	Onsala	34	T_{mb}	12.10 ± 1.41	1060 ± 124
Young et al. (1995)	FCRAO	45	T_A^*	4.21 ± 0.49	869 ± 101

Notes: a: determined using the combined spectrum.

Table 4. Main parameters of the different radio telescopes

Telescope	$\theta(^{\circ})$	Units	Jy/K ²
Kitt Peak ¹	55	T_R^*	39
IRAM	21	T_{mb}	4.8
FCRAO	45	T_A^*	42
SEST	43	T_{mb}	19
Onsala	34	T_{mb}	12
BELL	100	T_{mb}	108

Notes: 1: in some references CO fluxes are expressed in T_{mb} scale.

2: conversion between K and Jy (see eq. 8).

Table 5. Best fit to the relations between integrated CO fluxes: $SCO_y = a \times SCO_{Kuno} + b$

SCO_y	a	b	ρ^1	$SCO_{Kuno}/SCO_y(\text{corrected})^2$
SCO_{Helfer}	0.86(± 0.17)	-85.28(± 428.62)	0.90	1.02 \pm 0.18
SCO_{Chung}	0.65(± 0.08)	44.84(± 157.85)	0.93	1.10 \pm 0.43
SCO_{Young}^3	0.71(± 0.07)	183.61(± 140.59)	0.88	1.12 \pm 0.49

Notes: 1: Spearman correlation coefficient.

2: Ratio of the Kuno et al. (2007) to the Helfer et al. (2003), Chung et al. (2009a), and Young et al. (1995) SCO fluxes once these last have been corrected using the relations given in this table. For comparison, $SCO_{Kuno}/SCO_{IRAM} = 0.83 \pm 0.03$ for the two HRS galaxies we observed with the IRAM radio telescope.

3: This relation is not used to correct the Young et al. (1995) data (see text).

Table 6. Disc scale height for edge-on galaxies

Name	D Mpc	r_{25}^a kpc	$incl$ $^\circ$	z_{CO} kpc	r_{dust}^b kpc	z_{dust}^b kpc	Reference
NGC 891	9.5	16.79	88.3	0.160-0.276	7.54	0.200,0.240	1,2,3,4,5
NGC 4013	11.6	7.90	89.6	-	2.60	0.110	4
NGC 4565	16.9	35.17	87.2	-	40.36	0.181	7
NGC 5529	29.6	24.60	87.2	-	7.70	0.370	4
NGC 5907	11.0	18.39	87.2	-	5.30	0.100	4
IC 2531	22.0	21.60	89.6	-	8.43	0.210	4
UGC 1082	37.0	14.38	89.7	-	5.47	0.290	4
UGC 2048	63.0	33.23	89.6	-	16.50	0.500	6

Notes: a : from NED; b : measured from optical images in the i -band. References: 1: Scoville et al. (1993); 2: Yim et al. (2011); 3: Bianchi & Xilouris (2011); 4: Xilouris et al. (1999); 5: Xilouris et al. (1998); 6: Xilouris et al. (1997); 7: De Looze et al. (2012).

Table 7. Comparison between extrapolated single-beam observations and integrated fluxes from Kuno et al. (2007)

Sample	SCO_{3D}/SCO_{Kuno}	SCO_{2D}/SCO_{Kuno}	$SCO_{Saintonge}/SCO_{Kuno}$
All galaxies	1.33 \pm 1.01	1.32 \pm 0.98	0.64 \pm 0.48
All galaxies with $SCO_{Kuno} < 5000 \text{ Jy km s}^{-1}$ & $N.\text{Beam} \leq 5$	0.92 \pm 0.39	0.92 \pm 0.39	0.77 \pm 0.34
All galaxies with $N.\text{Beam} > 5$	1.55 \pm 1.17	1.54 \pm 1.13	0.57 \pm 0.53
All galaxies with $SCO_{Kuno} < 5000 \text{ Jy km s}^{-1}$ & $N.\text{Beam} \leq 5$ & ref FCRAO	1.02 \pm 0.47	1.01 \pm 0.47	0.85 \pm 0.46

Table 8. Total CO emission of edge-on galaxies

Name	$incl$ $^\circ$	$SCO(CB)$ Jy km s^{-1}	Ref	θ "	SCO_{2D} Jy km s^{-1}	SCO_{3D} Jy km s^{-1}	SCO_{Int} Jy km s^{-1}	Ref
NGC 891	88.3	606.5	1	45	3440	3579	5398-7197; 1970; 4570; 5226	4 ^a ; 5 ^b ; 1 ^c ; 2 ^c
		1509.3	2	55	7090	7288		
NGC 4565	87.2	177.6	3	34	1452	1550	1672; 1643	6 ^b ; 7 ^b
NGC 5907	87.2	173.0	1	45	952	985	1750; 725; 1230	8 ^b ; 9 ^b ; 1 ^c
		150.0	3	34	1097	1160		

Notes: a : from interferometric observations; b : from partial mapping along the major and minor axes; c : from mapping along the major axis; References: 1: Young et al. (1995; FCRAO); 2: Sage (1993); 3: Elfhag et al. (1996); 4: Scoville et al. (1993); the flux given in this reference is $5398 \text{ Jy km s}^{-1}$, and is estimated by the authors to represent between 75 and 100% of the total flux of the galaxy; 5: Sakamoto et al. (1997); 6: Neininger et al. (1996); 7: Sofue & Nakai (1994); 8: Dumke et al. (1997); 9: Sofue & Nakai (1993).

Table 9. Comparison between total CO fluxes extrapolated using the 3D aperture correction using only the central beam proposed in this work (eq. 11) and the Saintonge et al. (2011) multiple-beam prescriptions (eq. 13) for galaxies in the Kuno et al. (2007) sample

Sample	SCO_{3D}/SCO_{Kuno}	$SCO_{Saintonge_{MB}}/SCO_{Kuno}$
All galaxies	1.35 ± 1.08	0.54 ± 0.77
All galaxies with $SCO_{Kuno} < 5000 \text{ Jy km s}^{-1}$ & $\text{N.Beam} \leq 5$	1.03 ± 0.40	1.45 ± 0.95
All galaxies with $\text{N.Beam} > 5$	1.50 ± 1.27	0.65 ± 0.47

Table 10. Central beam observations of the HRS.

HRS (1)	Tel (2)	N. beam (3)	θ (4) arcsec	sign (5)	$I(\text{CO})$ (6) K km s^{-1}	rms (7) mK	δV_{CO} (8) km s^{-1}	T scale (9)	Ref (10)	Jy/K (11) Jy K^{-1}	SCO_{3D} (12) Jy km s^{-1}	ff (13)	flag (14)	Notes (15)
3	FCRAO	1	45	0	-	3.00	15.0	T_A^*	3	42	126.29	0.087	1	
3	FCRAO	1	45	0	-	8.00	15.0	T_A^*	1	42	336.78	0.087	1	
3	IRAM	1	22	0	-	3.52	31.0	T_{mb}	23	4.7	57.82	0.021	1	
4	IRAM	1	36	1	54.00	10.00	5.2	T_{mb}	22	4.8	1085.37	0.038	1	
7	IRAM	1	22	0	0.74	3.67	31.0	T_{mb}	23	4.7	37.54	0.029	1	
7	KP12m	1	55	0	-	3.00	30.0	T_R^*	4	39	94.70	0.182	1	
8	KP12m	1	55	0	-	3.00	15.7	T_R^*	5	39	91.43	0.194	1	
9	KP12m	1	55	1	1.79	3.00	15.7	T_R^*	5	39	119.08	0.220	1	
11	KP12m	1	55	0	-	5.00	15.7	T_R^*	5	39	68.49	0.395	1	
13	SEST	1	43	1	5.20	40.00	10.3	T_{mb}	6	19	241.68	0.110	1	
14	IRAM	1	22	0	-	3.57	31.0	T_{mb}	23	4.7	23.44	0.055	1	
15	FCRAO	1	45	1	3.04	2.00	15.0	T_A^*	1	42	443.49	0.054	1	
16	IRAM	1	22	1	3.58	5.00	10.0	T_{mb}	17	4.8	89.65	0.027	1	
16	KP12m	1	55	1	1.85	4.00	15.7	T_R^*	5	39	137.59	0.171	1	
17	KP12m	3	55	1	4.17	4.00	15.7	T_R^*	5	39	268.33	0.281	1	
20	FCRAO	1	45	0	-	23.00	10.0	T_A^*	21	42	338.01	0.279	1	2
20	IRAM	1	36	0	-	20.00	5.2	T_{mb}	22	4.8	28.51	0.179	1	
22	IRAM	1	22	0	-	1.30	30.0	T_{mb}	24	4.7	20.10	0.021	1	
23	IRAM	1	36	0	-	20.00	5.2	T_{mb}	22	4.8	41.80	0.207	1	
24	IRAM	1	36	0	-	89.00	5.2	T_{mb}	22	4.8	261.71	0.076	1	
25	FCRAO	3	45	1	2.24	8.00	15.0	T_A^*	1	42	153.54	0.329	1	
25	IRAM	1	22	1	18.30	5.00	20.0	T_{mb}	7	4.8	261.88	0.079	1	
25	SEST	1	43	1	9.70	5.00	20.0	T_{mb}	7	19	311.17	0.301	1	
27	FCRAO	1	45	0	-	16.10	10.0	T_A^*	21	42	132.38	1.580	1	2
31	KP12m	1	55	0	-	3.00	15.7	T_R^*	5	39	74.77	0.347	1	
32	IRAM	1	22	0	-	3.41	31.0	T_{mb}	23	4.7	12.06	0.165	1	
32	KP12m	1	55	0	-	4.00	15.7	T_R^*	5	39	51.10	1.030	1	
33	KP12m	1	55	1	1.81	4.00	15.7	T_R^*	5	39	115.22	0.260	1	
34	KP12m	1	55	1	1.94	3.00	15.7	T_R^*	5	39	126.54	0.475	1	
35	IRAM	1	22	0	-	3.57	31.0	T_{mb}	23	4.7	9.16	0.291	1	
36	FCRAO	1	45	1	5.24	7.00	10.0	T_A^*	21	42	503.71	0.112	1	2
36	FCRAO	2	45	1	7.55	8.00	15.0	T_A^*	1	42	725.76	0.112	1	
36	SEST	1	43	1	20.30	5.00	20.0	T_{mb}	7	19	922.15	0.102	1	
37	KP12m	1	55	1	2.00	3.00	15.7	T_R^*	5	39	105.39	0.511	1	
38	SEST	3	43	1	1.15	4.80	15.0	T_{mb}	8	19	34.43	0.504	1	
42	KP12m	5	55	1	4.34	3.00	15.7	T_R^*	5	39	331.23	0.161	1	
43	IRAM	1	22	0	-	3.80	30.0	T_{mb}	24	4.7	36.88	0.021	1	
45	IRAM	1	22	0	4.32	3.84	31.0	T_{mb}	23	4.7	48.39	0.025	1	
46	IRAM	1	22	0	7.00	5.25	31.0	T_{mb}	23	4.7	58.25	0.029	1	
48	FCRAO	6	45	1	4.21	8.00	15.0	T_A^*	1	42	659.12	0.046	1	
48	KP12m	1	55	1	6.33	4.67	15.7	T_R^*	5	39	728.40	0.069	1	
48	OSO	1	34	1	12.10	20.00	10.4	T_{mb}	6	12	779.72	0.026	1	
49	IRAM	1	22	0	-	2.85	31.0	T_{mb}	23	4.7	42.14	0.013	1	
50	SEST	1	43	1	9.90	5.00	20.0	T_{mb}	7	19	311.88	0.260	1	
53	KP12m	3	55	1	2.64	3.00	15.7	T_R^*	5	39	188.85	0.270	1	
54	KP12m	1	55	1	0.81	3.00	15.7	T_R^*	5	39	51.57	0.260	1	
55	KP12m	3	55	1	2.76	4.00	15.7	T_R^*	5	39	193.68	0.203	1	
56	FCRAO	3	45	1	6.97	6.00	15.0	T_A^*	1	42	464.97	0.325	1	
57	KP12m	3	55	1	4.55	4.00	15.7	T_R^*	5	39	366.58	0.143	1	
59	KP12m	1	55	0	-	4.00	15.7	T_R^*	5	39	98.95	0.506	1	
60	KP12m	3	55	1	4.18	3.00	15.7	T_R^*	5	39	296.57	0.195	1	
63	KP12m	3	55	1	2.67	3.00	15.7	T_R^*	5	39	220.01	0.147	1	
66	KP12m	1	55	1	5.97	4.00	15.7	T_R^*	5	39	360.55	0.359	1	
66	OSO	1	34	0	-	40.00	10.4	T_{mb}	6	12	286.42	0.137	1	
69	KP12m	1	55	0	-	2.00	15.7	T_R^*	5	39	75.10	0.107	1	
71	IRAM	1	22	0	-	4.07	31.0	T_{mb}	23	4.7	76.38	0.013	1	
73	FCRAO	8	45	1	4.13	6.00	15.0	T_A^*	1	42	751.42	0.038	1	
74	KP12m	1	55	1	5.48	4.00	15.7	T_R^*	5	39	320.81	0.343	1	
77	FCRAO	5	45	1	6.46	8.00	15.0	T_A^*	1	42	847.34	0.063	1	
78	BELL	1	100	0	-	10.00	5.3	T_{mb}	2	108	148.20	1.585	1	
78	FCRAO	1	45	0	-	8.00	15.0	T_A^*	1	42	105.46	0.321	1	
81	KP12m	3	55	1	8.51	3.00	15.7	T_R^*	5	39	575.63	0.224	1	
84	KP12m	1	55	1	1.29	3.00	15.7	T_R^*	5	39	60.99	0.907	1	
85	KP12m	3	55	1	8.29	3.00	15.7	T_R^*	5	39	754.29	0.136	1	
86	BELL	1	100	1	0.93	10.00	5.3	T_{mb}	2	108	138.27	0.520	1	
88	OSO	1	34	1	4.50	8.60	20.0	T_{mb}	9	12	200.49	0.047	1	
89	BELL	1	100	1	0.88	10.00	5.3	T_{mb}	2	108	148.24	0.425	1	
89	FCRAO	1	45	1	0.90	8.00	12.0	T_A^*	1	42	110.66	0.086	1	
89	SEST	1	43	1	0.90	7.00	18.0	T_{mb}	10	19	52.45	0.079	1	
90	IRAM	1	22	0	-	3.95	31.0	T_{mb}	23	4.7	38.09	0.036	1	

Continued on next page...

Table 10 – Continued

HRS (1)	Tel (2)	N. beam (3)	θ (4) arcsec	sign (5)	$I(\text{CO})$ (6) K km s^{-1}	rms (7) mK	δV_{CO} (8) km s^{-1}	T scale (9)	Ref (10)	Jy/K (11) Jy K^{-1}	SCO_3D (12) Jy km s^{-1}	ff (13)	flag (14)	Notes (15)
91	BELL	1	100	1	4.13	10.00	5.3	T_{mb}	2	108	984.56	0.167	1	
91	FCRAO	3	45	1	4.90	7.00	12.0	T_A^*	1	42	881.33	0.034	1	
91	KP12m	1	55	1	7.66	9.00	21.0	T_R^*	14	39	1066.73	0.050	1	
93	IRAM	1	22	1	1.88	1.59	26.0	T_{mb}	11	4.8	70.72	0.015	1	
94	BELL	1	100	1	0.83	10.00	5.3	T_{mb}	2	108	126.26	0.893	1	
94	FCRAO	5	45	0	-	8.00	15.0	T_A^*	1	42	249.45	0.181	1	
95	SEST	1	43	1	3.10	6.00	18.0	T_{mb}	10	19	87.32	0.390	1	
96	BELL	1	100	1	4.66	10.00	5.3	T_{mb}	2	108	661.75	0.620	1	
96	FCRAO	5	45	1	4.10	8.00	12.0	T_A^*	1	42	382.20	0.125	1	
97	BELL	1	100	1	1.04	10.00	5.3	T_{mb}	2	108	225.45	0.231	1	
97	FCRAO	9	45	0	-	8.00	12.0	T_A^*	1	42	540.05	0.047	1	
98	FCRAO	1	45	0	-	8.00	12.0	T_A^*	1	42	154.17	0.438	1	
98	KP12m	1	55	1	0.73	3.60	5.2	T_R^*	12	39	44.61	0.654	1	
100	BELL	1	100	1	5.25	10.00	5.3	T_{mb}	2	108	682.32	1.039	1	
100	FCRAO	1	45	1	1.42	8.00	12.0	T_A^*	1	42	106.44	0.210	1	
101	IRAM	1	22	0	-	3.51	13.0	T_{mb}	11	4.8	27.09	0.024	1	
101	KP12m	1	55	0	-	2.52	20.8	T_{mb}	11	32.9	60.44	0.150	1	
102	BELL	1	100	1	13.69	10.00	5.3	T_{mb}	2	108	3042.52	0.145	1	
102	FCRAO	7	45	1	10.60	10.00	12.0	T_A^*	1	42	2230.78	0.029	1	
103	OSO	1	34	0	-	20.00	10.4	T_{mb}	6	12	174.92	0.090	1	
105	IRAM	1	22	0	-	2.50	30.0	T_{mb}	24	4.7	21.25	0.057	1	
110	FCRAO	1	45	0	-	8.00	12.0	T_A^*	1	42	149.05	0.214	1	
110	KP12m	1	55	0	-	3.30	5.6	T_R^*	12	39	34.02	0.320	1	
111	FCRAO	5	45	1	6.00	8.00	12.0	T_A^*	1	42	633.38	0.099	1	
112	KP12m	1	55	1	0.63	3.00	15.7	T_R^*	5	39	32.55	0.629	1	
113	FCRAO	6	45	1	4.90	7.00	12.0	T_A^*	1	42	719.75	0.080	1	
114	BELL	1	100	1	10.16	10.00	5.3	T_{mb}	2	108	2472.74	0.116	1	
114	FCRAO	7	45	1	11.90	8.00	12.0	T_A^*	1	42	2889.91	0.024	1	
117	KP12m	3	55	1	3.27	3.00	15.7	T_R^*	5	39	212.46	0.339	1	
119	FCRAO	3	45	1	5.66	8.00	12.0	T_A^*	1	42	487.23	0.142	1	
120	KP12m	3	55	1	3.41	3.00	15.7	T_R^*	5	39	244.42	0.234	1	
121	KP12m	1	55	1	1.12	4.00	15.7	T_R^*	5	39	63.15	0.630	1	
122	BELL	1	100	1	12.59	10.00	5.3	T_{mb}	2	108	3585.05	0.085	1	
122	FCRAO	8	45	1	15.00	7.00	12.0	T_A^*	1	42	4582.71	0.017	1	
122	IRAM	1	36	1	1853.63	60.00	5.0	T_{mb}	22	4.8	90918.70	0.011	0	3
123	IRAM	1	22	0	2.95	3.57	31.0	T_{mb}	23	4.7	26.83	0.060	1	
124	KP12m	3	55	1	1.98	4.00	15.7	T_R^*	5	39	158.51	0.319	1	
125	IRAM	1	22	0	-	3.70	31.0	T_{mb}	23	4.7	25.01	0.033	1	
126	IRAM	1	22	0	-	4.10	31.0	T_{mb}	23	4.7	40.18	0.029	1	
127	BELL	1	100	0	-	10.00	5.3	T_{mb}	2	108	262.66	1.376	1	
129	IRAM	1	22	0	-	3.77	31.0	T_{mb}	23	4.7	34.13	0.035	1	
130	BELL	1	100	0	-	10.00	5.3	T_{mb}	2	108	141.60	1.195	1	
130	FCRAO	3	45	0	-	8.00	12.0	T_A^*	1	42	93.40	0.242	1	
130	SEST	1	43	0	-	7.40	18.0	T_{mb}	10	19	49.34	0.221	1	
133	KP12m	1	55	1	0.76	8.00	20.0	T_R^*	13	39	45.60	0.413	1	
135	IRAM	1	22	0	-	3.80	30.0	T_{mb}	24	4.7	128.23	0.006	1	
136	KP12m	1	55	0	-	4.00	15.7	T_R^*	5	39	71.81	0.559	1	
137	IRAM	1	22	0	-	3.58	31.0	T_{mb}	23	4.7	53.15	0.018	1	
138	IRAM	1	22	0	-	2.50	30.0	T_{mb}	24	4.7	91.54	0.003	1	
138	OSO	1	34	0	-	40.00	10.4	T_{mb}	6	12	1051.40	0.007	1	
140	KP12m	1	55	0	-	3.00	15.7	T_R^*	5	39	94.11	0.122	1	
141	FCRAO	3	45	0	-	8.00	12.0	T_A^*	1	42	231.42	0.105	1	
141	KP12m	1	55	1	1.86	2.00	21.0	T_R^*	14	39	147.36	0.157	1	
142	FCRAO	1	45	0	-	9.20	10.0	T_A^*	21	42	146.29	0.258	1	2
142	FCRAO	1	45	1	1.60	3.00	15.0	T_A^*	3	42	111.84	0.258	1	
142	FCRAO	1	45	1	1.60	8.00	15.0	T_A^*	1	42	111.84	0.258	1	
142	KP12m	1	55	1	2.20	2.00	30.0	T_R^*	4	39	126.61	0.385	1	
144	BELL	1	100	1	2.01	10.00	5.3	T_{mb}	2	108	363.57	0.379	1	
144	FCRAO	1	45	1	2.70	5.00	12.0	T_A^*	1	42	355.57	0.077	1	
144	SEST	1	43	1	2.70	5.40	18.0	T_{mb}	10	19	168.20	0.070	1	
145	OSO	1	34	0	-	15.00	20.0	T_{mb}	10	12	84.67	0.189	1	
148	KP12m	1	55	1	2.37	10.00	10.0	T_{mb}	15	32.9	137.16	0.326	1	
149	BELL	1	100	1	4.70	10.00	5.3	T_{mb}	2	108	703.34	0.693	1	
149	FCRAO	4	45	1	6.80	8.00	12.0	T_A^*	1	42	660.05	0.140	1	
150	IRAM	1	22	0	-	5.10	27.3	T_{mb}	25	4.7	388.53	0.002	1	
150	KP12m	1	55	0	-	0.63	5.0	T_R^*	16	39	36.21	0.011	1	1
151	BELL	1	100	0	-	10.00	5.3	T_{mb}	2	108	189.90	0.971	1	
151	FCRAO	1	45	0	-	8.00	15.0	T_A^*	1	42	146.50	0.197	1	
151	SEST	1	43	0	-	9.80	18.0	T_{mb}	10	19	91.95	0.180	1	
152	KP12m	1	55	1	1.71	4.00	15.7	T_R^*	5	39	93.51	0.438	1	
153	IRAM	1	22	1	5.08	5.00	10.0	T_{mb}	17	4.8	71.81	0.069	1	

Continued on next page...

Table 10 – Continued

HRS (1)	Tel (2)	N. beam (3)	θ (4) arcsec	sign (5)	$I(\text{CO})$ (6) K km s^{-1}	rms (7) mK	δV_{CO} (8) km s^{-1}	T scale (9)	Ref (10)	Jy/K (11) Jy K^{-1}	SCO_{3D} (12) Jy km s^{-1}	ff (13)	flag (14)	Notes (15)
154	IRAM	1	22	1	0.88	5.00	10.0	T_{mb}^*	17	4.8	21.27	0.029	1	
154	KP12m	1	55	1	0.52	3.00	21.0	T_R^*	14	39	37.86	0.180	1	
155	IRAM	1	22	0	-	3.14	31.0	T_{mb}^*	23	4.7	29.42	0.037	1	
156	FCRAO	5	45	1	10.20	7.00	12.0	T_A^*	1	42	839.34	0.189	1	
157	KP12m	1	55	1	2.30	4.00	21.0	T_R^*	14	39	124.81	0.533	1	
158	OSO	1	34	1	9.70	22.00	20.0	T_{mb}^*	10	12	229.67	0.308	1	
159	FCRAO	3	45	1	1.51	5.00	12.0	T_A^*	1	42	153.12	0.105	1	
160	SEST	1	43	1	2.70	7.10	18.0	T_{mb}^*	10	19	112.47	0.124	1	
161	IRAM	1	22	1	6.77	3.03	31.0	T_{mb}^*	23	4.7	356.85	0.009	1	
161	KP12m	1	55	1	0.70	2.00	30.0	T_R^*	4	39	89.13	0.059	1	
162	IRAM	1	22	1	4.36	2.47	31.0	T_{mb}^*	23	4.7	128.03	0.021	1	
162	KP12m	1	55	1	1.80	2.00	30.0	T_R^*	4	39	150.18	0.131	1	
163	BELL	1	100	1	3.27	10.00	5.3	T_{mb}^*	2	108	844.66	0.117	1	
163	FCRAO	3	45	1	2.90	7.00	12.0	T_A^*	1	42	721.22	0.024	1	
164	BELL	1	100	1	0.78	10.00	5.3	T_{mb}^*	2	108	98.68	1.126	1	
166	IRAM	1	22	0	-	3.84	31.0	T_{mb}^*	23	4.7	50.68	0.022	1	
170	BELL	1	100	1	0.57	10.00	5.3	T_{mb}^*	2	108	113.02	0.177	1	
170	FCRAO	4	45	1	2.50	9.00	12.0	T_A^*	1	42	429.00	0.036	1	
170	SEST	1	43	1	6.90	7.00	18.0	T_{mb}^*	10	19	567.07	0.033	1	
171	KP12m	1	55	1	1.79	4.00	15.7	T_R^*	5	39	91.58	0.618	1	
172	KP12m	1	55	1	2.70	4.00	15.7	T_R^*	5	39	162.46	0.369	1	
173	FCRAO	1	45	1	4.70	5.00	15.0	T_A^*	3	42	594.82	0.066	1	
173	FCRAO	1	45	1	4.70	8.00	15.0	T_A^*	1	42	594.82	0.066	1	
174	FCRAO	1	45	1	1.30	5.00	15.0	T_A^*	3	42	180.70	0.056	1	
174	FCRAO	1	45	1	1.30	8.00	15.0	T_A^*	1	42	180.70	0.056	1	
174	IRAM	1	22	1	10.90	3.00	30.0	T_{mb}^*	24	4.7	446.74	0.013	1	
174	KP12m	1	55	1	3.60	2.00	20.0	T_R^*	4	39	372.69	0.083	1	
175	IRAM	1	22	0	-	3.72	31.0	T_{mb}^*	23	4.7	34.85	0.037	1	
177	KP12m	1	55	1	1.72	4.00	21.0	T_R^*	14	39	85.52	0.704	1	
178	IRAM	1	22	0	-	4.12	31.0	T_{mb}^*	23	4.7	367.41	0.002	1	
178	KP12m	1	55	0	-	0.97	5.0	T_R^*	16	39	60.45	0.011	1	1
179	IRAM	1	22	0	-	2.50	30.0	T_{mb}^*	24	4.7	45.14	0.013	1	
180	IRAM	1	22	0	2.10	3.00	30.0	T_{mb}^*	24	4.7	34.57	0.015	1	
181	IRAM	1	22	0	-	2.91	31.0	T_{mb}^*	23	4.7	15.50	0.061	1	
182	KP12m	1	55	1	1.23	3.00	21.0	T_R^*	14	39	68.62	0.468	1	
183	IRAM	1	22	0	-	2.50	30.0	T_{mb}^*	24	4.7	157.91	0.003	1	
183	KP12m	1	55	0	-	11.00	5.2	T_R^*	18	39	529.71	0.016	1	1
184	OSO	1	34	1	2.96	13.00	20.0	T_{mb}^*	10	12	64.45	0.208	1	
185	KP12m	1	55	1	1.10	3.00	15.7	T_R^*	5	39	79.50	0.184	1	
186	IRAM	1	22	1	-	3.51	31.0	T_{mb}^*	23	4.7	0.00	0.009	1	
186	IRAM	1	22	1	1.44	4.40	12.0	T_{mb}^*	19	4.8	79.86	0.009	1	
187	IRAM	1	22	1	2.17	5.00	10.0	T_{mb}^*	17	4.8	70.01	0.019	1	
187	KP12m	1	55	1	0.93	2.00	21.0	T_R^*	14	39	80.98	0.120	1	
188	FCRAO	1	45	0	-	8.00	15.0	T_A^*	1	42	172.43	0.175	1	
188	SEST	1	43	0	-	6.40	18.0	T_{mb}^*	10	19	70.95	0.160	1	
190	BELL	1	100	1	13.31	10.00	5.3	T_{mb}^*	2	108	2969.20	0.154	1	
190	FCRAO	7	45	1	12.00	9.00	12.0	T_A^*	1	42	2457.03	0.031	1	
193	SEST	1	43	1	0.90	8.80	18.0	T_{mb}^*	10	19	30.04	0.221	1	
194	BELL	1	100	1	2.47	10.00	5.3	T_{mb}^*	2	108	612.35	0.224	1	
194	KP12m	5	55	1	7.40	8.00	20.0	T_R^*	13	39	1134.06	0.068	1	
195	KP12m	1	55	0	-	4.00	15.7	T_R^*	5	39	68.93	0.566	1	
196	FCRAO	3	45	0	-	8.00	15.0	T_A^*	1	42	182.06	0.133	1	
196	IRAM	1	22	1	2.93	5.00	10.0	T_{mb}^*	17	4.8	67.23	0.032	1	
196	KP12m	1	55	1	1.08	3.00	21.0	T_R^*	14	39	76.86	0.198	1	
197	FCRAO	3	45	0	-	8.00	15.0	T_A^*	1	42	197.43	0.196	1	
197	KP12m	1	55	1	4.33	6.60	5.6	T_R^*	12	39	305.80	0.293	1	
198	KP12m	1	55	1	0.81	8.00	20.0	T_R^*	13	39	47.82	0.371	1	
200	FCRAO	1	45	0	-	5.00	15.0	T_A^*	3	42	310.27	0.034	1	
200	FCRAO	3	45	0	-	10.00	12.0	T_A^*	1	42	555.02	0.034	1	
200	IRAM	1	22	1	23.80	3.00	30.0	T_{mb}^*	24	4.7	1315.70	0.008	1	
200	KP12m	1	55	1	3.80	2.00	30.0	T_R^*	4	39	528.52	0.051	1	
201	BELL	1	100	1	17.77	10.00	5.3	T_{mb}^*	2	108	3423.86	0.268	1	
201	FCRAO	6	45	1	15.60	10.00	12.0	T_A^*	1	42	2409.90	0.054	1	
203	FCRAO	3	45	0	-	8.00	12.0	T_A^*	1	42	153.83	0.201	1	
203	KP12m	1	55	1	1.17	2.00	21.0	T_R^*	14	39	76.33	0.300	1	
204	BELL	1	100	1	5.26	10.00	5.3	T_{mb}^*	2	108	1303.76	0.116	1	
204	FCRAO	7	45	1	4.70	8.00	12.0	T_A^*	1	42	1160.95	0.023	1	
205	BELL	1	100	0	-	10.00	5.3	T_{mb}^*	2	108	487.38	0.170	1	
205	FCRAO	6	45	1	10.10	10.00	12.0	T_A^*	1	42	2023.98	0.034	1	
205	KP12m	1	55	0	-	13.30	10.0	T_R^*	21	39	578.05	0.051	1	
205	OSO	1	34	1	20.20	20.00	10.4	T_{mb}^*	6	12	1678.53	0.020	1	

Continued on next page...

Table 10 – Continued

HRS (1)	Tel (2)	N. beam (3)	θ (4) arcsec	sign (5)	$I(\text{CO})$ (6) K km s^{-1}	rms (7) mK	δV_{CO} (8) km s^{-1}	T scale (9)	Ref (10)	Jy/K (11) Jy K^{-1}	SCO_{3D} (12) Jy km s^{-1}	ff (13)	flag (14)	Notes (15)
206	OSO	1	34	1	8.50	18.00	20.0	T_{mb}	10	12	170.65	0.249	1	
207	FCRAO	1	45	1	2.36	8.00	15.0	T_A^*	1	42	196.50	0.156	1	
207	FCRAO	1	45	1	2.36	10.00	12.0	T_A^*	20	42	196.50	0.156	1	2
207	IRAM	1	22	1	5.57	5.00	10.0	T_{mb}	17	4.8	113.75	0.037	1	
208	BELL	1	100	1	2.16	10.00	5.3	T_{mb}	2	108	464.32	0.155	1	
208	FCRAO	7	45	1	3.70	5.00	12.0	T_A^*	1	42	738.70	0.031	1	
209	IRAM	1	22	0	-	2.50	30.0	T_{mb}	24	4.7	24.55	0.041	1	
210	IRAM	1	22	0	-	4.22	31.0	T_{mb}	23	4.7	27.61	0.071	1	
211	IRAM	1	22	0	-	3.80	30.0	T_{mb}	24	4.7	97.60	0.006	1	
212	FCRAO	1	45	0	-	8.00	15.0	T_A^*	1	42	102.17	0.334	1	
213	IRAM	1	36	1	23.33	10.00	10.5	T_{mb}	22	4.8	748.24	0.018	1	
213	OSO	1	34	1	14.80	20.00	10.4	T_{mb}	6	12	1263.00	0.016	1	
214	IRAM	1	22	0	-	4.00	31.0	T_{mb}	23	4.7	38.36	0.035	1	
215	BELL	1	100	1	5.98	10.00	5.3	T_{mb}	2	108	921.12	0.422	1	
215	FCRAO	4	45	1	4.70	7.00	12.0	T_A^*	1	42	521.53	0.085	1	
216	BELL	1	100	1	8.72	10.00	5.3	T_{mb}	2	108	1491.64	0.358	1	
216	FCRAO	5	45	1	10.50	10.00	12.0	T_A^*	1	42	1350.48	0.072	1	
216	OSO	3	34	1	35.50	30.00	10.4	T_{mb}	6	12	1795.68	0.041	1	
217	BELL	1	100	1	11.84	10.00	5.3	T_{mb}	2	108	2699.35	0.106	1	
217	FCRAO	5	45	1	14.60	10.00	12.0	T_A^*	1	42	2477.93	0.022	1	
217	OSO	1	34	1	38.70	20.00	20.0	T_{mb}	10	12	2446.40	0.012	1	
217	SEST	1	43	1	33.60	10.00	18.0	T_{mb}	10	19	2689.90	0.020	1	
218	IRAM	1	22	0	-	5.10	30.0	T_{mb}	24	4.7	47.71	0.037	1	
219	IRAM	1	22	0	-	3.27	31.0	T_{mb}	23	4.7	32.13	0.028	1	
220	BELL	1	100	1	2.76	10.00	5.3	T_{mb}	2	108	640.67	0.130	1	
220	FCRAO	6	45	1	4.10	6.00	12.0	T_A^*	1	42	923.18	0.026	1	
220	IRAM	1	36	1	283.40	1.00	15.6	T_{mb}	22	4.8	10024.99	0.017	1	
220	OSO	1	34	1	23.10	40.00	10.4	T_{mb}	6	12	2224.42	0.015	1	
221	FCRAO	1	45	0	-	8.00	15.0	T_A^*	1	42	151.41	0.181	1	
221	OSO	1	34	1	5.30	17.00	20.0	T_{mb}	10	12	151.85	0.103	1	
224	BELL	1	100	1	0.74	10.00	5.3	T_{mb}	2	108	106.38	0.774	1	
229	IRAM	1	22	0	-	3.23	31.0	T_{mb}	23	4.7	7.47	0.242	1	
230	SEST	1	43	1	3.30	6.90	18.0	T_{mb}	10	19	101.97	0.277	1	
231	FCRAO	1	45	0	-	8.00	15.0	T_A^*	1	42	323.90	0.048	1	
231	IRAM	1	22	0	1.25	3.36	31.0	T_{mb}	23	4.7	59.31	0.011	1	
231	OSO	1	34	0	-	17.00	20.0	T_{mb}	10	12	325.60	0.027	1	
233	KP12m	3	55	1	4.03	4.00	15.7	T_R^*	5	39	245.56	0.515	1	
234	IRAM	1	22	0	-	3.38	31.0	T_{mb}	23	4.7	40.32	0.017	1	
235	IRAM	1	22	0	-	3.13	31.0	T_{mb}	23	4.7	27.57	0.029	1	
236	IRAM	1	22	0	-	3.94	31.0	T_{mb}	23	4.7	88.62	0.007	1	
237	KP12m	1	55	1	4.45	7.00	10.0	T_{mb}	15	32.9	216.63	0.367	1	
239	SEST	1	43	1	6.50	8.90	18.0	T_{mb}	10	19	254.54	0.253	1	
240	IRAM	1	22	0	-	3.73	31.0	T_{mb}	23	4.7	27.77	0.042	1	
241	IRAM	1	22	1	0.24	2.90	12.0	T_{mb}	19	4.8	31.39	0.003	1	
242	BELL	1	100	0	-	10.00	5.3	T_{mb}	2	108	267.73	0.705	1	
242	FCRAO	3	45	0	-	5.00	12.0	T_A^*	1	42	128.18	0.143	1	
242	KP12m	1	55	0	-	10.00	21.0	T_R^*	14	39	268.17	0.213	1	
243	IRAM	1	22	0	-	3.76	31.0	T_{mb}	23	4.7	83.20	0.013	1	
244	BELL	1	100	1	6.30	10.00	5.3	T_{mb}	2	108	1090.39	0.284	1	
244	FCRAO	5	45	1	5.00	9.00	12.0	T_A^*	1	42	691.12	0.058	1	
245	IRAM	1	22	1	-	8.87	31.0	T_{mb}	23	4.7	0.00	0.003	1	
245	KP12m	1	55	1	0.80	2.00	30.0	T_R^*	4	39	209.05	0.019	1	
246	BELL	1	100	1	1.29	10.00	5.3	T_{mb}	2	108	208.45	0.364	1	
246	FCRAO	4	45	1	4.20	7.00	12.0	T_A^*	1	42	508.64	0.074	1	
246	IRAM	1	36	1	4.20	7.00	12.0	T_{mb}	22	4.8	75.08	0.047	1	
247	BELL	1	100	1	7.10	10.00	5.3	T_{mb}	2	108	1348.59	0.228	1	
247	FCRAO	5	45	1	3.30	8.00	12.0	T_A^*	1	42	529.26	0.046	1	
247	IRAM	1	36	1	926.82	60.00	5.0	T_{mb}	22	4.8	22587.53	0.030	1	
248	IRAM	1	22	0	-	3.73	31.0	T_{mb}	23	4.7	25.35	0.048	1	
251	FCRAO	7	45	1	16.56	8.00	15.0	T_A^*	1	42	2034.74	0.085	1	
253	IRAM	1	22	0	1.54	3.86	31.0	T_{mb}	23	4.7	30.76	0.049	1	
254	BELL	1	100	1	1.74	10.00	5.3	T_{mb}	2	108	299.99	0.284	1	
254	FCRAO	5	45	1	3.60	5.00	12.0	T_A^*	1	42	495.42	0.057	1	
255	IRAM	1	22	1	0.44	5.00	10.0	T_{mb}	17	4.8	9.24	0.036	1	
255	KP12m	1	55	0	-	8.00	10.0	T_{mb}	15	32.9	50.75	0.223	1	
256	FCRAO	1	45	1	2.64	8.00	15.0	T_A^*	1	42	299.82	0.080	1	
256	SEST	1	43	1	7.30	40.00	10.3	T_{mb}	6	19	393.62	0.073	1	
257	BELL	1	100	0	0.94	10.00	5.3	T_{mb}	2	108	411.20	0.243	1	
257	FCRAO	3	45	0	-	8.00	12.0	T_A^*	1	42	332.92	0.049	1	
257	SEST	1	43	0	-	7.20	18.0	T_{mb}	10	19	172.28	0.045	1	
258	IRAM	1	22	0	-	3.86	31.0	T_{mb}	23	4.7	177.03	0.004	1	
258	IRAM	1	22	0	-	5.20	10.0	T_{mb}	19	4.8	138.33	0.004	1	

Continued on next page...

Table 10 – Continued

HRS (1)	Tel (2)	N. beam (3)	θ (4) arcsec	sign (5)	$I(\text{CO})$ (6) K km s^{-1}	rms (7) mK	δV_{CO} (8) km s^{-1}	T scale (9)	Ref (10)	Jy/K (11) Jy K^{-1}	SCO_3D (12) Jy km s^{-1}	ff (13)	flag (14)	Notes (15)
259	BELL	1	100	1	0.51	10.00	5.3	T_{mb}	2	108	66.51	0.954	1	
259	IRAM	1	22	1	2.90	5.00	10.0	T_{mb}	17	4.8	52.06	0.046	1	
259	KP12m	1	55	1	4.85	8.00	10.0	T_{mb}	15	32.9	253.43	0.288	1	
260	FCRAO	5	45	1	4.30	5.00	12.0	T_A^*	1	42	440.19	0.111	1	
260	FCRAO	5	45	1	4.30	5.00	15.0	T_A^*	3	42	440.19	0.111	1	
260	IRAM	1	22	1	31.70	8.40	31.0	T_{mb}	23	4.7	785.53	0.027	1	
260	KP12m	5	55	1	8.90	2.00	20.0	T_R^*	4	39	715.75	0.166	1	
262	FCRAO	3	45	0	-	9.00	12.0	T_A^*	1	42	166.01	0.159	1	
262	KP12m	1	55	1	3.61	5.00	10.0	T_{mb}	15	32.9	201.23	0.238	1	
263	FCRAO	9	45	1	1.42	8.00	15.0	T_A^*	1	42	541.45	0.012	1	
266	KP12m	1	55	1	0.77	4.00	15.7	T_R^*	5	39	119.66	0.042	1	
268	SEST	1	43	1	4.60	2.50	20.0	T_{mb}	7	19	130.16	0.451	1	
270	FCRAO	1	45	0	-	5.00	15.0	T_A^*	3	42	342.60	0.028	1	
270	FCRAO	1	45	0	-	8.00	15.0	T_A^*	1	42	548.15	0.028	1	
270	IRAM	1	22	0	11.17	4.51	31.0	T_{mb}	23	4.7	145.75	0.007	1	
272	IRAM	1	22	0	-	4.14	31.0	T_{mb}	23	4.7	72.97	0.011	1	
273	KP12m	1	55	1	2.42	3.00	15.7	T_R^*	5	39	168.12	0.322	1	
274	KP12m	1	55	0	-	3.00	15.7	T_R^*	5	39	115.68	0.114	1	
275	IRAM	1	22	1	1.63	5.00	10.0	T_{mb}	17	4.8	30.02	0.044	1	
276	FCRAO	1	45	0	-	13.80	10.0	T_A^*	21	42	230.24	0.234	1	2
280	KP12m	1	55	0	-	5.00	15.7	T_R^*	5	39	91.63	1.077	1	
282	IRAM	1	22	0	-	3.80	31.0	T_{mb}	23	4.7	11.40	0.310	1	
283	BELL	1	100	1	0.46	10.00	5.3	T_{mb}	2	108	59.39	1.278	1	
283	FCRAO	3	45	0	-	9.00	12.0	T_A^*	1	42	185.68	0.259	1	
283	IRAM	1	22	1	11.30	5.00	20.0	T_{mb}	7	4.8	181.05	0.062	1	
283	SEST	1	43	1	6.20	5.00	20.0	T_{mb}	7	19	212.31	0.236	1	
284	KP12m	1	55	1	5.07	5.00	15.7	T_R^*	5	39	253.77	0.906	1	
285	FCRAO	3	45	1	3.34	8.00	15.0	T_A^*	1	42	321.09	0.103	1	
286	FCRAO	3	45	0	-	6.00	12.0	T_A^*	1	42	227.17	0.142	1	
286	KP12m	1	55	0	-	4.00	21.0	T_R^*	14	39	160.90	0.213	1	
287	KP12m	1	55	1	2.24	3.00	15.7	T_R^*	5	39	137.74	0.301	1	
288	KP12m	1	55	1	2.05	3.00	15.7	T_R^*	5	39	132.52	0.226	1	
289	KP12m	1	55	1	4.01	4.00	15.7	T_R^*	5	39	260.80	0.261	1	
290	FCRAO	1	45	0	-	16.10	10.0	T_A^*	21	42	131.64	0.773	1	2
291	IRAM	1	22	0	-	4.13	31.0	T_{mb}	23	4.7	12.85	0.096	1	
291	KP12m	1	55	0	-	3.00	15.7	T_R^*	5	39	29.74	0.602	1	
292	KP12m	1	55	1	6.44	4.00	15.7	T_R^*	5	39	308.98	0.832	1	
293	KP12m	1	55	1	0.99	3.00	15.7	T_R^*	5	39	58.19	0.342	1	
295	FCRAO	5	45	1	10.72	8.00	15.0	T_A^*	1	42	2123.21	0.032	1	
296	IRAM	1	22	0	1.30	2.90	31.0	T_{mb}	23	4.7	21.51	0.034	1	
297	KP12m	3	55	1	2.35	4.00	15.7	T_R^*	5	39	166.05	0.290	1	
299	KP12m	1	55	1	1.01	3.00	15.7	T_R^*	5	39	80.37	0.152	1	
301	KP12m	1	55	1	1.17	3.00	15.7	T_R^*	5	39	104.44	0.115	1	
304	KP12m	3	55	1	1.69	4.00	15.7	T_R^*	5	39	106.76	0.405	1	
306	FCRAO	1	45	0	-	5.00	15.0	T_A^*	3	42	463.40	0.032	1	
306	FCRAO	1	45	0	-	8.00	15.0	T_A^*	1	42	741.44	0.032	1	
306	KP12m	1	55	1	2.20	2.00	20.0	T_R^*	4	39	315.87	0.048	1	
306	OSO	1	34	0	-	20.00	10.4	T_{mb}	6	12	650.81	0.018	1	
307	FCRAO	5	45	0	-	8.00	15.0	T_A^*	1	42	550.83	0.029	1	
307	IRAM	1	36	1	5.00	0.00	5.2	T_{mb}	22	4.8	167.47	0.018	1	
307	OSO	1	34	0	-	40.00	10.4	T_{mb}	6	12	973.88	0.016	1	
310	KP12m	3	55	1	2.11	3.00	15.7	T_R^*	5	39	123.51	0.426	1	
311	KP12m	1	55	1	3.64	3.00	15.7	T_R^*	5	39	327.73	0.093	1	
312	IRAM	1	22	0	-	3.06	31.0	T_{mb}	23	4.7	44.14	0.017	1	
313	KP12m	1	55	1	0.77	3.00	15.7	T_R^*	5	39	48.63	0.394	1	
316	IRAM	1	22	0	-	3.08	31.0	T_{mb}	23	4.7	22.78	0.029	1	
318	KP12m	1	55	0	-	5.00	15.7	T_R^*	5	39	85.08	0.291	1	
319	IRAM	1	22	1	2.28	5.00	10.0	T_{mb}	17	4.8	67.38	0.022	1	
320	IRAM	1	22	1	1.78	5.00	10.0	T_{mb}	17	4.8	50.82	0.023	1	
323	KP12m	1	55	1	2.03	4.00	15.7	T_R^*	5	39	108.47	0.664	1	

References to the CO data:

1: Young et al. (1995), 2: Stark et al. (1986), 3: Thronson et al. (1989), 4: Sage & Wrobel (1989), 5: This work, 6: Elfhag et al. (1996), 7: Albrecht et al. (2007), 8: Sauty et al. (2003), 9: Gondhalekar et al. (1998), 10: Boselli et al. (1995), 11: Welch & Sage (2003), 12: Smith & Madden (1997), 13: Sage (1993), 14: Boselli et al. (2002), 15: Leroy et al. (2005), 16: Bregman & Hogg (1988), 17: Böker et al. (2003), 18: Jaffe (1987), 19: Sage et al. (2007), 20: Kenney, private communication, 21: Jackson et al. (1989), 22: Braine et al. (1993), 23: Young et al. (2011), 24: Combes et al. (2007), 25: Wiklind et al. (1995)

Notes: 1: assumed in T_R^* . 2: transformed from the original table to this scale. 3: partly mapped galaxy, with an equivalent beamsize assumed to be $\theta=36$ arcsec.

Table 11. Integrated CO fluxes and molecular hydrogen masses of the HRS of the HRS.

HRS (1)	sgn (2)	S_{CO} (3) Jy km s $^{-1}$	err (4) Jy km s $^{-1}$	S/N (5)	ff (6)	$\log M(H_2)_c$ (7) M_{\odot}	$\log M(H_2)_v$ (8) M_{\odot}	Ref (9)
1	-	-	-	-	-	-	-	-
2	-	-	-	-	-	-	-	-
3	0	57.81	-	-	0.021	8.16	8.05	23
4	1	1085.00	1230.39	21.72	0.038	9.42	9.17	22
5	-	-	-	-	-	-	-	-
6	-	-	-	-	-	-	-	-
7	0	37.54	-	-	0.029	8.07	7.86	23
8	0	91.42	-	-	0.194	8.49	8.39	5
9	1	118.90	50.33	1.90	0.220	8.64	8.57	5
10	-	-	-	-	-	-	-	-
11	0	68.48	-	-	0.395	8.34	8.43	5
12	-	-	-	-	-	-	-	-
13	1	241.70	102.31	0.42	0.111	9.04	8.80	6
14	0	23.44	-	-	0.055	7.89	7.78	23
15	1	443.50	502.93	4.26	0.054	9.14	8.94	1
16	1	113.60	23.97	4.51	0.027	8.52	8.50	5,17
17	1	268.30	113.57	3.21	0.281	8.91	8.93	5
18	-	-	-	-	-	-	-	-
19	-	-	-	-	-	-	-	-
20	0	28.51	-	-	0.179	8.14	8.14	22
21	-	-	-	-	-	-	-	-
22	0	20.10	-	-	0.021	7.87	7.65	24
23	0	41.80	-	-	0.207	8.24	8.16	22
24	0	261.70	-	-	0.076	9.08	8.94	22
25	1	190.00	90.26	-	MA	8.75	8.72	1
26	-	-	-	-	-	-	-	-
27	0	132.40	-	-	1.580	8.86	9.06	7
28	-	-	-	-	-	-	-	-
29	-	-	-	-	-	-	-	-
30	-	-	-	-	-	-	-	-
31	0	74.74	-	-	0.347	8.41	8.32	5
32	0	12.06	-	-	0.165	7.47	7.58	23
33	1	115.20	48.76	1.97	0.260	8.64	8.61	5
34	1	126.50	53.55	1.90	0.475	8.47	8.64	5
35	0	9.16	-	-	0.291	7.59	7.69	23
36	1	637.40	76.62	-	Int	9.44	9.25	26
37	1	105.40	44.62	2.39	0.511	8.56	8.62	5
38	1	34.43	14.57	0.88	0.504	8.10	8.30	8
39	-	-	-	-	-	-	-	-
40	-	-	-	-	-	-	-	-
41	-	-	-	-	-	-	-	-
42	1	331.20	140.20	6.72	0.161	8.94	8.83	5
43	0	36.88	-	-	0.021	7.92	7.81	24
44	-	-	-	-	-	-	-	-
45	0	48.39	-	-	0.025	8.32	8.17	23
46	0	58.25	-	-	0.029	8.38	8.17	23
47	-	-	-	-	-	-	-	-
48	1	1093.00	131.39	-	Int	9.43	9.27	26
49	0	42.14	-	-	0.013	8.08	7.86	23
50	1	311.70	131.94	5.25	0.260	9.11	9.02	7
51	-	-	-	-	-	-	-	-
52	-	-	-	-	-	-	-	-
53	1	188.80	79.92	2.78	0.270	8.59	8.65	5
54	1	51.57	21.83	1.07	0.260	8.16	8.14	5
55	1	193.50	81.91	2.40	0.203	8.68	8.72	5
56	1	390.00	185.26	-	MA	9.32	9.15	1
57	1	366.50	155.14	4.18	0.143	8.95	8.82	5
58	-	-	-	-	-	-	-	-
59	0	98.96	-	-	0.506	8.73	8.65	5
60	1	296.30	125.42	3.29	0.195	8.78	8.72	5
61	-	-	-	-	-	-	-	-
62	-	-	-	-	-	-	-	-
63	1	220.00	93.13	2.66	0.147	8.83	8.67	5
64	-	-	-	-	-	-	-	-
65	-	-	-	-	-	-	-	-
66	1	360.40	152.56	4.46	0.359	9.15	9.07	5
67	-	-	-	-	-	-	-	-
68	-	-	-	-	-	-	-	-
69	0	75.09	-	-	0.107	8.28	8.05	5
70	-	-	-	-	-	-	-	-

Continued on next page...

Table 11 – Continued

HRS (1)	sgn (2)	SCO (3) Jy km s $^{-1}$	err (4) Jy km s $^{-1}$	S/N (5)	ff (6)	$\log M(H_2)_c$ (7) M \odot	$\log M(H_2)_v$ (8) M \odot	Ref (9)
71	0	76.38	-	-	0.013	8.35	8.09	23
72	-	-	-	-	-	-	-	-
73	1	1790.00	850.30	-	MA	9.56	9.32	1
74	1	320.80	135.79	4.93	0.343	8.86	8.85	5
75	-	-	-	-	-	-	-	-
76	-	-	-	-	-	-	-	-
77	1	1050.00	498.78	-	MA	9.61	9.29	1
78	0	105.50	-	-	0.321	8.49	8.74	1
79	-	-	-	-	-	-	-	-
80	-	-	-	-	-	-	-	-
81	1	575.60	243.65	8.19	0.224	9.17	9.15	5
82	-	-	-	-	-	-	-	-
83	-	-	-	-	-	-	-	-
84	1	60.98	25.81	1.43	0.907	8.20	8.39	5
85	1	754.20	319.25	7.20	0.136	9.20	9.04	5
86	1	138.00	58.42	0.57	0.520	8.55	8.67	2
87	-	-	-	-	-	-	-	-
88	1	200.50	227.37	1.65	0.047	8.72	8.81	9
89	1	103.70	39.33	0.75	0.079	8.43	8.41	1,2,10
90	0	38.09	-	-	0.036	7.99	7.85	23
91	1	940.00	446.52	-	MA	9.39	9.07	1
92	-	-	-	-	-	-	-	-
93	1	70.72	80.20	2.99	0.015	8.19	7.98	11
94	1	126.30	53.46	0.51	0.894	8.52	8.59	2
95	1	87.20	36.91	1.73	0.390	8.35	8.46	10
96	1	491.80	59.12	-	Int	9.11	8.99	1,2
97	1	620.00	294.52	-	MA	9.21	8.84	1
98	1	44.61	18.88	1.18	0.654	8.06	8.29	12
99	-	-	-	-	-	-	-	-
100	1	391.80	285.43	2.46	1.039	9.01	8.98	1,2
101	0	27.09	-	-	0.024	7.75	7.62	11
102	1	4033.00	484.80	-	Int	10.02	9.73	26
103	0	174.90	-	-	0.090	8.92	8.76	6
104	-	-	-	-	-	-	-	-
105	0	21.25	-	-	0.057	7.74	7.66	24
106	-	-	-	-	-	-	-	-
107	-	-	-	-	-	-	-	-
108	-	-	-	-	-	-	-	-
109	-	-	-	-	-	-	-	-
110	0	34.01	-	-	0.320	7.95	8.06	12
111	1	559.50	230.99	-	Int	9.16	9.07	27
112	1	32.45	13.74	0.65	0.629	8.19	8.18	5
113	1	758.60	313.19	-	Int	9.29	9.14	27
114	1	3344.00	401.98	-	Int	9.94	9.63	26
115	-	-	-	-	-	-	-	-
116	-	-	-	-	-	-	-	-
117	1	212.40	89.91	3.11	0.339	9.00	8.97	5
118	-	-	-	-	-	-	-	-
119	1	487.30	206.27	2.77	0.142	9.10	9.09	1
120	1	244.40	103.45	3.54	0.234	8.80	8.75	5
121	1	63.14	26.73	0.80	0.630	8.48	8.45	5
122	1	3148.00	378.42	-	Int	9.91	9.55	26
123	0	26.83	-	-	0.060	7.84	7.78	23
124	1	158.50	67.09	1.61	0.319	8.61	8.72	5
125	0	25.01	-	-	0.033	8.07	7.92	23
126	0	40.18	-	-	0.029	8.02	7.91	23
127	0	261.20	-	-	1.376	9.09	9.03	2
128	-	-	-	-	-	-	-	-
129	0	34.13	-	-	0.035	7.95	7.78	23
130	0	49.28	-	-	0.221	8.11	8.31	10
131	-	-	-	-	-	-	-	-
132	-	-	-	-	-	-	-	-
133	1	45.58	19.29	0.29	0.413	8.12	8.39	13
134	-	-	-	-	-	-	-	-
135	0	128.20	-	-	0.006	8.78	8.31	24
136	0	71.70	-	-	0.559	8.53	8.52	5
137	0	53.15	-	-	0.018	8.14	7.97	23
138	0	91.54	-	-	0.003	8.38	8.00	24
139	-	-	-	-	-	-	-	-
140	0	94.10	-	-	0.122	8.39	8.28	5
141	1	147.30	62.35	2.48	0.157	8.84	8.66	14
142	1	116.50	23.30	2.58	0.385	8.48	8.56	1,3,4

Continued on next page...

Table 11 – Continued

HRS (1)	sgn (2)	SCO (3) Jy km s $^{-1}$	err (4) Jy km s $^{-1}$	S/N (5)	ff (6)	$\log M(H_2)_c$ (7) M \odot	$\log M(H_2)_v$ (8) M \odot	Ref (9)
143	-	-	-	-	-	-	-	-
144	1	230.00	109.26	-	MA	8.78	8.64	1
145	0	84.66	-	-	0.189	8.60	8.75	10
146	-	-	-	-	-	-	-	-
147	-	-	-	-	-	-	-	-
148	1	137.20	58.08	1.08	0.326	8.55	8.74	15
149	1	786.90	94.59	-	Int	9.31	9.23	26
150	0	36.21	-	-	0.011	7.97	7.52	16
151	0	91.87	-	-	0.180	8.38	8.49	10
152	1	93.51	39.58	1.99	0.438	8.38	8.59	5
153	1	71.81	81.43	5.55	0.069	8.27	8.44	17
154	1	29.56	8.29	1.71	0.029	8.15	8.26	14,17
155	0	29.42	-	-	0.037	8.14	7.87	23
156	1	491.80	59.12	-	Int	9.11	8.94	26
157	1	124.50	52.70	1.88	0.533	8.51	8.61	14
158	1	229.70	97.23	1.51	0.308	9.04	9.28	4
159	1	153.10	64.81	2.23	0.105	8.86	8.79	1
160	1	112.50	47.62	1.52	0.124	8.73	8.71	10
161	1	223.00	133.87	3.04	0.009	8.76	8.45	4,23
162	1	139.10	27.82	4.71	0.021	8.56	8.34	4,23
163	1	390.90	161.39	-	Int	9.01	8.76	27
164	1	98.66	41.76	0.58	1.126	8.41	8.35	2
165	-	-	-	-	-	-	-	-
166	0	50.68	-	-	0.022	8.38	8.04	23
167	-	-	-	-	-	-	-	-
168	-	-	-	-	-	-	-	-
169	-	-	-	-	-	-	-	-
170	1	450.00	213.76	-	MA	9.07	8.78	1
171	1	91.47	38.72	1.57	0.618	8.64	8.68	5
172	1	162.40	68.74	2.48	0.369	8.62	8.67	5
173	1	594.80	0.00	4.56	0.066	9.19	9.01	1,3
174	1	295.20	117.46	6.19	0.013	8.88	8.62	1,3,4,24
175	0	34.85	-	-	0.037	7.96	7.82	23
176	-	-	-	-	-	-	-	-
177	1	85.40	36.15	1.61	0.704	8.35	8.52	14
178	0	60.45	-	-	0.011	8.20	7.63	16
179	0	45.14	-	-	0.013	8.07	7.82	24
180	0	34.57	-	-	0.015	7.95	7.69	24
181	0	15.50	-	-	0.061	7.60	7.54	23
182	1	68.44	28.97	1.02	0.468	8.25	8.35	14
183	0	157.90	-	-	0.003	8.61	8.17	24
184	1	64.40	27.26	0.63	0.208	8.22	8.37	10
185	1	79.50	33.65	1.37	0.184	8.31	8.33	5
186	1	39.93	39.93	0.77	0.009	8.10	8.22	19,23
187	1	75.49	15.10	2.39	0.019	8.29	8.61	14,17
188	0	70.95	-	-	0.160	8.26	8.39	10
189	-	-	-	-	-	-	-	-
190	1	2951.00	354.73	-	Int	9.88	9.50	26
191	-	-	-	-	-	-	-	-
192	-	-	-	-	-	-	-	-
193	1	30.01	12.70	0.44	0.221	7.89	8.16	10
194	1	873.20	260.82	1.84	0.068	9.35	9.13	2,13
195	0	68.92	-	-	0.566	8.25	8.44	5
196	1	72.01	14.40	3.05	0.032	8.27	8.37	14,17
197	1	305.80	129.45	3.84	0.293	8.90	9.02	12
198	1	47.76	20.22	0.38	0.371	8.08	8.26	13
199	-	-	-	-	-	-	-	-
200	1	922.10	393.55	11.90	0.008	9.38	8.99	4,24
201	1	1862.00	768.74	-	Int	9.68	9.41	27
202	-	-	-	-	-	-	-	-
203	1	76.30	32.30	1.86	0.300	8.30	8.40	14
204	1	1377.00	165.53	-	Int	9.55	9.33	26
205	1	1082.00	130.07	-	Int	9.45	9.25	26
206	1	170.60	72.21	2.25	0.249	8.65	8.96	10
207	1	168.90	39.00	9.93	0.156	8.64	8.69	1,17,20
208	1	295.10	35.47	-	Int	8.88	8.61	26
209	0	24.55	-	-	0.041	7.70	7.49	24
210	0	27.61	-	-	0.071	7.85	7.82	23
211	0	97.60	-	-	0.006	8.40	8.08	24
212	0	102.20	-	-	0.334	8.57	8.80	1
213	1	1672.00	427.86	-	Int	9.67	9.23	28
214	0	38.36	-	-	0.035	8.00	7.86	23

Continued on next page...

Table 11 – Continued

HRS (1)	sgn (2)	SCO (3) Jy km s $^{-1}$	err (4) Jy km s $^{-1}$	S/N (5)	ff (6)	$\log M(H_2)_c$ (7) M \odot	$\log M(H_2)_v$ (8) M \odot	Ref (9)
215	1	2229.00	920.26	-	Int	9.76	9.67	27
216	1	1050.00	498.78	-	MA	9.43	9.23	1
217	1	1869.00	224.67	-	Int	9.69	9.35	26
218	0	47.71	-	-	0.037	8.09	7.91	24
219	0	32.13	-	-	0.028	7.92	7.85	23
220	1	885.30	106.42	-	Int	9.36	9.01	26
221	1	151.90	64.30	1.12	0.103	8.60	8.58	10
222	-	-	-	-	-	-	-	-
223	-	-	-	-	-	-	-	-
224	1	106.30	45.00	0.41	0.774	8.44	8.39	2
225	-	-	-	-	-	-	-	-
226	-	-	-	-	-	-	-	-
227	-	-	-	-	-	-	-	-
228	-	-	-	-	-	-	-	-
229	0	7.47	-	-	0.242	7.29	7.61	23
230	1	101.90	43.13	1.91	0.277	8.42	8.55	10
231	0	59.31	-	-	0.011	8.19	7.94	23
232	-	-	-	-	-	-	-	-
233	1	245.60	103.96	3.77	0.515	8.80	8.90	5
234	0	40.32	-	-	0.017	8.02	7.83	23
235	0	27.57	-	-	0.029	7.85	7.83	23
236	0	88.62	-	-	0.007	8.36	8.03	23
237	1	216.50	91.64	3.46	0.367	8.75	8.88	15
238	-	-	-	-	-	-	-	-
239	1	254.50	107.73	2.10	0.253	8.82	8.90	10
240	0	27.77	-	-	0.042	7.86	7.76	23
241	1	31.38	35.58	0.18	0.003	7.91	7.55	19
242	0	128.20	-	-	0.143	8.52	8.49	1
243	0	83.20	-	-	0.013	8.33	8.16	23
244	1	881.20	363.81	-	Int	9.36	9.25	27
245	1	104.50	104.50	0.54	0.003	8.43	7.98	4,23
246	1	350.00	166.26	-	MA	8.96	8.83	1
247	1	1574.00	189.21	-	Int	9.61	9.43	26
248	0	25.35	-	-	0.048	7.82	7.72	23
249	-	-	-	-	-	-	-	-
250	-	-	-	-	-	-	-	-
251	1	2130.00	1011.81	-	MA	9.95	9.56	1
252	-	-	-	-	-	-	-	-
253	0	30.76	-	-	0.049	8.10	7.93	23
254	1	786.90	94.59	-	Int	9.31	9.22	26
255	1	9.24	10.48	0.79	0.036	7.38	7.63	17
256	1	346.70	69.34	1.72	0.073	8.90	8.83	1,6
257	0	172.30	-	-	0.045	8.65	8.43	10
258	0	138.30	-	-	0.004	8.59	8.15	19
259	1	123.90	91.71	6.56	0.046	8.51	8.65	2,15,17
260	1	200.00	95.01	-	MA	8.71	8.51	1
261	-	-	-	-	-	-	-	-
262	1	201.10	85.13	3.55	0.238	8.72	8.80	15
263	1	1950.00	926.30	-	MA	9.72	9.29	1
264	-	-	-	-	-	-	-	-
265	-	-	-	-	-	-	-	-
266	1	119.70	135.74	0.67	0.042	8.69	8.69	5
267	-	-	-	-	-	-	-	-
268	1	130.20	55.11	4.50	0.451	8.53	8.65	7
269	-	-	-	-	-	-	-	-
270	0	145.80	-	-	0.007	8.61	8.24	23
271	-	-	-	-	-	-	-	-
272	0	72.97	-	-	0.011	8.28	8.03	23
273	1	168.10	71.16	2.45	0.322	8.64	8.65	5
274	0	115.70	-	-	0.114	8.48	8.41	5
275	1	30.03	34.05	2.14	0.044	8.13	8.13	17
276	0	230.20	-	-	0.234	8.78	8.94	7
277	-	-	-	-	-	-	-	-
278	-	-	-	-	-	-	-	-
279	-	-	-	-	-	-	-	-
280	0	91.38	-	-	1.077	8.37	8.53	5
281	-	-	-	-	-	-	-	-
282	0	11.40	-	-	0.310	7.47	7.71	23
283	1	150.90	66.00	5.18	0.062	8.59	8.62	2,7,7
284	1	253.70	107.39	3.17	0.906	8.89	8.89	5
285	1	321.10	135.92	1.12	0.103	8.92	8.77	1
286	0	160.90	-	-	0.213	8.62	8.48	14

Continued on next page...

Table 11 – Continued

HRS (1)	sgn (2)	SCO (3) Jy km s $^{-1}$	err (4) Jy km s $^{-1}$	S/N (5)	ff (6)	$\log M(H_2)_c$ (7) M \odot	$\log M(H_2)_v$ (8) M \odot	Ref (9)
287	1	137.60	58.25	2.77	0.301	8.55	8.61	5
288	1	132.50	56.09	2.02	0.226	8.48	8.40	5
289	1	260.70	110.35	3.21	0.261	9.13	8.93	5
290	0	131.50	-	-	0.773	8.49	8.66	21
291	0	12.85	-	-	0.096	7.60	7.64	23
292	1	308.90	130.76	5.48	0.832	8.93	8.98	5
293	1	58.18	24.63	1.40	0.342	8.10	8.25	5
294	-	-	-	-	-	-	-	-
295	1	2425.00	291.50	-	Int	9.77	9.61	26
296	0	21.51	-	-	0.034	7.65	7.62	23
297	1	166.00	70.27	1.71	0.290	8.84	8.75	5
298	-	-	-	-	-	-	-	-
299	1	80.37	34.02	1.18	0.152	8.30	8.25	5
300	-	-	-	-	-	-	-	-
301	1	104.40	44.19	1.36	0.115	8.56	8.47	5
302	-	-	-	-	-	-	-	-
303	-	-	-	-	-	-	-	-
304	1	106.80	45.21	1.28	0.405	8.56	8.62	5
305	-	-	-	-	-	-	-	-
306	1	315.90	358.23	2.05	0.048	8.87	8.57	4
307	1	167.50	189.94	0.00	0.018	8.67	8.44	22
308	-	-	-	-	-	-	-	-
309	-	-	-	-	-	-	-	-
310	1	123.50	52.28	2.33	0.427	8.82	8.85	5
311	1	327.80	371.73	3.01	0.093	9.13	8.81	5
312	0	44.14	-	-	0.017	8.25	7.99	23
313	1	48.63	20.59	0.82	0.394	8.30	8.33	5
314	-	-	-	-	-	-	-	-
315	-	-	-	-	-	-	-	-
316	0	22.78	-	-	0.029	8.07	7.84	23
317	-	-	-	-	-	-	-	-
318	0	85.07	-	-	0.291	8.47	8.52	5
319	1	67.38	76.41	2.07	0.022	8.36	8.38	17
320	1	50.82	57.63	2.29	0.023	8.37	8.33	17
321	-	-	-	-	-	-	-	-
322	-	-	-	-	-	-	-	-
323	1	108.40	45.89	1.45	0.664	8.73	8.70	5

References to the CO data:

1: Young et al. (1995), 2: Stark et al. (1986), 3: Thronson et al. (1989), 4: Sage & Wrobel (1989), 5: This work, 6: Elfhag et al. (1996), 7: Albrecht et al. (2007), 8: Sauty et al. (2003), 9: Gondhalekar et al. (1998), 10: Boselli et al. (1995), 11: Welch & Sage (2003), 12: Smith & Madden (1997), 13: Sage (1993), 14: Boselli et al. (2002), 15: Leroy et al. (2005), 16: Bregman & Hogg (1988), 17: Böker et al. (2003), 18: Jaffe (1987), 19: Sage et al. (2007), 20: Kenney, private communication, 21: Jackson et al. (1989), 22: Braine et al. (1993), 23: Young et al. (2011), 24: Combes et al. (2007), 25: Wiklind et al. (1995), 26: Kuno et al. (2007), 27: Chung et al. (2009a), 28: Neining et al. (1996).

Table 12. HI data.

HRS	sgn	rms mJy	SHI Jy km s^{-1}	$\log M(HI)$ M_{\odot}	WHI km s^{-1}	$HI - def$	flag	Ref
(1)	(2)	(3)	(4)	(5)	(6)	(7)	(8)	(9)
1	-	-	-	-	-	-	-	-
2	1	2.55	3.32	8.42	185	0.07	1	1
3	1	-	6.79	8.65	388	0.38	1	3
4	1	-	15.00	8.98	475	0.57	2	4
5	1	1.14	2.41	8.20	286	0.66	1	2
6	1	9.42	9.29	8.89	177	0.62	1	2
7	0	1.05	1.57	8.12	-	1.02	-	2
8	1	13.74	51.37	9.66	394	0.07	1	2
9	1	1.37	4.65	8.65	250	0.49	1	2
10	1	-	5.25	8.76	178	0.12	2	6
11	1	1.21	7.33	8.79	138	0.24	1	2
12	1	2.19	1.83	8.23	76	0.06	1	1
13	1	3.81	17.70	9.32	377	0.25	1	2
14	1	0.31	0.72	7.79	214	1.43	1	2
15	1	2.72	114.44	9.97	334	-0.15	1	1
16	1	2.62	18.09	9.14	157	0.01	1	1
17	1	2.55	33.30	9.42	268	-0.09	1	2
18	1	1.42	2.78	8.54	113	0.59	1	2
19	1	5.05	16.21	9.32	58	-0.18	1	2
20	1	4.01	23.52	9.47	175	-0.32	1	2
21	1	2.24	2.85	8.28	175	0.72	1	1
22	1	1.94	1.37	8.12	369	1.14	1	1
23	1	-	13.70	9.17	346	0.32	1	7
24	1	16.11	91.32	10.04	338	-0.37	1	2
25	1	2.86	22.24	9.24	305	-0.08	1	2
26	1	1.04	3.05	8.56	174	0.44	1	8
27	1	1.07	2.89	8.62	121	0.03	1	2
28	1	2.19	8.34	8.85	232	0.05	1	1
29	1	1.38	5.96	8.54	206	0.37	1	2
30	1	2.11	22.32	9.12	201	0.12	1	2
31	1	-	64.80	9.77	387	-0.12	2	4
32	1	0.70	1.29	7.92	184	0.82	1	5
33	1	2.47	26.14	9.41	130	-0.10	1	1
34	1	0.89	22.49	9.14	295	0.17	1	2
35	-	-	-	-	-	-	-	-
36	1	2.04	4.86	8.74	190	0.60	1	1
37	1	1.96	7.69	8.84	194	0.04	1	1
38	1	2.44	10.44	9.00	191	0.03	1	1
39	1	2.14	11.46	9.13	236	0.16	1	1
40	1	2.94	8.58	9.02	199	0.30	1	1
41	1	1.19	4.21	8.54	184	0.38	1	2
42	1	2.20	35.70	9.39	113	0.08	1	1
43	1	0.30	0.21	7.09	141	1.89	2	9
44	1	1.41	3.89	8.37	48	0.34	1	5
45	1	1.81	6.79	8.89	308	0.22	1	2
46	1	1.30	9.84	9.02	296	0.07	1	2
47	1	2.13	18.99	9.32	192	-0.15	1	1
48	1	-	50.70	9.51	103	0.09	1	10
49	0	8.12	12.18	8.96	-	0.29	-	11
50	1	2.75	15.85	9.23	284	-0.32	1	2
51	1	1.51	25.14	9.31	178	-0.29	1	2
52	1	5.12	32.19	9.35	184	-0.65	1	2
53	1	2.39	44.96	9.39	250	0.05	1	1
54	1	2.00	34.80	9.41	154	-0.15	1	12
55	1	5.00	29.20	9.27	204	0.08	1	7
56	1	3.06	8.27	9.06	341	0.09	1	2
57	1	2.00	12.70	8.91	182	0.50	1	7
58	1	-	3.60	8.29	144	0.61	1	13
59	1	2.34	12.37	9.24	403	0.38	1	1
60	1	14.84	54.81	9.47	456	-0.29	1	2
61	1	3.63	14.52	9.01	205	-0.08	1	2
62	1	16.86	37.90	9.65	258	-0.17	1	2
63	1	8.74	27.24	9.34	286	0.27	1	2
64	1	5.72	8.15	8.76	216	0.24	1	2
65	1	11.16	20.32	9.27	172	-0.18	1	2
66	1	4.08	24.28	9.40	285	-0.05	1	2
67	1	5.00	9.28	8.96	125	0.06	1	14
68	1	3.19	1.07	8.01	103	0.27	1	2
69	1	-	46.82	9.49	463	-0.03	1	15
70	1	-	6.68	8.92	162	0.16	2	16
71	-	-	-	-	-	-	-	-

Continued on next page...

Table 12. HI data.

HRS	sgn	rms mJy	SHI Jy km s $^{-1}$	$\log M(HI)$ M $_{\odot}$	WHI km s $^{-1}$	$HI - def$	flag	Ref
(1)	(2)	(3)	(4)	(5)	(6)	(7)	(8)	(9)
72	1	10.00	14.31	9.23	194	-0.27	2	17
73	1	10.28	47.79	9.40	402	0.36	1	2
74	1	-	22.54	9.12	186	0.10	1	18
75	0	9.90	14.85	9.07	-	-0.28	-	14
76	1	10.00	7.80	8.63	134	0.24	1	19
77	1	5.77	64.15	9.82	325	-0.14	1	2
78	1	-	22.10	9.23	105	-0.30	1	20
79	1	1.97	12.18	9.12	197	0.28	1	1
80	1	2.23	5.03	8.53	85	0.77	1	1
81	1	3.27	17.73	9.08	306	0.19	1	2
82	1	2.07	1.72	8.07	125	0.37	1	1
83	1	-	1.70	8.09	114	0.68	1	21
84	1	2.45	4.86	8.52	226	0.38	1	1
85	1	12.19	43.74	9.38	375	0.26	1	2
86	1	15.00	50.94	9.54	198	-0.21	1	22
87	0	0.56	0.84	7.76	-	1.48	-	23
88	1	13.00	55.20	9.58	200	0.05	2	44
89	1	2.81	62.20	9.63	250	-0.09	1	1
90	0	1.56	2.34	8.20	-	0.98	-	23
91	1	2.25	74.14	9.70	459	0.18	1	1
92	1	1.79	10.49	8.85	294	0.28	1	1
93	1	-	48.11	9.44	238	-0.41	1	15
94	1	2.11	40.52	9.44	270	0.23	1	1
95	1	2.47	6.57	8.65	193	0.27	1	1
96	1	2.20	13.92	8.98	253	0.40	1	1
97	1	2.74	31.56	9.33	512	0.67	1	1
98	1	2.50	18.68	9.10	221	0.25	1	1
99	1	2.11	1.04	7.85	117	0.91	1	1
100	1	1.87	3.44	8.37	230	0.81	1	1
101	0	0.80	1.20	7.82	-	1.24	-	24
102	1	2.42	77.05	9.72	224	0.06	1	1
103	0	0.76	1.14	8.15	-	1.36	-	25
104	-	-	-	-	-	-	-	-
105	1	1.66	8.65	8.77	401	-0.14	1	1
106	1	2.41	5.04	8.80	123	0.40	1	1
107	1	2.29	4.05	8.44	250	0.46	1	1
108	1	2.22	1.10	8.14	167	0.93	1	1
109	1	2.24	23.17	9.20	348	0.21	1	2
110	1	2.86	29.79	9.31	191	0.04	1	1
111	1	1.92	18.26	9.09	295	0.28	1	2
112	0	1.10	1.65	8.31	-	0.94	-	26
113	1	2.27	32.63	9.35	359	0.50	1	1
114	1	3.14	84.71	9.76	153	0.05	1	1
115	1	2.38	0.80	7.74	268	1.14	1	1
116	0	0.89	1.33	7.96	-	1.24	-	23
117	1	2.30	1.32	8.22	307	1.50	1	1
118	1	2.73	21.35	9.16	115	-0.26	1	1
119	1	2.45	1.93	8.12	212	1.42	1	1
120	1	2.07	1.66	8.05	257	1.49	1	1
121	1	2.48	9.55	9.08	310	0.37	1	1
122	1	2.90	48.86	9.52	246	0.46	1	1
123	1	2.73	9.11	8.79	309	0.33	1	1
124	1	2.64	6.92	8.67	236	0.92	1	1
125	0	2.40	3.60	8.65	-	0.38	-	1
126	0	0.67	1.00	7.84	-	1.30	-	23
127	1	2.25	5.49	8.84	323	0.63	1	1
128	1	2.16	2.21	8.44	154	0.65	1	1
129	0	0.78	1.17	7.90	-	1.15	-	23
130	1	2.43	5.57	8.58	91	0.68	1	1
131	1	2.19	1.78	8.35	54	0.62	1	1
132	1	2.46	7.06	8.94	81	0.16	1	1
133	1	-	22.29	9.23	212	0.19	2	28
134	1	2.17	0.92	8.06	232	1.46	1	1
135	0	2.40	3.60	8.65	-	1.41	-	1
136	1	0.70	0.71	7.95	298	1.20	1	27
137	0	0.78	1.17	7.90	-	1.51	-	23
138	0	2.40	3.60	8.39	-	1.55	-	1
139	1	2.28	6.16	8.89	140	0.18	1	1
140	1	2.53	11.80	8.90	335	0.37	1	1
141	1	2.09	2.61	8.51	263	1.14	1	1
142	1	2.50	44.20	9.48	200	-0.28	1	20

Continued on next page...

Table 12. HI data.

HRS	sgn	rms mJy	SHI Jy km s^{-1}	$\log M(HI)$ M_{\odot}	WHI km s^{-1}	$HI - def$	flag	Ref
(1)	(2)	(3)	(4)	(5)	(6)	(7)	(8)	(9)
143	1	2.59	27.42	9.53	276	-0.06	1	1
144	1	2.68	7.57	8.71	356	0.98	1	1
145	1	2.75	7.27	8.96	124	0.42	1	1
146	1	2.26	4.67	8.76	177	0.40	1	1
147	1	1.54	7.71	8.72	308	0.45	1	2
148	1	2.66	16.55	9.05	188	0.20	1	1
149	1	2.62	7.73	8.72	234	0.83	1	1
150	1	2.75	1.31	7.95	178	2.08	1	1
151	1	3.45	3.16	8.33	157	0.92	1	1
152	1	2.65	3.69	8.40	113	0.75	1	1
153	1	2.50	4.22	8.46	129	0.53	1	1
154	1	2.71	21.03	9.42	78	0.03	1	1
155	0	0.78	1.17	8.16	-	1.21	-	23
156	1	2.51	1.44	7.99	182	1.36	1	1
157	1	2.30	11.51	8.89	178	0.28	1	2
158	1	2.86	14.99	9.27	165	0.11	1	1
159	1	3.10	3.49	8.64	57	0.98	1	1
160	1	2.40	6.60	8.92	135	0.65	1	1
161	0	0.89	1.33	7.96	-	1.81	-	23
162	0	0.67	1.00	7.84	-	1.14	-	23
163	1	4.14	8.01	8.74	239	1.20	1	1
164	0	0.89	1.33	7.96	-	1.10	-	23
165	1	2.40	2.06	8.41	187	0.68	1	1
166	0	0.78	1.17	8.16	-	1.47	-	23
167	1	2.25	0.81	8.00	211	1.45	1	1
168	1	2.78	15.78	9.29	172	-0.03	1	1
169	1	-	2.15	8.48	111	0.31	2	29
170	1	2.90	6.60	8.65	302	0.99	1	20
171	1	2.58	2.84	8.55	203	0.78	1	1
172	1	2.04	1.19	7.91	183	1.48	1	1
173	1	4.18	3.97	8.43	113	0.95	1	2
174	0	2.40	3.60	8.39	-	0.70	-	1
175	0	0.44	0.66	7.65	-	1.47	-	30
176	1	2.66	0.35	7.64	32	1.88	1	1
177	1	2.39	7.30	8.70	131	0.32	1	1
178	0	2.40	3.60	8.39	-	1.56	-	1
179	0	2.40	3.60	8.39	-	0.84	-	1
180	0	0.67	1.00	7.84	-	1.30	-	23
181	0	2.40	3.60	8.39	-	0.25	-	1
182	1	2.35	11.31	8.89	304	0.05	1	1
183	0	2.40	3.60	8.39	-	1.61	-	1
184	0	0.57	0.85	7.77	-	1.27	-	30
185	1	2.19	0.61	7.62	177	1.43	1	1
186	0	2.40	3.60	8.47	-	0.96	-	1
187	1	2.80	43.41	9.47	148	-0.01	1	1
188	1	2.39	19.14	9.12	180	0.04	1	2
189	1	2.24	3.60	8.39	119	0.42	1	1
190	1	2.28	29.10	9.30	506	0.58	1	1
191	1	1.60	2.35	8.20	166	0.55	1	31
192	0	0.60	0.90	7.79	-	1.31	-	32
193	1	2.16	4.00	8.44	113	0.66	1	1
194	1	16.07	138.30	9.97	301	-0.00	1	2
195	0	2.40	3.60	8.39	-	0.71	-	1
196	1	2.79	46.92	9.50	164	-0.21	1	1
197	1	2.53	7.17	8.69	204	0.68	1	1
198	1	1.46	9.94	8.82	141	0.36	1	2
199	1	1.68	1.20	7.91	108	1.00	1	1
200	0	0.70	1.05	7.85	-	1.80	-	27
201	1	6.50	108.50	9.87	354	-0.12	1	33
202	0	2.40	3.60	8.39	-	-0.17	-	1
203	1	2.49	41.56	9.45	183	-0.36	1	1
204	1	2.96	71.66	9.69	265	0.32	1	1
205	1	15.00	74.90	9.71	354	0.15	2	6
206	1	2.12	1.39	7.98	84	0.96	1	1
207	1	2.22	4.64	8.50	106	0.60	1	1
208	1	1.84	10.18	8.84	229	0.94	1	1
209	1	2.80	3.38	8.25	358	0.72	2	17
210	0	2.40	3.60	8.39	-	0.82	-	1
211	0	2.40	3.60	8.39	-	1.29	-	1
212	1	1.29	26.16	9.40	107	-0.53	1	2
213	1	3.60	259.15	10.28	504	-0.01	1	1

Continued on next page...

Table 12. HI data.

HRS	sgn	rms mJy	SHI Jy km s^{-1}	$\log M(HI)$ M_{\odot}	WHI km s^{-1}	$HI - def$	flag	Ref
(1)	(2)	(3)	(4)	(5)	(6)	(7)	(8)	(9)
214	0	2.40	3.60	8.39	-	0.89	-	1
215	1	0.36	15.64	9.03	192	0.35	1	34
216	1	0.36	25.11	9.23	309	0.44	1	34
217	1	2.43	11.15	8.88	377	1.05	1	1
218	0	0.67	1.00	7.84	-	1.29	-	23
219	0	0.56	0.84	7.76	-	1.42	-	23
220	1	2.24	9.67	8.82	355	0.98	1	1
221	1	2.04	0.58	7.60	150	1.50	1	1
222	1	2.16	0.40	7.44	110	1.61	1	1
223	1	2.32	3.05	8.32	145	0.58	1	1
224	1	2.07	1.56	8.03	246	1.43	1	1
225	1	2.18	1.00	7.83	65	1.28	1	1
226	1	2.00	3.54	8.38	295	0.79	1	1
227	1	18.78	162.65	9.95	196	-0.44	1	2
228	-	-	-	-	-	-	-	-
229	1	0.70	0.26	7.25	107	1.61	2	32
230	1	1.75	7.10	8.68	134	0.54	1	1
231	0	0.50	0.75	7.71	-	1.65	-	30
232	1	2.09	0.79	7.73	139	1.81	1	1
233	1	2.31	3.25	8.34	177	1.20	1	1
234	0	0.89	1.33	7.96	-	1.32	-	23
235	0	0.78	1.17	7.90	-	0.84	-	23
236	0	2.40	3.60	8.39	-	1.34	-	1
237	1	2.76	7.53	8.71	130	0.31	1	1
238	1	-	29.20	9.24	142	-0.57	1	35
239	1	2.14	7.59	8.71	263	0.45	1	1
240	0	0.89	1.33	7.96	-	0.73	-	23
241	1	-	14.65	9.00	668	0.90	2	29
242	1	2.28	19.00	9.11	275	0.31	1	1
243	1	3.00	1.70	8.06	349	0.94	1	23
244	1	2.94	7.86	8.73	161	0.40	1	1
245	0	2.40	3.60	8.39	-	1.02	-	1
246	1	15.24	62.99	9.63	358	-0.20	1	2
247	1	2.52	50.59	9.54	284	-0.05	1	1
248	0	2.40	3.60	8.39	-	0.25	-	1
249	1	2.10	1.00	7.83	67	1.49	1	1
250	0	14.87	22.30	9.18	-	0.13	-	36
251	1	3.14	81.10	9.95	384	-0.21	1	2
252	1	2.86	11.90	9.18	135	-0.28	1	2
253	1	3.79	1.56	8.22	-	0.92	-	2
254	1	2.09	8.36	8.76	178	0.99	1	1
255	1	2.23	31.65	9.33	42	0.08	1	1
256	1	3.40	4.74	8.46	132	0.75	2	17
257	1	3.19	30.06	9.31	413	0.29	1	1
258	-	-	-	-	-	-	-	-
259	1	27.50	55.60	9.58	177	-0.28	2	28
260	1	2.28	0.84	7.76	296	1.52	1	1
261	1	-	8.24	8.73	226	0.52	2	26
262	1	2.71	47.65	9.51	160	-0.29	1	1
263	1	4.06	116.03	9.91	384	-0.03	1	1
264	1	2.08	3.20	8.40	177	0.48	1	2
265	-	-	-	-	-	-	-	-
266	1	17.70	131.20	10.15	211	-0.35	1	2
267	1	2.51	28.55	9.28	176	0.06	1	1
268	1	2.43	17.60	9.08	330	0.15	1	1
269	0	0.89	1.33	7.96	-	1.44	-	23
270	0	3.29	4.93	8.56	-	1.07	-	2
271	1	2.66	13.07	8.95	172	0.23	1	1
272	0	2.40	3.60	8.39	-	1.43	-	1
273	1	12.52	12.62	8.93	276	0.42	1	2
274	1	0.44	15.10	9.01	463	0.24	2	37
275	1	5.34	36.86	9.64	93	-0.49	1	2
276	1	2.40	8.81	8.78	213	0.42	1	1
277	1	2.21	0.87	7.77	235	0.85	1	1
278	1	2.19	0.74	7.65	128	1.67	1	1
279	1	11.23	23.70	9.21	187	-0.01	1	2
280	1	0.47	6.09	8.62	376	0.44	1	38
281	1	2.08	1.96	8.13	58	0.33	1	1
282	0	2.40	3.60	8.39	-	-0.30	-	1
283	1	2.21	69.65	9.68	259	-0.58	1	1
284	1	-	10.50	8.93	255	0.00	1	39

Continued on next page...

Table 12. HI data.

HRS	sgn	rms mJy	SHI Jy km s^{-1}	$\log M(HI)$ M_{\odot}	WHI km s^{-1}	$HI - def$	flag	Ref
(1)	(2)	(3)	(4)	(5)	(6)	(7)	(8)	(9)
285	1	0.55	2.56	8.24	373	1.31	1	2
286	1	9.99	29.36	9.30	521	0.23	1	2
287	1	3.38	14.49	8.99	185	0.05	1	2
288	1	2.68	5.41	8.51	292	0.82	1	2
289	1	14.12	35.61	9.68	249	-0.16	1	2
290	1	2.70	6.10	8.58	90	0.37	1	2
291	1	4.73	3.33	8.43	98	0.51	1	2
292	1	-	14.60	9.02	220	0.17	2	41
293	1	2.94	15.73	8.96	142	-0.10	1	2
294	1	2.97	6.23	8.89	252	0.50	1	2
295	1	3.09	73.58	9.67	267	0.08	1	1
296	0	3.86	5.79	8.50	-	0.35	-	40
297	1	10.29	32.83	9.55	302	0.13	1	2
298	1	-	9.80	8.98	163	-0.41	1	39
299	1	2.75	16.76	9.04	201	0.38	1	1
300	1	-	2.80	8.39	256	0.65	1	39
301	1	6.47	32.91	9.48	209	0.12	1	2
302	1	2.67	17.44	9.24	179	0.34	1	1
303	-	-	-	-	-	-	-	-
304	1	2.42	4.87	8.64	273	0.84	1	1
305	1	2.07	0.61	7.60	73	1.38	1	1
306	1	2.76	1.87	8.06	572	1.28	1	1
307	1	2.76	52.35	9.59	270	0.25	1	1
308	0	2.40	3.60	8.31	-	0.39	-	1
309	1	-	13.04	9.08	207	-0.10	2	6
310	1	2.53	7.22	9.01	228	0.71	1	1
311	1	2.57	11.12	9.08	410	0.72	1	1
312	1	0.44	0.27	7.45	228	1.84	2	9
313	1	-	10.50	9.05	240	0.52	1	7
314	1	5.99	20.07	9.27	207	-0.18	1	2
315	1	-	20.05	9.30	193	0.47	2	41
316	1	1.25	0.68	7.96	122	1.22	1	42
317	1	1.60	4.72	8.82	197	0.23	1	2
318	1	2.69	21.38	9.29	180	-0.15	1	1
319	1	1.92	38.09	9.53	189	-0.10	1	1
320	1	2.83	39.81	9.68	93	-0.26	1	1
321	1	-	3.76	8.66	208	0.24	2	43
322	1	4.63	64.59	9.85	115	-0.27	1	1
323	1	2.74	17.65	9.36	305	0.06	1	1

References to the HI data:

1: Haynes et al. (2011), 2: Springob et al. (2005), 3: Chamaroux et al. (1987), 4: Davis & Seaquist (1983), 5: Bica & Giovanelli (1987), 6: Peterson (1979), 7: Helou et al. (1982), 8: Bica & Giovanelli (1986), 9: Lake & Schommer (1984), 10: Staveley-Smith & Davies (1988), 11: Krumm & Salpeter (1979), 12: Helou et al. (1981), 13: O'Neil (2004), 14: Schneider et al. (1992), 15: Noordermeer et al. (2005), 16: Courtois et al. (2009), 17: Richter & Huchtmeier (1987), 18: Huchtmeier & Seiradakis (1985), 19: Huchtmeier et al. (2005), 20: Helou et al. (1984), 21: Lu et al. (1993), 22: Bottinelli et al. (1982), 23: Giovanardi et al. (1983a), 24: Wardle & Knapp (1986), 25: van Driel et al. (2000), 26: Hoffman et al. (1989), 27: Taylor et al. (2012), 28: Fisher & Tully (1981), 29: Bottinelli et al. (1990), 30: Magri (1994), 31: Hoffman et al. (1987), 32: Haynes & Giovanelli (1986), 33: Wong et al. (2006), 34: Chung et al. (2009b), 35: Koribalski et al. (2004), 36: Giovanardi et al. (1983b), 37: Haynes et al. (2000), 38: Gavazzi et al. (2005), 39: Theureau et al. (1998), 40: Haynes & Giovanelli (1991), 41: de Vaucouleurs et al. (1991), 42: Lewis (1987), 43: Huchtmeier & Richter (1989), 44: Smoker et al. (2000).

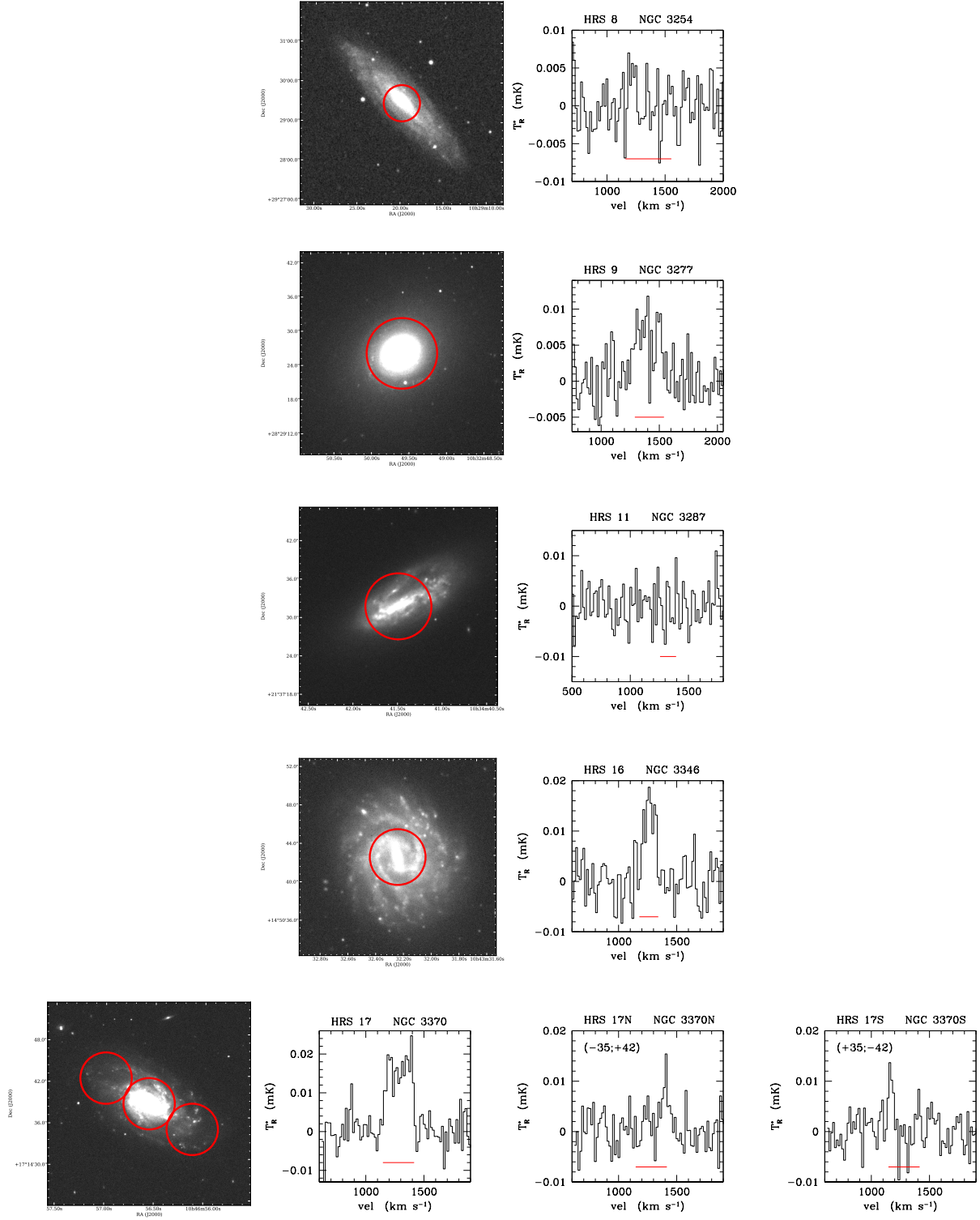


Fig. 9. CO data of the HRS galaxies observed in this work, in order of increasing HRS name. Left: the r -band SDSS image of the observed galaxies with superimposed the position covered by the beam of the telescope (red solid line). Right: observed $^{12}\text{CO}(1-0)$ spectra smoothed to a velocity resolution of 15.7 km s^{-1} . Intensities are in T_R^* scale.

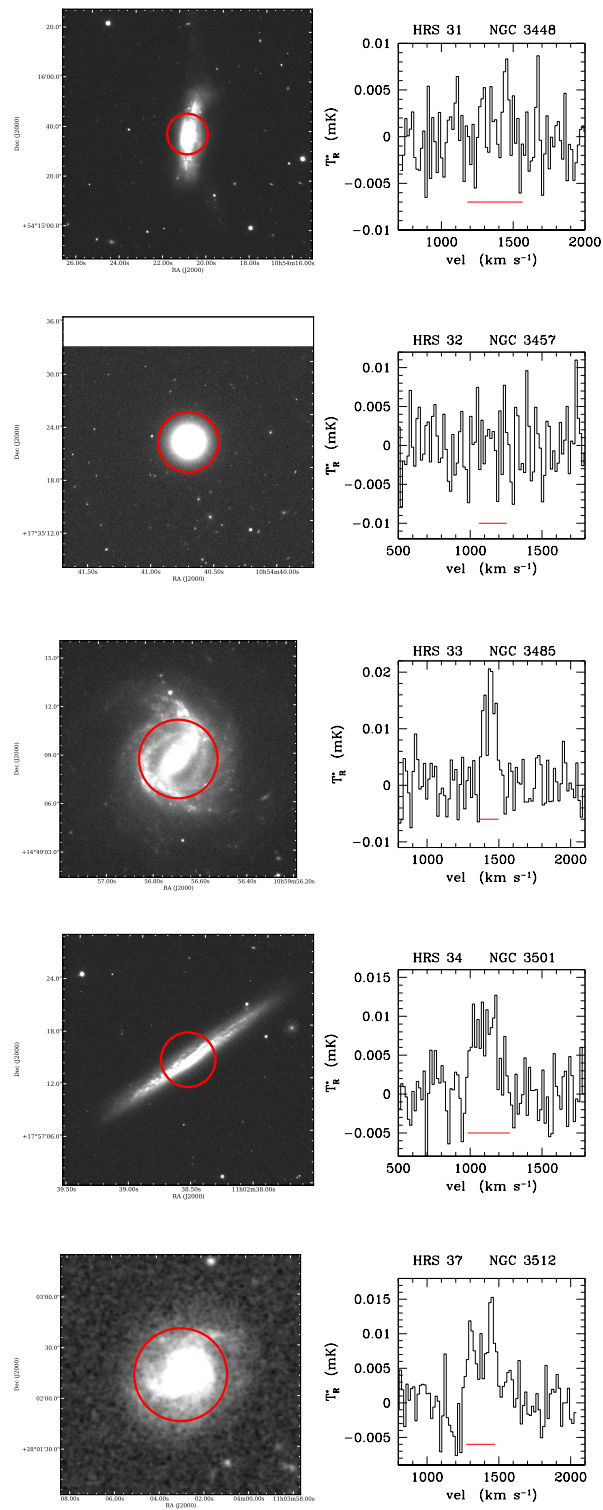


Fig. 9. Continued.

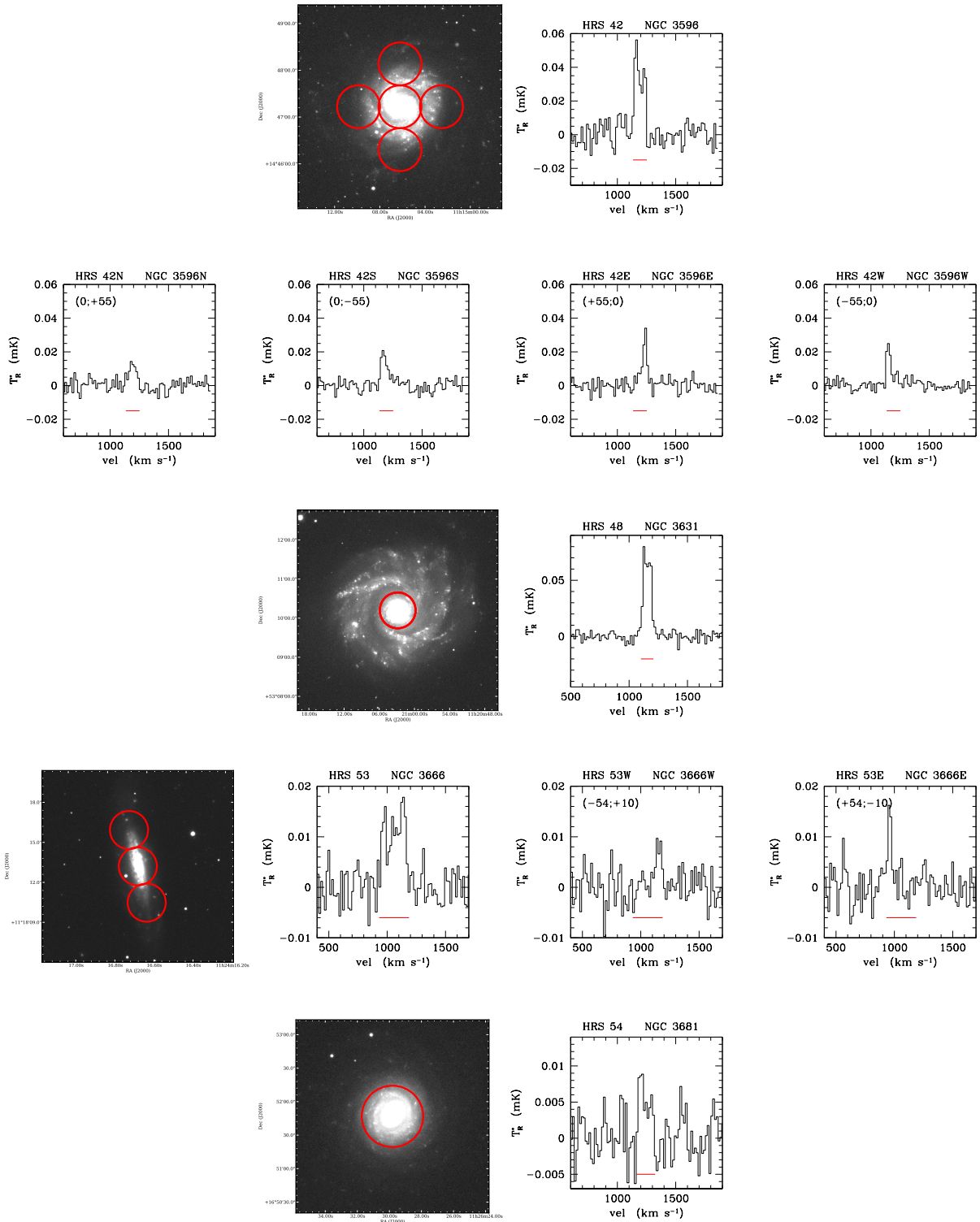


Fig. 9. Continued.

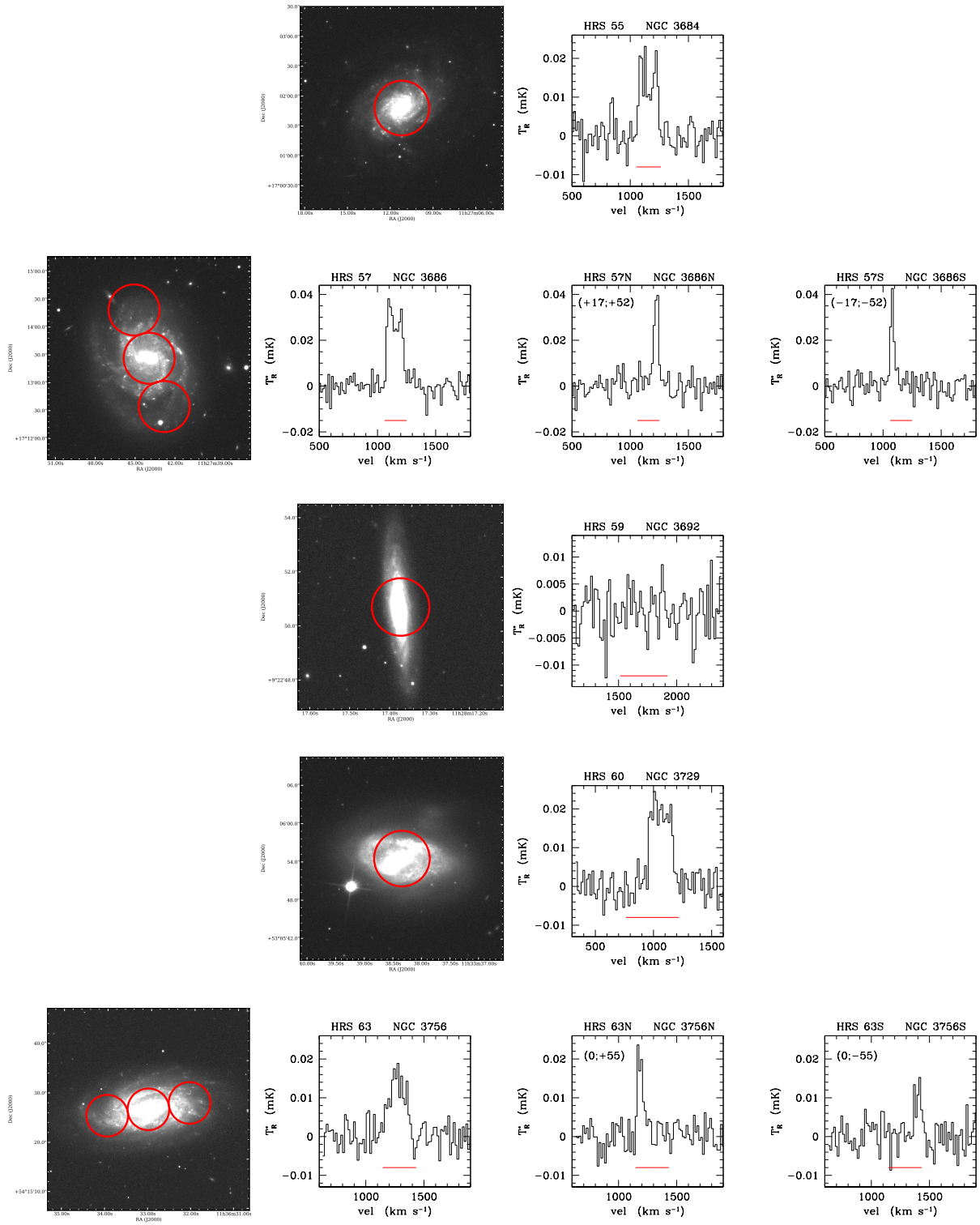


Fig. 9. Continued.

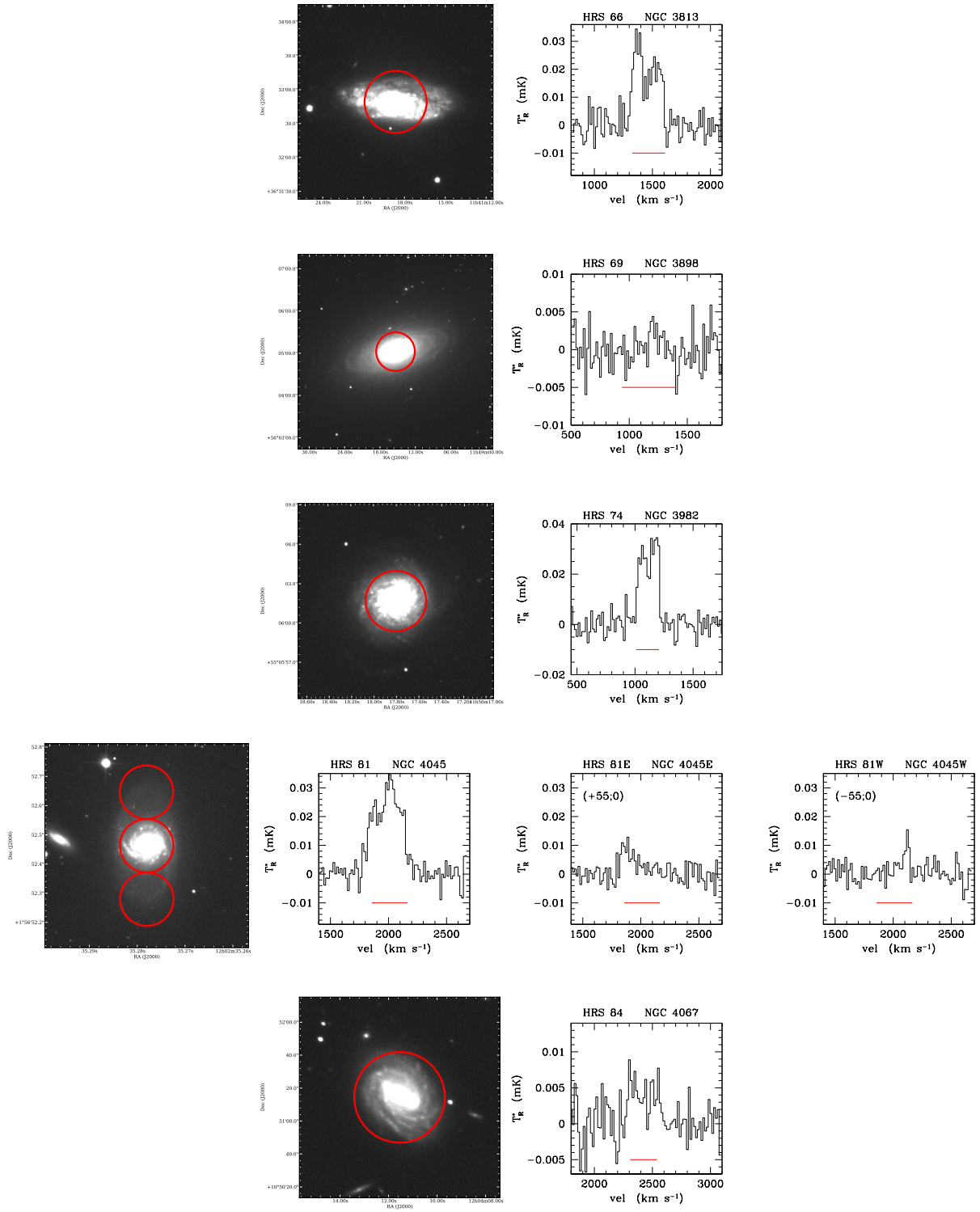


Fig. 9. Continued.

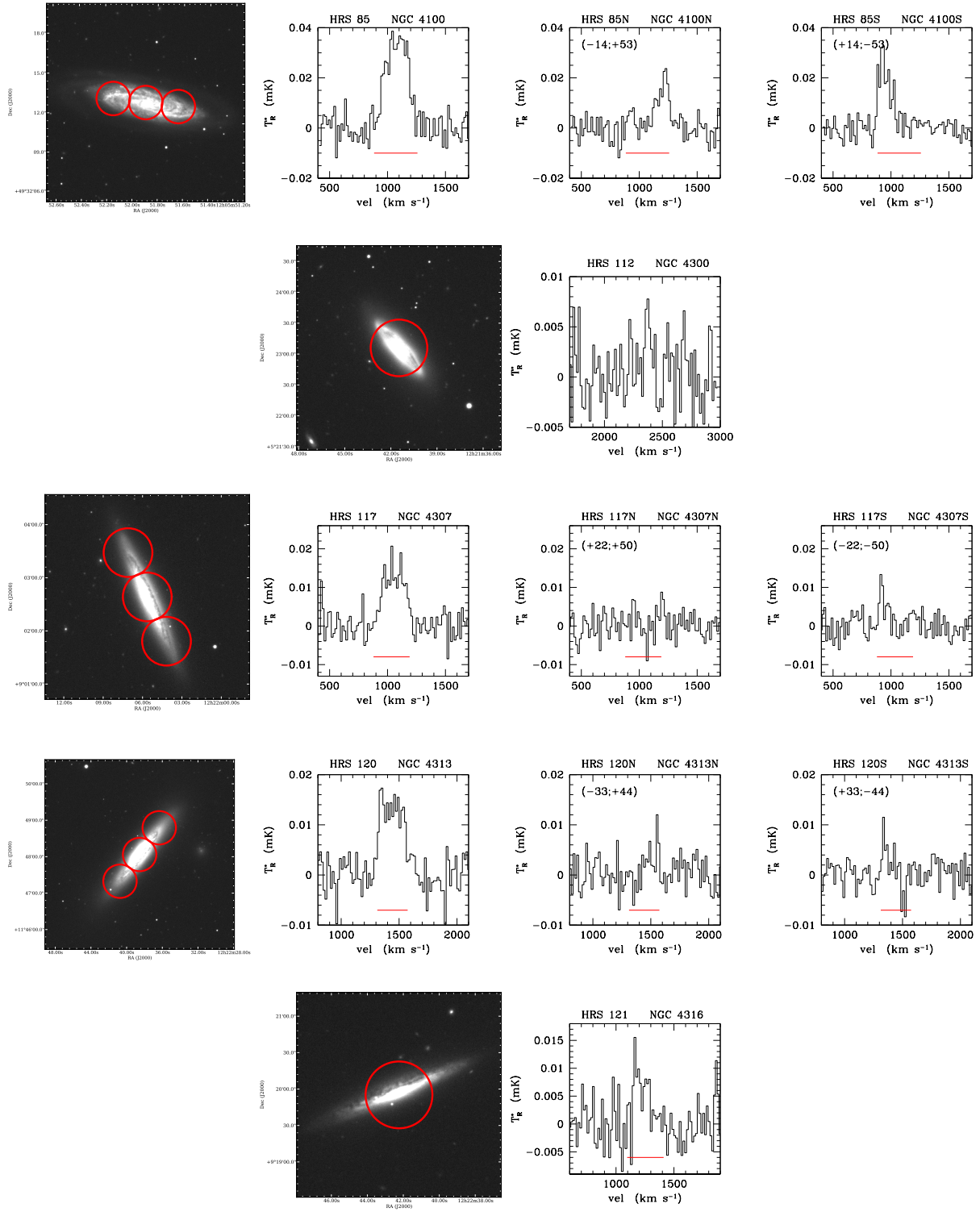


Fig. 9. Continued.

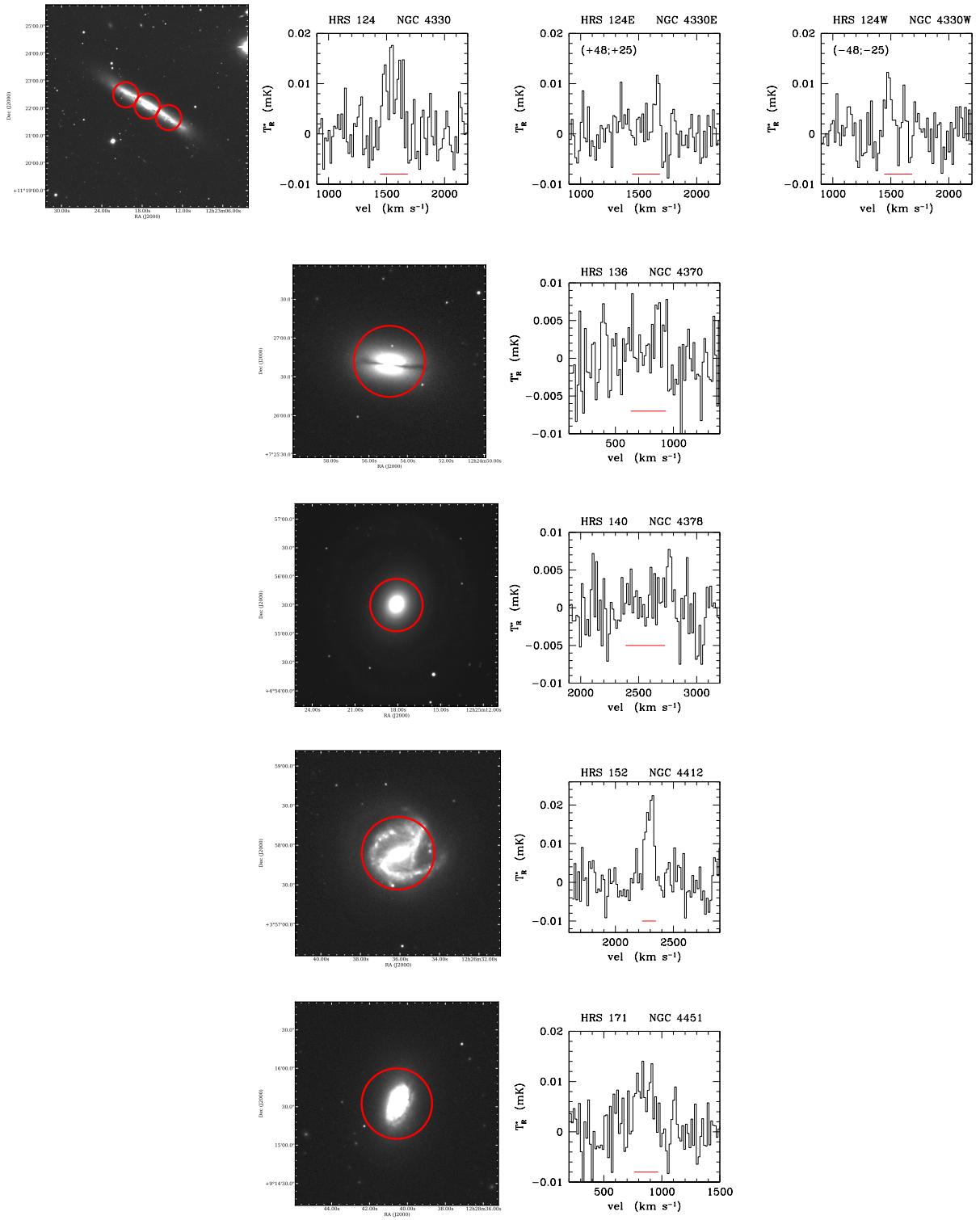


Fig. 9. Continued.

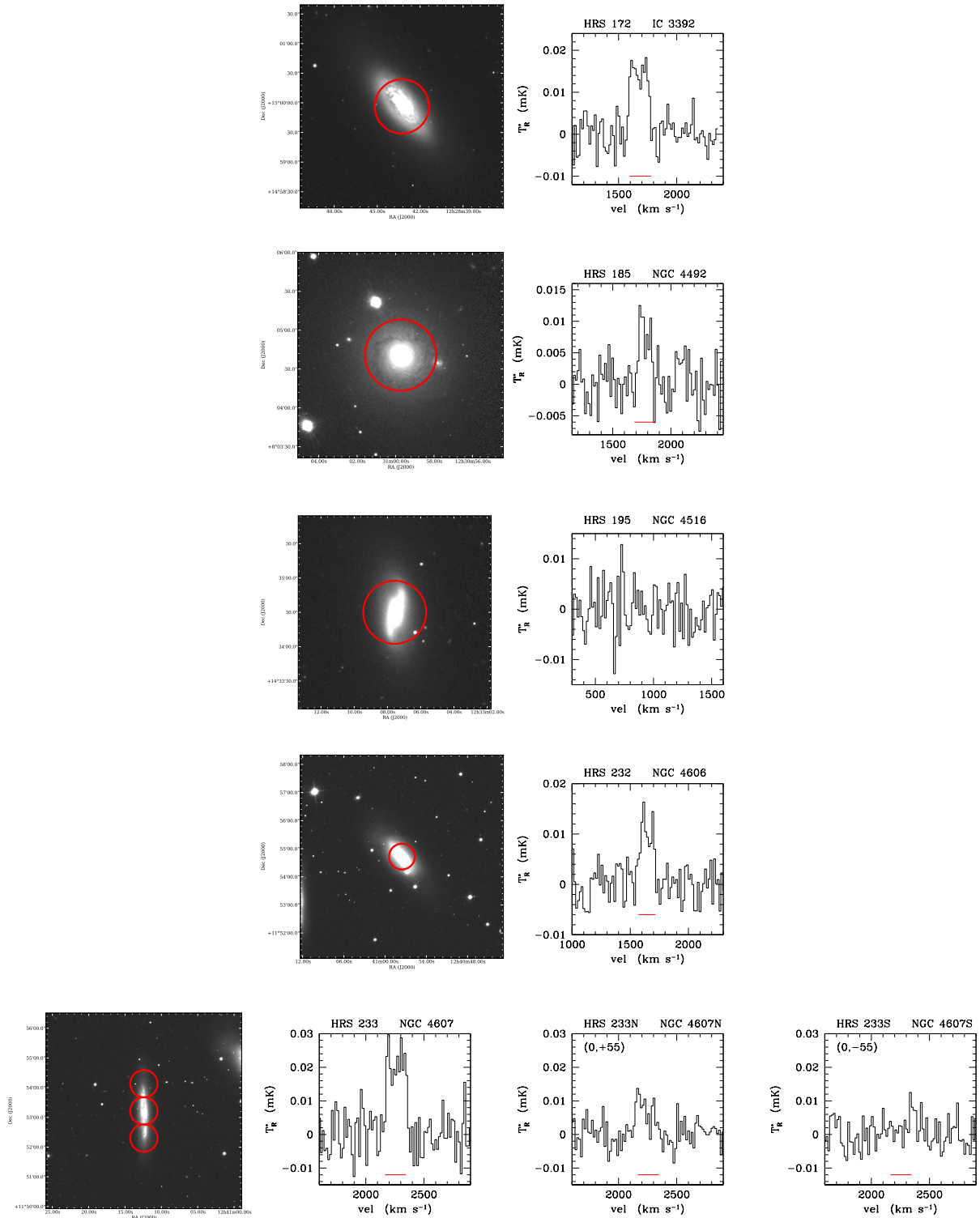


Fig. 9. Continued.

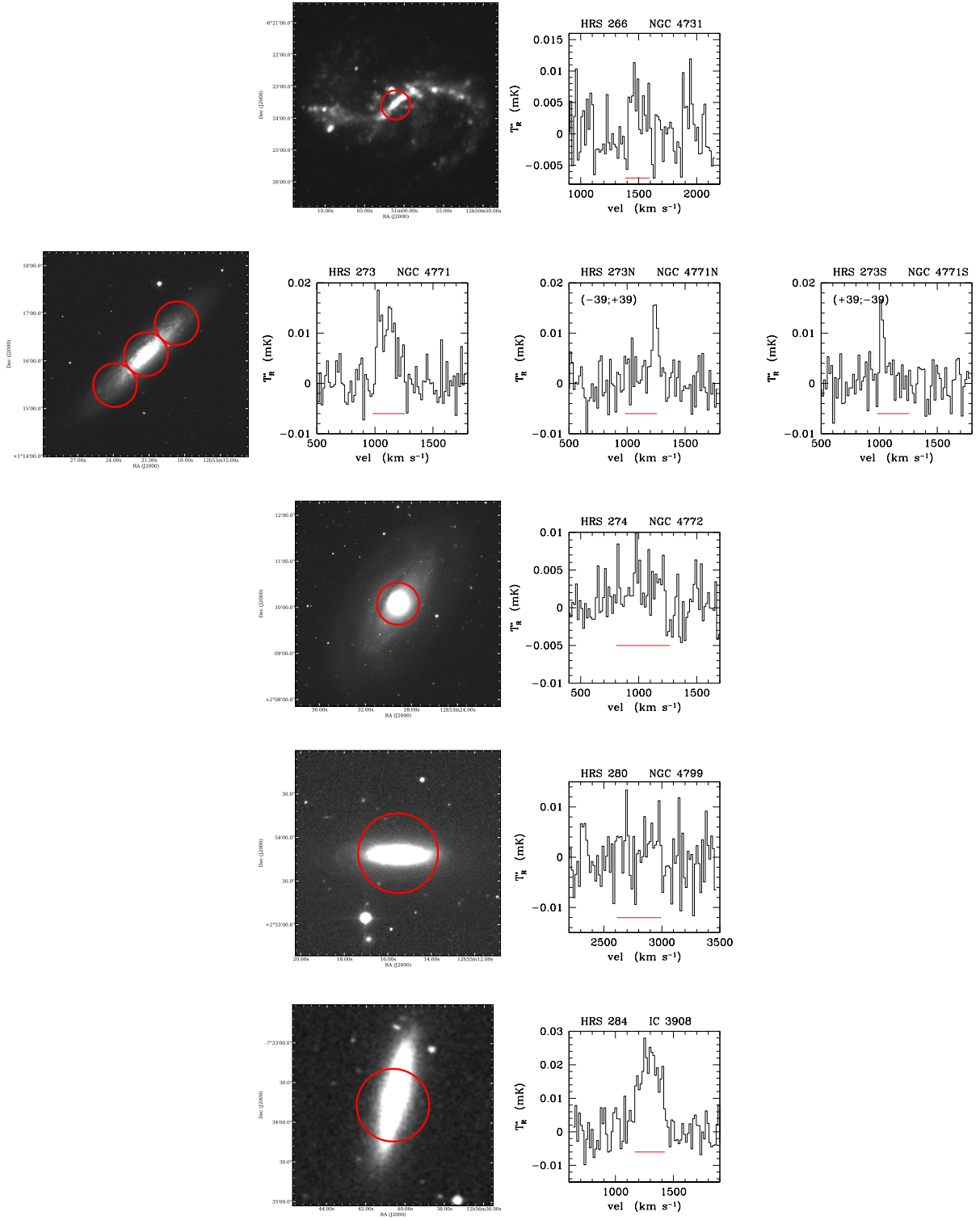


Fig. 9. Continued.

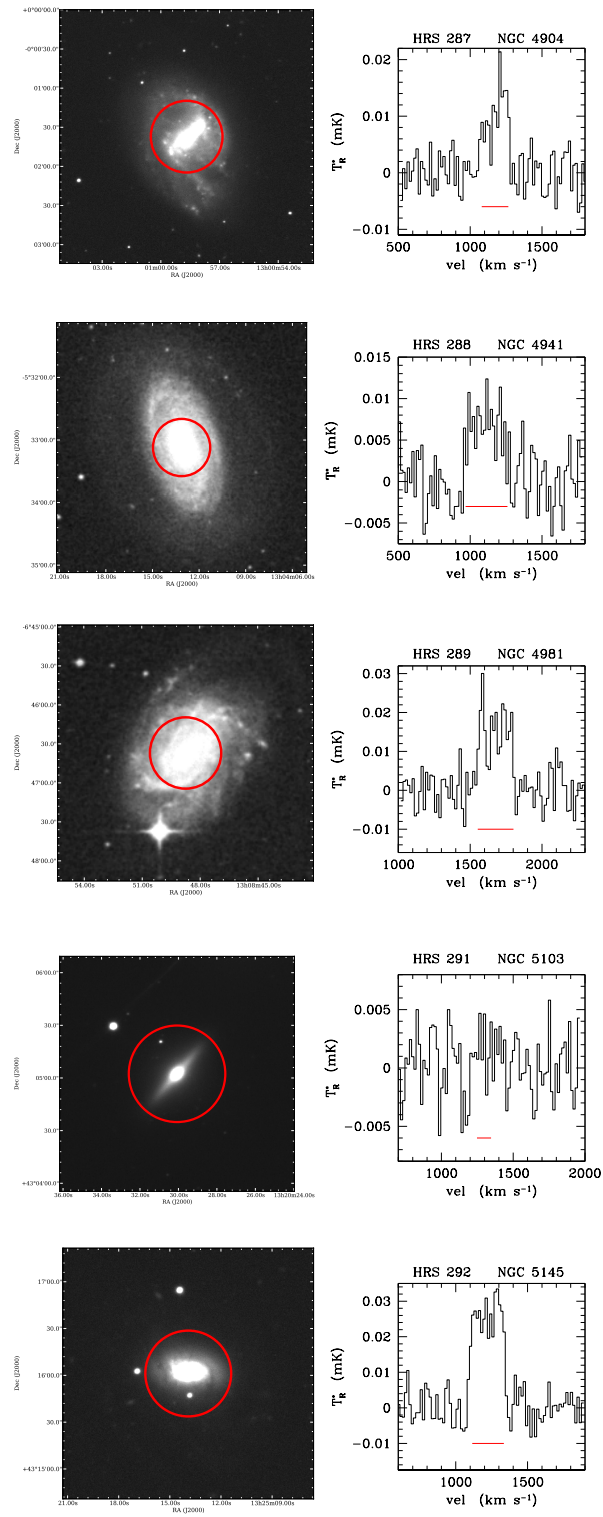


Fig. 9. Continued.

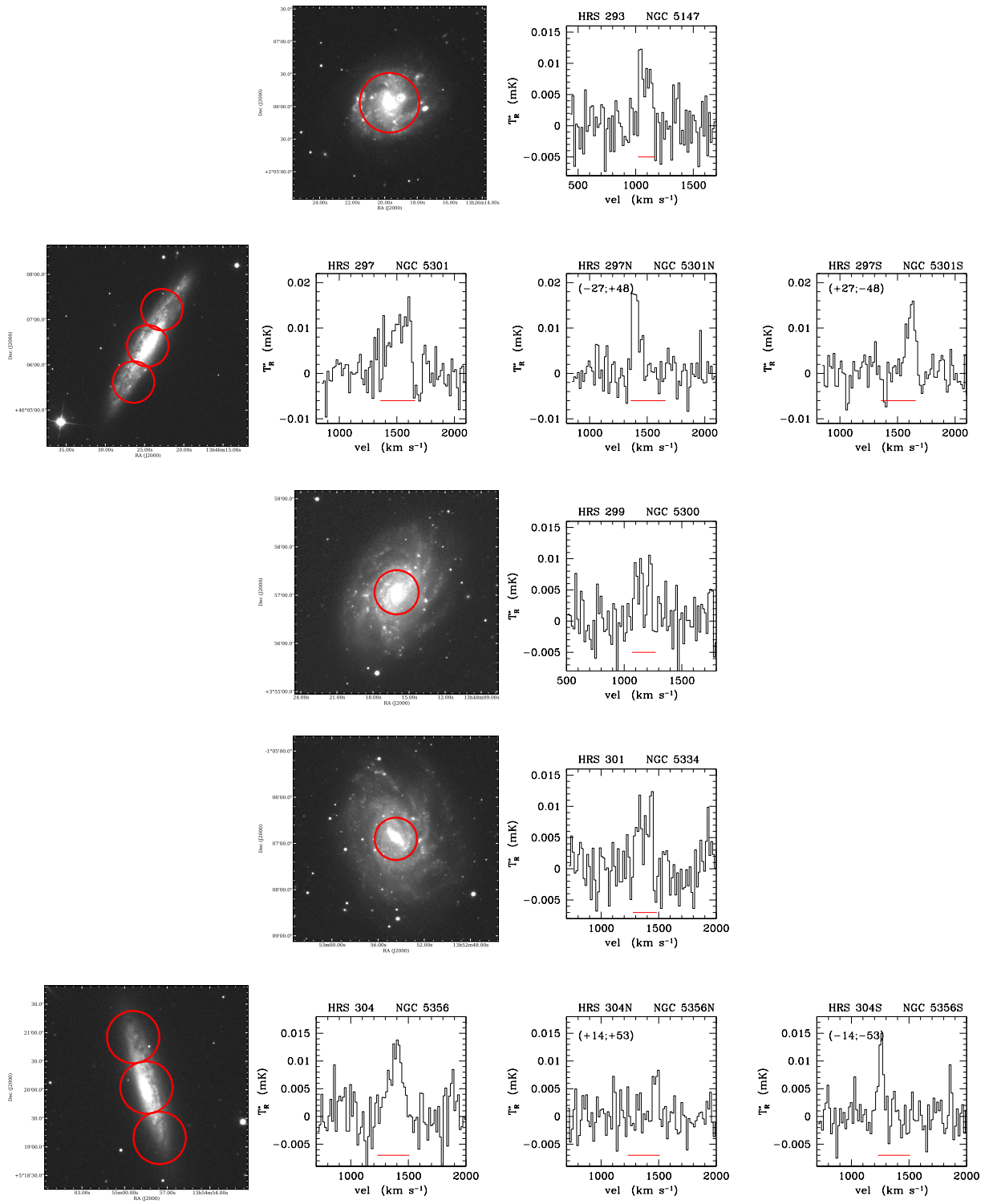


Fig. 9. Continued.

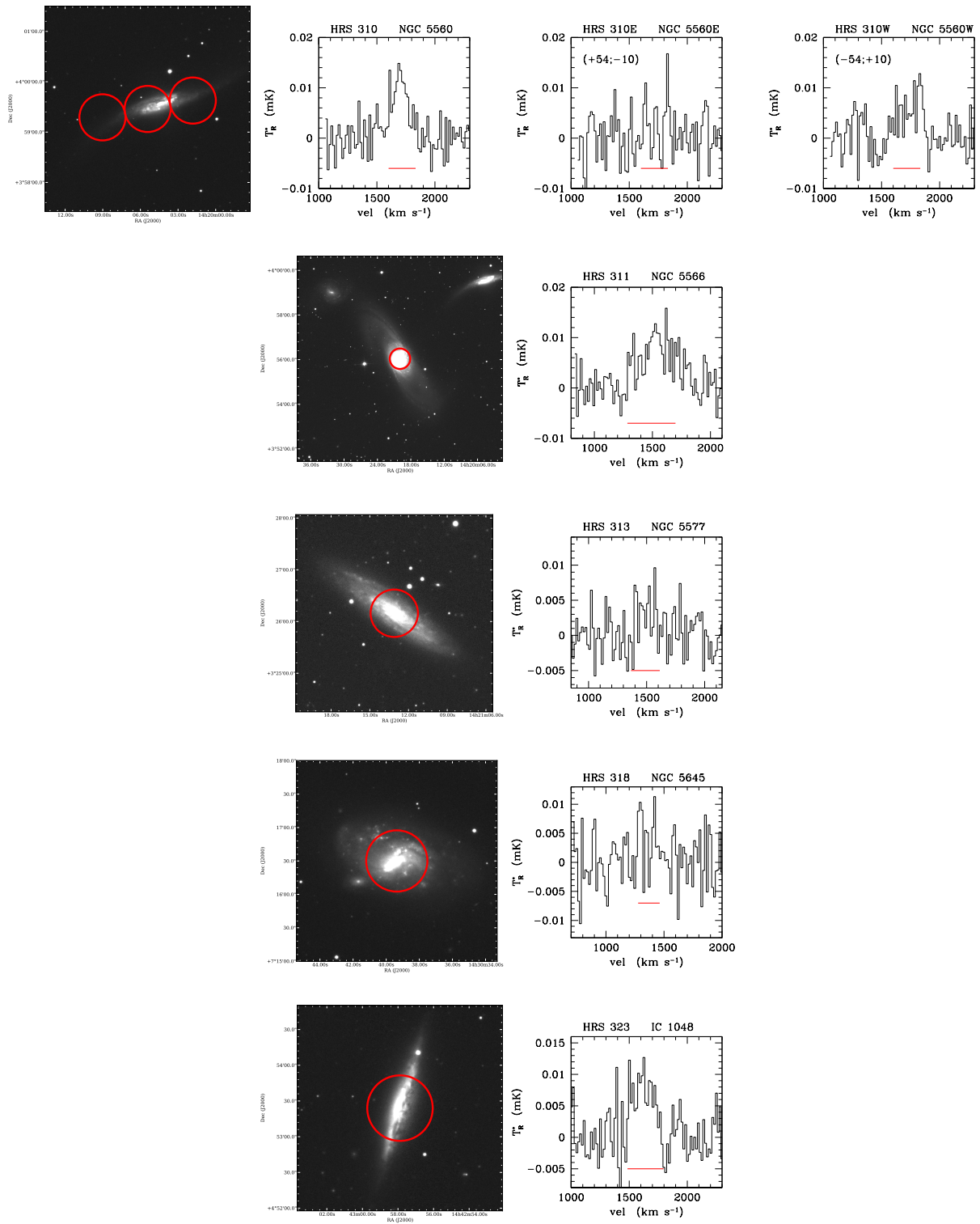


Fig. 9. Continued.